■

■

■

JOURNAL OF

THE INDIAN INSTITUTE OF SCIENCE

CONTENTS

PAGE

PROPAGATION OF LONG WAVES OF FINITE AMPLITUDE

By P. L. SACHDEV

(Department of Applied Mathematics, Indian Institute of Science, Bangalore-12, India)

[Received : July 11, 1970]

ABSTRACT

We consider the radiation problem for long waves of small amplitude, caused by an instantaneous disturbance of unit height at the origin. The equations governing this phenomenon were derived by Long (1964). The asymptotic expressions for the wave front and for large times are obtained. The initial value problem for the non-linear system of equations is also solved, using a perturbation scheme based on the small parameter α, the non-dimensional amplitude of the disturbance. The solution holds only for $t < < 1/\alpha$ as a result of the appearance of a secular term in the first order solution.

1. INTRODUCTION

Long (1964) derived a set of equations governing the development of arbitrary, small but finite amplitude long waves. These waves are, therefore, characterised by the inequalities

$$(a/h) < < 1, \quad (\lambda/h) > > 1 \qquad [1.1]$$

where h is the uniform depth of the water, a is a length representative of the amplitude and λ is a length representative of the wavelength of the disturbance. In contrast to the theory of Airy[1] which imposes the additional restriction that

$$(a/h) \ (\lambda^2/h^2) > > 1 \qquad [1.2]$$

and of Jeffereys and Jeffereys (1946) which requires

$$(a/h) \ (\lambda^2/h^2) < < 1 \qquad [1.3]$$

Boussinesq[2] derived an equation which governs the propagation of long waves when

$$(a/h) \ (\lambda^2/h^2) \sim 1. \qquad [1.4]$$

The initial-value problems for the Boussinesq equation which were discussed by Korteweg and de Vries[7], for example, were for waves for which the wave heights travel only in one direction with not an arbitrary speed but one nearly equal to $(gh)^{1/2}$. Long (1964), following Raye gl.[1], expanded the complex potential for the unsteady motion and derived a set of equations which govern arbitrary long waves of small but finite amplitude without any restriction on their speed to $(gh)^{1/2}$ or the direction of their propagation. With these restrictions these equations properly reduce to Boussinesq equations, Long has shown that these equations also yield the solitary wave which is a long wave that propagates without change of form. He has also considered numerical solutions of his equations for some symmetric initial values of elevation and zero initial velocity. After some time, the wave profile in either of the two directions is very nearly that corresponding to a solitary wave.

The purpose of this paper is to study the non-linear hyperbolic system of equations derived by Long (1964). These equations govern the development of an arbitrary, small (but finite) amplitude long wave disturbances and also yield the solitary wave when they are suitably approximated. Our treatment follows the well-known approach of Lighthill and Whitham[9] and Whitham[13], particularly the latter, to the system which is obtained by linearising the non-linear system. Whitham showed that the highest order derivative in a partial and differential equation governing wave propagation, yield the phenomenon in the earlier stages of propagation, coupled with a damping caused by lower order terms, while it is the lowest order terms which finally govern the phenomenon, these being accompanied by a diffusion due to the higher order terms. The characteristics of differential equations that we consider have constant slopes $\pm\sqrt{3}$, 0, 0, which, however, do not introduce any simplicity in the analysis of the equations. First we consider the radiation problem for the linearised form of these equations and derive the form of the wave for small and large times respectively. The solution for the initial boundary conditions $t=0$, $\eta = \eta_t = \eta_{tt} = \eta_{ttt} = 0$, $x > 0$ and $\eta = \delta(t)$ at $x=0$, is expressed in terms of Bessel function of first order for small time, that is, when the high frequency waves dominate or in the region where the discontinuities in the wave form appear. The solution is expressed in terms of Airy function when we consider the wave form after a large time. We also consider an initial value problem for the non-linear system in a power series in the small parameter α, characterising the non-dimensional amplitude of the disturbance. The first order term in the solution contains a secular term, that is, one containing the independent variable t, so that the solution is valid only for $\alpha t < < 1$.

2. DIFFERENTIAL EQUATIONS AND THEIR CHARACTERISTIC FORM

The differential equations describing the two dimensional long gravity waves and satisfying the kinematic and dynamic conditions on the surface of

water were written by Long in terms of the non-dimensional height $\eta = (\eta'/h)$ of the disturbance above the undisturbed level and a non-dimensional velocity $U = -F_x = -[F'_{x'}(x', t')/\sqrt{(gh)}]$. Here the primed quantities denote the dimensional variables so that $y' = 0$ is the x'—axis along the bottom of the channel and $y' = h$ is the vertical undisturbed height as shown in the fiigure. t' is time. The function F' is a function of x' and t' in terms of which the real part of the complex velocity potential ϕ' is expanded about $y' = 0$, that is,

$$\phi'(x', y', t') = F'(x', t') - (y'^2/2) \ F'_{x'x'}(x', t') + \ . \ . \ . \qquad [2.1]$$

The dimensionless quantities are expressed as

$$x = (x'/h), \ \ y = (y'/h), \ \ t = t'/\sqrt{(g/h)},$$

$$\phi(x, \ y, \ t) = \frac{\phi'(x', y', t')}{h\sqrt{(gh)}}, \ \ \eta = (\eta'/h), \ \ F(x, t) = \frac{F'(x', t')}{h\sqrt{(gh)}}. \ \ [2.2]$$

U, in fact, is the velocity at the bottom of the channel. Long made certain assumptions as to the order of different terms, which correspond to those employed in the derivation of the solitary wave. Thus, he assumed that if the non-dimensional amplitude of the disturbance is of the order α, a small quantity, that is, if

$$\eta \sim \alpha, \qquad [2.3]$$

then

$$(\partial/\partial x) \sim \alpha^{1/2}. \qquad [2.4]$$

This, in fact, expresses [1.4]. Besides, he assumed that

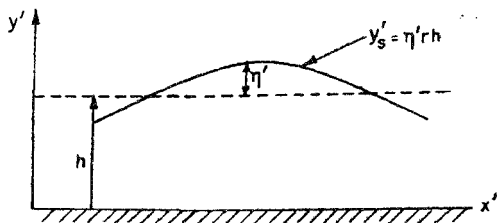$$U \equiv -F_x \sim \alpha, \ \ (\partial/\partial t) \sim (\partial/\partial x). \qquad [2.5]$$

Fɪɢ. 1
Long-wave Propagation

By substituting the non-dimensional velocity potential in the non-dimensional form of surface condition, Long obtained the following equations for η and U with an error of $0(\alpha^3)$ in η,

$$\eta_t + U\eta_x + U_x - \eta\,\eta_z + \tfrac{1}{6}\,\Omega_t = 0, \qquad [2.6]$$

$$\eta_x + U_t - U\,\eta_t + \tfrac{1}{2}\,\Omega_x = 0, \qquad [2.7]$$

$$\eta_t - \omega = 0, \qquad [2.8]$$

$$\omega_t - \Omega = 0. \qquad [2.9]$$

The equations [2.8] and [2.9] are already in characteristic form. The former two equations, [2.6] and [2.7], can be suitably combined to give the characteristic form :

$$\partial(\eta + \sqrt{3}\,U + \tfrac{1}{2}\,\Omega)/\partial z + \sqrt{3}\,U\,(\partial\eta/\partial z)$$
$$= \tfrac{1}{2}\,w\,[\sqrt{3}\,\eta + 2\,U - (2/\sqrt{3})] \qquad [2.6]'$$

$$\partial(-\eta + \sqrt{3}\,U - \tfrac{1}{2}\,\Omega)/\partial\bar{z} + \sqrt{3}\,U\,(\partial\eta/\partial\bar{z})$$
$$= \tfrac{1}{2}\,w\,[\sqrt{3}\,\eta - 2\,U - (2/\sqrt{3})] \qquad [2.7]'$$

where the independent variables are the characteristics $z = x + \sqrt{3}\,t$, $z = x - 3\sqrt{t}$. Thus, we have a hyperbolic system of equations with explicit characteristics, having constant slopes $\pm\sqrt{3}$, 0, 0.

3. SOLUTION OF THE LINEARISED EQUATIONS

If we put $U = U_0 + U$, $\eta = \eta_0 + \eta$, where U_0 and η_0 (in particular $\eta_0 = 0$) are the solutions of equations [2.6]' and [2.7]' giving uniform flow and U and η are of order $0(\alpha^2)$, and linearise (thus omitting terms of $0(\alpha^{1/2})$, we obtain, after elimination of U, a linear equation in η.

$$\left[\frac{\partial^2}{\partial z^2}\left(\frac{\partial^2}{\partial t^2} - 3\,\frac{\partial^2}{\partial x^2}\right) + 6\,(1 - \eta_0)\frac{\partial^2}{\partial t^2} + 12\,U_0\,\frac{\partial^2}{\partial t\,\partial x} - 6\,\frac{\partial^2}{\partial x^2}\,\right]\eta = 0. \qquad [3.1]$$

Thus the second order operator gives the lower order waves with speeds $[U_0 \pm \sqrt{(U_0^2 + 1 - \eta_0)}/1 - \eta_0]$ and the fourth order operator gives the higher order waves with speeds $o, o, \pm\sqrt{3}$. Unlike the differential operators considered by Whitham (1959), here the order of the adjacent differential operators differs by two. If we substitute

$$\eta \propto \exp(ikx - \alpha t) \qquad [3.2]$$

in equation [3.1] where k is real and consider long waves so that $k << 1$, we easily verify that all roots α of the dispersion relation are pure imaginary. This shows that we have a stable situation, with progressive waves as solutions. Similarly, if we consider a periodic wave maintained at $x = o$ so that

$$\eta \propto \exp.(\beta x - iwt) \tag{3.3}$$

with ω (real) $<< 1$, we again get all four roots corresponding to β pure imaginary, leading to the same result as noted above. Thus, for large times, we again have a stable situation. However, to be able to study the general wave motion, we consider the following signalling problem for the differential equation [3.1], an unsteady wave phenomenon on a running stream.

Initial conditions : $\qquad \eta = \eta_t = \eta_{tt} = \eta_{ttt} = 0$ at $t = o, \ x > 0$

Boundary conditions : $\quad \eta = f(t)$ at $x = 0$ $\qquad\qquad$ [3.4]

In the above we consider waves propagating in the $x > 0$ direction due to the signal at $x = 0$, but we could also consider the waves in the opposite direction. We find the Laplace transform of the equation [3.1] with the initial conditions [3.4]. We have

$$(3p^2 + 6) \ \overline{\eta}_{xx} - 12 \ U_0 \ p \ \overline{\eta}_x - [6 (1 - \eta_0) p^2 + p^4] \ \overline{\eta} = 0. \tag{3.5}$$

The solution of this equation is

$$\overline{\eta} = A_1 (p) \exp.[\gamma_1 (p) x] + A_2 (p) \exp.[\gamma_2(p)x] \tag{3.6}$$

where A_1 and A_2 are some functions of p and

$$\gamma_{1,2} = \frac{6 \ U_0 \ p \pm p \ \{36 \ U_0^2 + (3 \ p^2 + 6)[p^2 + 6 \ (1 - \eta_0)]\}^{1/2}}{3 \ (p^2 + 2)}. \tag{3,7}$$

This expression is rather complicated and therefore we approximate this for the following two situations (a) when p is very large *i.e.*, t is small, this approximation is valid when the high frequency waves dominate or near discontinuities in the wave form. (b) when p is very small so that we consider the solution for large times.

(a) When p is large. In this case,

$$\gamma_{1,2} \approx \frac{\pm p}{\sqrt{(3)}} + \frac{1}{3p} [6 \ U_0 \pm \sqrt{(3)} \ (2 - 3 \ \eta_0)]. \tag{3.8}$$

For the forward moving wave we take negative sign, with $A_1(p) = 0$, and inverting equation [3.6],

$$\eta = \frac{1}{2\pi i} \int_{\gamma-i\infty}^{\gamma+i\infty} A_2(p) \exp\left\{ p\left(t - \frac{x}{\sqrt{(3)}}\right) + [6U_0 - \sqrt{(3)}(2-3\eta_0)]\frac{x}{3p}\right\} dp \quad [3.9]$$

where $\gamma = \text{Re}p$ is such that all singularities of the integrand are to the left of $\text{Re}p = \gamma$. It is obvious that

$$A_2(p) = \int_0^\infty \exp.(-pt) f(t) \, dt. \qquad [3.10]$$

If we take $f(t) = \delta(t)$, the Dirac delta function, so that $A_2(p) = 1$, the above integral is easily evaluated, Roberts and Kaufmann[12], the solution $\hat{\eta}$ is

$$\hat{\eta}(x,t) = 0 \qquad 0 < t < x/\sqrt{3} \qquad [3.11]$$

$$= \delta\left(t - \frac{x}{\sqrt{(3)}}\right) - \left(\frac{x}{3}\right)^{1/2} \left[\frac{\sqrt{(3)}\,(2-3\,\eta_0) - 6\,U_0}{t - [x/\sqrt{(3)}]}\right]^{1/2} \times$$

$$\times J_1 \left\{2\left(\frac{x}{3}\right)^{1/2}\left(t - \frac{x}{\sqrt{(3)}}\right)^{1/2} [\sqrt{(3)}\,(2-3\eta_0) - 6\,U_0]^{1/2}\right\}$$

$$t \geqslant [x/\sqrt{(3)}].$$

For any other $f(t)$, we can use the faltung theorem to obtain

$$\eta = \int_0^t \hat{\eta}(x, u) \, f(t-u) \, du. \qquad [3.12]$$

If we were to consider wave propagation in the negative direction, we would have

$$\hat{\eta} = \delta\left(t + \frac{x}{\sqrt{(3)}}\right) - (-x)^{1/2} \frac{[\sqrt{(3)}\,(2-3\eta_0) + 6U_0]^{1/2}}{\sqrt{3}\,[\,t + x/\sqrt{3}]\frac{1}{2}} \times$$

$$J_1\left\{\frac{2}{\sqrt{(3)}}\,(-x)^{1/2}\,[\sqrt{(3)}\,(2-3\eta_0) + 6U_0]^{1/2}\left(t + \frac{x}{\sqrt{(3)}}\right)^{1/2}\right\}.$$

$$t \geqslant -[x/\sqrt{(3)}]$$

$$= 0. \qquad\qquad\qquad t < -[x/\sqrt{(3)}] \quad [3.13]$$

The above solution represents higher order progressive waves with speeds $+\sqrt{(3)}$ and $-\sqrt{(3)}$ respectively. The wave height near the front initially decreases from 1 as x increases. We also note that if $\eta_0 = 0$, $U_0 = [1/\sqrt{3}]$, $\eta(x,t) = \delta[t - x/\sqrt{(3)}]$ in equation [3.11] which gives $\eta(x,t) = 1$ on $t = [x/\sqrt{(3)}]$ and $\eta = 0$ elsewhere. Of course these results are based on linear theory, the non-linear effects will alter the situation considerably. Unlike the exponential damping of dynamic waves by the kinematic waves, in the flood wave problem of Lighthill and Whitham, we have near the wave front a diminishing of the amplitude from unity and an oscillatory character, given by Bessel function of order one.

(*b*) In this case p is small, we approximate $\gamma_{1,2}$ to

$$\gamma_{1,2} = p\left[U_0^2 \pm (U_0^2 + 1 - \eta_0)^{1/2}\right] + p^3\left[\pm \frac{4 - 3\eta_0}{12(U_0^2 + 1 - \eta_0)} - \frac{1}{2} U_0 \mp \frac{1}{2} (U_0^2 + 1 - \eta_0)^{1/2}\right]$$

$$\equiv B_{1,2}\, p + C_{1,2}\, p^3. \tag{3.14}$$

Again if we consider wave propagation in the positive direction only, then taking the lower sign,

$$\eta = \frac{1}{2\pi i} \int_{\gamma - i\infty}^{\gamma + i\infty} \overline{f}(p)\, \exp.\, [p(t + B_2 x) + C_2 x p^3]\, dp \tag{3.15}$$

where $Rl\,\gamma$ is defined in the usual way. Again if we choose $f(t) = \delta(t)$ so that $\overline{f}(p) = 1$, the above integral can be easily integrated, Magnus *et al*[10]. We can transform this integral into the form

$$\hat{\eta} = (1/\pi) \int_0^\infty \cos\,[z\,(t + B_2 x) - c_2\, x z^3]\, dz \tag{3.16}$$

which is expressible in terms of Airy functions

$$\hat{\eta} = \frac{1}{(3\,C_2\,x)^{1/3}}\, A_i\left(-3^{-1/3}\frac{B_2 x + t}{(C_2 x)^{1/3}}\right) \qquad \cdots$$

$$\approx \frac{1}{\sqrt{\pi}\,[3\,C_2\,x\,(B_2 x + t)]^{1/4}}\, \cos\left[\frac{2}{3}\frac{(B_2 x + t)^{3/2}}{(3\,C_2 x)^{1/2}} - \pi/4\right], \tag{3.16'}$$

the asymptotic expression of *Ai* for large value of t when x/t is kept fixed. We briefly verify this result by the method of saddle points. The exponential term in the integral [3.15] can be written as

$$\exp t\,\{p\,[1 + B_2\,(x/t)] + C_2\,(x/t)\,p^3\}.$$

For fixed value of x/t, we evaluate this integral for large t. The saddle points of $F(p) = p[1 + B_2(x/t)] + C_2(x/t)]p^3$ are

$$p_{0,1} = \pm i[(t/x + B_2)(1/3 C_2)]^{1/2}, \tag{3.16}"$$

both of these being equally important. Therefore, by the usual method of saddle points,

$$\eta \sim \frac{1}{[48 \pi^2 C_2 x (t + B_2 x)]^{\frac{1}{4}}} [\bar{\eta}(p_0) \exp i \left\{\tfrac{2}{3}(t + B_2 x)\sqrt{[(t/x + B_2)(1/3 C_2)]} - \pi/4\right\}$$

$$+ \bar{\eta}(p_1) \exp -i \left\{\tfrac{2}{3}(t + B_2 x) \sqrt{[(t/x + B_2)(1/3 C_2)]} - \pi/4\right\}]$$

$$= \frac{1}{\sqrt{\pi}[3 C_2 x (B_2 x + t)]^{1/4}} \cos \left[\tfrac{2}{3} \frac{(B_2 x + t)^{\frac{3}{2}}}{(3 C_2 x)^{1/2}} - \pi/4\right] \tag{3.17}$$

when $\bar{\eta}(p) = 1$. This is the same as in [3.16]. This represents essentially the lower order waves. We find that the solution does not hold at the observation point $x = 0$ and the front $B_2 x + t = 0$, Lighthill and Whitham[9]. We also note that $\eta \propto (1/\sqrt{x})$ or $\eta \propto (1/\sqrt{t})$ for fixed x/t, showing diffusion of the lower order wave by the higher order ones.

The solution in the negative x direction can be easily obtained by changing B_2 and C_2 to B_1 and C_1 respectively.

Before we consider the non-linear wave propagation, we briefly indicate the results as obtained by the quick method, Whitham[13]. For example, for the wave corresponding to $(\partial x/\partial t) = \sqrt{3}$ we put $(\partial/\partial t) = -\sqrt{3}(\partial/\partial x)$ in equation [3.1] and introduce the variable $\xi = x - \sqrt{3} t$, we get the equation

$$(\partial^2 \eta/\partial x \partial \xi) = -\tfrac{1}{3}[2 - 3 \eta_0 - 2\sqrt{3} U_0]\eta. \tag{3.18}$$

With the conditions that $\eta = 0$ on the front $x - \sqrt{3} t = \xi = 0$ and $\eta = f(t)$ on $x = 0$, the solution of equation [3.18] can be written in the form, Garabedian[5],

$$\eta(x, \xi) = \frac{f(0) J_0(2\sqrt{\lambda x \xi})}{2} + \int_0^\xi f'(\eta_1) J_0[2\sqrt{\lambda(\xi - \eta_1)}] d\eta_1. \tag{3.19}$$

Similarly, the solution near the wave front $x = -\sqrt{3} t$ is obtained by simply changing ξ to $\xi' = x + \sqrt{3} t$. For the lower order waves, if we put $(\partial/\partial t) = -C_{1,2}(\partial/\partial x)$ in equation where $C_{1,2} = [U_0 \pm \sqrt{(U_0^2 + 1 - \eta_0)}/1 - \eta_0}$,

we get

$$\frac{\partial \eta}{\partial t} + C_i \frac{\partial \eta}{\partial x} - \frac{C_i^2 (C_i^2 - 3)}{6 (1 - \eta_0)} \frac{\partial^3 \eta}{\partial x^3} = 0, \quad i = 1, 2 \qquad [3.20]$$

after integrating out once with respect to x. The solution of this equation can be expressed in terms of Bessel functions.

4. INITIAL VALUE PROBLEM

Now we consider the initial value problem for the hyperbolic system $(2.6)' - (2.9)'$ where equations [2.8] and [2.9] are expressed in terms of the characteristic variables z and $\bar{z}$ as

$$(\partial \eta / \partial z) - (\partial \eta / \partial \bar{z}) = (w / \sqrt{3}). \qquad [2.8]'$$

$$(\partial w / \partial z) - (\partial w / \partial \bar{z}) = (\Omega / \sqrt{3}). \qquad [2.9]'$$

We assume that $\eta (x, 0)$ and $U (x, 0)$ are given. We seek the solution in the form

$$\eta = \alpha (\eta_0 + \alpha \eta_1), \quad U = \alpha (U_0 + \alpha U_1), \quad \omega = \alpha^{3/2}(\omega_0 + \alpha \omega_1),$$
$$\Omega = \alpha^2 (\Omega_0 + \alpha \Omega_1), \qquad [4.1]$$

since the equations of Long give η with an error of $0 (\alpha^3)$. Here η and U are functions of z and $\bar{z}$. We substitute the expressions [4.1] in equations $[2.6]' - [2.9]'$, taking note of the assumptions [2.4] and [2.5].

After some calculation, we get the following equations. **Zero order** system :

$$\frac{\partial (\eta_0 + \sqrt{3} U_0)}{\partial z} = - (1 / \sqrt{3}) \omega_0. \qquad [4.2]$$

$$(\partial / \partial \bar{z}) (- \eta_0 + \sqrt{3} U_0) = (- \omega_0 / \sqrt{3}), \qquad [4.3]$$

$$(\partial \eta_0 / \partial z) - (\partial \eta_0 / \partial \bar{z}) = (\omega^0 / \sqrt{3}), \qquad [4.4]$$

$$(\partial \omega_0 / \partial z) - (\partial \omega_0 / \partial \bar{z}) = (\Omega_0 / \sqrt{3}). \qquad [4.5]$$

First order system :

$$\frac{\partial [\eta_1 + \sqrt{3} U_1 + (\Omega_0 / 2)]}{\partial z} + \sqrt{3} U_0 (\partial \eta_0 / \partial z)$$
$$\cdot (\omega_0 / 2) (\sqrt{3} \eta_0 + 2 U_0) - (\omega_1 / \sqrt{3}), \qquad [4.6]$$

$$\frac{\partial\,[-\eta_1 + \sqrt{3}\,U_1 - (\Omega_0/2)]}{\partial \bar{z}} + \sqrt{3}\,U_0\,(\partial\,\eta_0/\partial \bar{z})$$

$$= (\omega_0/2)\,(\sqrt{3}\,\eta_0 - 2\,U_0) - (\omega_1/\sqrt{3}), \qquad\qquad [4.7]$$

$$(\partial\eta_1/\partial z) - (\partial\eta_1/\partial\bar{z}) = (\omega_1/\sqrt{3}), \qquad\qquad [4.8]$$

$$(\partial\omega_1/\partial z) - (\partial\omega_1/\partial\bar{z}) = (\Omega_1/\sqrt{3}). \qquad\qquad [4.9]$$

The equations satisfied by η_0 and η_1 are found to be

$$\left(\frac{\partial^2}{\partial z^2} + \frac{\partial^2}{\partial\bar{z}^2} - 4\,\frac{\partial^2}{\partial z\,\partial\bar{z}}\right)\eta_0 = 0, \qquad\qquad [4.10]$$

$$\left(\frac{\partial^2}{\partial z^2} + \frac{\partial^2}{\partial\bar{z}^2} - 4\,\frac{\partial^2}{\partial z\,\partial\bar{z}}\right)\eta_1 = F\,(z,\,\bar{z}) \qquad\qquad [4\,11]$$

Where $F(z,\,\bar{z})$

$$= \frac{\partial^3\Omega_0}{\partial z\,\partial\bar{z}} + \sqrt{3}\left[\frac{\partial}{\partial\bar{z}}\!\left(U_0\frac{\partial\eta_0}{\partial z}\right) - \frac{\partial}{\partial z}\!\left(U_0\frac{\partial\eta_0}{\partial\bar{z}}\right)\right]$$

$$-\frac{\sqrt{3}}{2}\,\frac{\partial}{\partial\bar{z}}\left(\frac{\partial\eta_0}{\partial z} - \frac{\partial\eta_0}{\partial\bar{z}}\right)(\sqrt{3}\,\eta_0 + 2\,U_0)$$

$$+(\sqrt{3}/2)\,(\partial/\partial z)\,[(\partial\eta_0/\partial z) - (\partial\eta_0/\partial z)]\,(\sqrt{3}\,\eta_0 - 2\,U_0). \qquad [4.12]$$

We easily verify that the characteristics of the differential operator on the left hand side equations [4.1] and [4.2] are $\bar{z} + (2\pm\sqrt{3})\,z = (3\pm\sqrt{3})\,(x\mp t) =$ const, agreeing with the linearised equation [29] of Long (1964). Thus the characteristic slopes of the zero order solutions are ± 1, while those of the non-linear system are $\pm\sqrt{3}$. We consider, in particular, the initial value problem $\eta\,(x,\,0) = 2\,\alpha\,\cos x,\,U(x,\,0) = 0$, so that we find from equations [4.10], [4.2] and [4.3] that

$$\eta_0\,(x,\,t) = \cos\,(x+t) + \cos\,(x-t),\ \ U_0\,(x,\,t) = \cos\,(x-t) - \cos\,(x+t). \quad [4.13]$$

Thus, it is more convenient to introduce the characteristic variables

$$\alpha_1 = x - t,\ \ \beta_1 = x + t \qquad\qquad [4.13]$$

so that η_1 can be shown to satisfy the equation

$$(\partial^2 \eta_1 / \partial \alpha_1 \partial \beta_1) = -\tfrac{1}{2} \cos (\alpha_1 + \beta_1) + \tfrac{3}{4} [\cos 2\,\alpha_1 + \cos 2\,\beta_1]$$
$$-\tfrac{1}{12} (\cos \alpha_1 + \cos \beta_1). \qquad\qquad [4.14]$$

The solution of this hyperbolic differential equation with **the initial** condition $\eta_1 = (\partial \eta_1 / \partial \alpha_1) = (\partial \eta_1 / \partial \beta_1) = 0$ on the initial line $\alpha_1 = \beta_1$ **from** equations [4.6] and [4.7] is

$$\eta_1 = (\beta_1 - \alpha_1) [\tfrac{3}{8} (\sin 2\,\alpha_1 - \sin 2\,\beta_1) + \tfrac{1}{12} \sin \beta_1 - \sin \alpha_1)]$$
$$+ \tfrac{1}{2} \cos (\alpha_1 + \beta_1) - \cos 2\,\alpha_1] + \tfrac{1}{4} (\cos 2\,\alpha_1 - \cos 2\,\beta_1)$$

$$= t [\tfrac{3}{4} \left\{ \sin 2\,(x-t) - \sin 2\,(x+t) \right\} + \tfrac{1}{6} \left\{ \sin (x+t) - \sin (x-t) \right\}]$$
$$+ \tfrac{1}{2} [\cos 2 x - \cos 2\,(x-t)] + \tfrac{1}{4} [\cos 2\,(x-t) - \cos 2\,(x+t)]. \qquad [4.15]$$

We find that a secular term in the first order term of the solution appears so that the solution is valid only for $\alpha\,t < < 1$. While the secular terms in ordinary differential equations have been treated quite successfully, there does not seem to be any general way of tackling them for partial differential equations. For example, Broer (1965) has considered some simple cases when a transformation of the time variable can be guessed from the solution. The term $(\alpha\,t/6) [\sin (x+t) - \sin (x-t)]$ in [4.15] can be easily combined with the zero order term by the transformation $t' = 1 + (\alpha\,t/6)$ but the other secular terms cannot be removed. The divergence of the solution for large t is not due to the linearising of the characteristics since we can easily fit **the exact** characteristics by stretching the x-co-ordinate by $1/\sqrt{3}$, but does **not remove** the singularity for large t. This perturbation scheme is not suited **to give** solution for the far field for which a different procedure similar to that given by Cole (1968) would lead to the Korteweg equation which provides the solitary wave and other periodic solutions, Kruskal and Zabusky[8]. In any case, the above solution for $t < (1/\alpha)$ shows that in the first order solution we get zero order solution and its double harmonic out of phase with the zero order solution by $\pi/2$ and these together have their amplitude increasing linearly with time while the other double harmonic in η_1 remains bounded.

5. ACKNOWLEDGEMENT

REFERENCES

1. Airy, G. È.   Encyclopaedia Metropolitanar. 1845, 241.

2. Boussinesq, J.   *J. Math. pures appl.*, 1872, **17**, 55.

3. Broer, L. J. F.   *Z. angew. Math. Phys.*, 1965, **16**, 13.

4. Cole, J. D.   Perturbation Methods in Applied Mathematics.
                                          Blaisdell Publishing Company, London, 1968,
                                          252.

5. Garabedian, P. R.   Partial Differential Equations.   John Wiley
                                          and Sons, 1964.

6. Jaffereys, H and Jaffereys, B. S.   Methods of Mathematical Physics, Cambridge
                                          University Press, 1946.

7. Korteweg, D. J. and DE Vries, G.   *Phil. Mag*, 1895, **39**, 422.

8. Krushkal, M. D. and Zabusky. N. J   *J. math. Phys.*, 1964, **5**, 231.

9. Lighthill, M. J. and Whitham. G. B.   *Proc, R. Soc.* 1955, 229A, 281.

10. Magnus, W., Oberheittinger, F.   Formulas and Theorems for the special func-
    and Soni, P. R.   tions of Mathematical Physics, 1966, 75.

11. Rayleigh, Lord   *Phil. Mag*, 1876, **1**, 257.

12. Roberts, G. E. and Kaufman, H.   Table of Laplace Transform. W. P Saunders
                                          Company, 1966, 60.

13. Whitham, G. B.   *Communs. pure appl Math.*, 1959, **12**, 113.

RAMAN SPECTRA OF 1,2-DICLOROETHANE AND 2-CHLOROETHANOL

By A. SELVARAJAN AND K. KRISHNAN

(Department of Physics, Indian Institute of Science, Bangalore-12, India.)

[Received: August 17, 1970]

ABSTRACT

Raman spectra of 1,2-dichloroethane and 2-chloroethanol have been recorded using both the 4358 Å and the 2537 Å excitations In the spectra obtained with the latter excitation, many new Raman lines are found for the first time. Assignments of these lines are discussed. When the exciting wavelength is changed from 4358 Å to 2537 Å, the relative intensities and depolarization ratios of some of the Raman lines of the two substances are seen to change also. These changes are explained on the basis of the resonance Raman effect.

1. INTRODUCTION

The Raman spectrum of 1,2-dichloroethane and 2-chloroethanol has been studied by numerous investigators[1-5]. The problem of internal rotation in substituted ethanes has been studied in detail by Mizushima[2]. It is now well known that both in the gaseous and liquid states 1,2-dichloroethane exists as a mixture of two rotational isomers, having the trans- and the gauche- forms respectively. The trans- form of the molecule belongs to the symmetry point group C_{2h} and the gauche- form to the point group symmetry C_2. Complete vibrational assignments from normal coordinate analyses for these two forms has been given by Nakagawa and Mizushima[6]. The molecular structure of 1,2-dichloroethane has also been studied by X-ray[7], electron diffraction[8] and infrared[2,9] methods.

The Raman spectrum of 2-chloroethanol has also been the subject of numerous investigations[10-15]. Infrared obsorption[16-18], electron difraction[19,20] and microwave[21] studies of 2-chloroethanol have also been reported in the literature. These studies have shown that the 2-chloroethanol molecule also exists in two rotational isomeric forms—the trans- and the gauche-ones. Whereas in 1,2-dichloroethane the trans- form is more stable, in 2-chloroethanol the guache- form is the more stable one. In the latter case, the chlorine atom and the hydroxyl groups take part in the formation of an internal hydrogen bond.

All these earlier studies on the Raman spectra of the above two compounds had been carried-out using the visible mercury 4358 Å excitation methods. Pure 1,2-d.chloroethane and 2-chloroethanol were found to be sufficiently transparant to the 2537 Å mercury radiation. It was thought worthwhile, therefore. to re-examine the Raman spectra of the above two liquids using the 2537 Å excitation, with a view to find out the changes if any, which take place in the spectra, as the exciting frequency in this case will be much closer to the electronic absorption frequencies of the compounds.

2. EXPERIMENTAL DETAILS

Two sets of Raman spectra were recorded for each compound, one using the v.s.ble mercury 4358 Å excitation and the other us'ng the ultraviolet mercury 2537 Å radiation. A Toronto type hel:cal mercury. arc was the sources of the visible radiation, while a water-cooled, magnet-controlled quartz mercury are served to produce an intense beam of the ultraviolet radiation. A saturated solution of sod:um nitrite was used to cut off all radiations of wavelength less than 4358 Å in the firs: case ; for the ultra-violet studies, a filter of dilute acetic acid was used to cut off all radiations of wavelength less than 2537 Å   The vis'ble Raman spectra were recorded using a Hlger two prism spectrograph on Ilford Astra III plates. For the ultraviolet Raman spectra, a Hilger med um quartz spectrograph was used, the spectra beirg photographed en Ilford Zenith Astronomical plates. For the depolarization measurements, a double image prism was inserted in the path of the scattered light. The light coming cut of the double image prism was condensed on to the slit of the spectrograph using a crystal quartz lens. The lens was so chosen that by its opt cal activity and biref-ringence the two componets of the scattered light com ng out of the double image prism, were effectively depolarized. Thus the two beams d.d not suffer unequal reflection losses inside the spectrograph. The Raman spectra were microphotometered using a Moll m'crophotometer.

Analar qu lity 1, 2-d:chloroethane, and 2-chlorcethanol were used in the study. Both the liquids were distilled twice before use. For the ultraviolet study, the samples were kept in a high optical quality fused silica Wood's tube.

3. RESULTS

Figures 1a and 1b show the Raman spectra and the microphotometer tracings of 1, 2-dichloroethane as excited by the 2537 Å and the 4358 Å radiations, respectively. Figures 2a and 2b show the corresponding Raman spectra of 2-chloroethanol. The observed Raman frequency shifts, their visually estimated relative intensities, and depolarization ratios of 1, 2-dich-loroethane are listed in Table 1. The frequency shifts of the Raman lines of 2-Chloroethanol, along with their visually estimated relative intensities are given in Table 2.

TABLE 1

Raman Spectrum of 1,2-Dichloroethane

7537 Å excitation		4538 Å excitation		Assignments		Species	
Frequencies $(cm^{-1})(a)$	ρ	Frequencies (cm^{-1})	$\rho^{(b)}$			Trans C_{2h}	Gachue C_2
125(3)	dp	125(4)	0.63	ν'_{10}	torsion		a
223(0)		223(1)		ν_{18}	C-Cl bending	b_u	
265(2)	0.47	263(2)	0.31	ν'_6	C-Cl bending		a
301(8)	0.54	300(8)	0.40	ν_6	C-Cl bending	a_g	
414(4)	0.94	412(4)	0.81	ν'_{18}	C-Cl bending		b
465(0)	. .			ν_5-ν_6	or ν_{16}-ν^9	A_g or B_g	
537(0)				ν'_5-ν_6	or $2\nu_6$	A_g	A
650(10)	0.13	652(10)	0.18	ν'_5	C-Cl stretching		a
680(8)	0.88	678(6)	dp	ν'_{17}	C-Cl stretching		b
752(10)	0.39	754(10)	0.23	ν_5	C-Cl stretching	a_g	
883(4)	0.18	881(3)	0.88	ν'_{13}	CH_2 rocking		b
944(5)	0.34	942(4)	0.26	ν'_9	CH_2 rocking		a
990(1)		989(1)	p	ν_{13}	CH_2 rocking	b_g	
1032(1)		1032(1)		ν'_4	C-C stretching		a
1054(3)	0.57	1052(4)	0.47	ν_4	C-C stretching	a_g	
1145(2)	dp	1143(2)	dp	ν'_{12}	CH_2 twisting		b
1169(0)				ν_2-ν'_6			A
1209(7)	0.71	1206(6)	0.65	ν'_8	CH_2 twisting		a
1264(0)		1262(1)	dp	ν'_3, ν_{12}	CH_2 wagging	b_g	a
1305(9)	0.35	1303(7)	0.45	ν_3, ν'_{16}	CH_2 twisting	a_g	b
1432(8)	0.72	1439(8)	0.82	ν'_2, ν'_{15}	CH_2 bending		a, b
1444(6)		1443(5)	dp	ν_2	CH_2 bending	a_g	
1507(1)				$2\nu_3$		A_g	

TABLE 1 — (contd.)

2537 Å excitation		4358 Å excitation		Assignmets	Species	
Frequencies. $(cm^{-1})(a)$	$\rho^{(a)}$	Frequencies $(cm^{-1})(a)$	$\rho^{(b)}$		Trans C_{2h}	Cauch C_2
1630(0)	· ·	· ·	· ·	$\nu'_{17} + \nu'_9$		B
2062(1)	· ·	· ·	· ·	$\nu_3 + \nu_5$	A_g	
2095(1)	· ·	· ·	· ·	$\nu_8' + \nu'_{13}$ or $\nu_2' + \nu_5'$		B or A
$2260(\frac{1}{2})$	· ·	· ·	· ·	$\nu_8' + \nu_4'$		A
2316(0)	· ·	· ·	· ·	$\nu_2' + \nu'_{13}$		B
2470(1)	· ·	· ,	· ·	$\nu_2'' + \nu_4'$ or $\nu_8' + \nu_3'$		A
$2525(\frac{1}{2})$	· ·	· ·	· ·	$\nu_8' + \nu'_{16}$		B
2569(1)	· ·	· ·	· ·	$\nu_2' + \nu_{12}$ or $\nu_3 + \nu_{12}$		A
2603(0)	· ·	· ·	· ·	$2\nu_3$ or $2\nu'_{16}$	A	A
$2712(\frac{1}{2})$	· ·	· ·	· ·	$\nu_2 + \nu_{12}$	B_g	
2744(1)	· ·	· ·	· ·	$\nu_2 + \nu_3$	A_g	
2844(5)	p	2841(4)	p	$2\nu_2'$		A
2875(5)	p	2875(4)	p	$2\nu_2$	A_g	
2958(10)	0.23	2960(10)	0.23	$\nu_1 \nu_1' \nu'_{14}$ CH stretching a_g		a,b
3005(8)	1.00	3007(7)	dp	$\nu_{11} \nu_7' \nu'_{11}$ C-H stretching b_g		a,b

(a) Numbers within brakets give the relative intensities estimated vissually.

(b) Values reported by Neu et al. (4).

4. DISCUSSION

A study of the Tables 1 and 2 shows that besides the Raman lines already reported by earlier workers, the Raman spectra of 1, 2-dichloroethane and 2-chloroethanol excited by the 2537 Å radiation contain many new lines. These lines are mainly in the region of combination and overtone bands. We have used the assignments for the fundamental vibrations of 1,2 dichloroethane as given by Nakagawa and M zushima [6]. Table 1 gives these assignments, together with our assignments of the newly observed Raman lines which have been assigned as combinations and overtones. In making the latter assignments, the following facts were taken into account : (i) only the overtones and combinations expected are these involving in general, the stronger fundamentals and (ii) the resultant states of the combinations and the overtones should belong to a Raman active species.
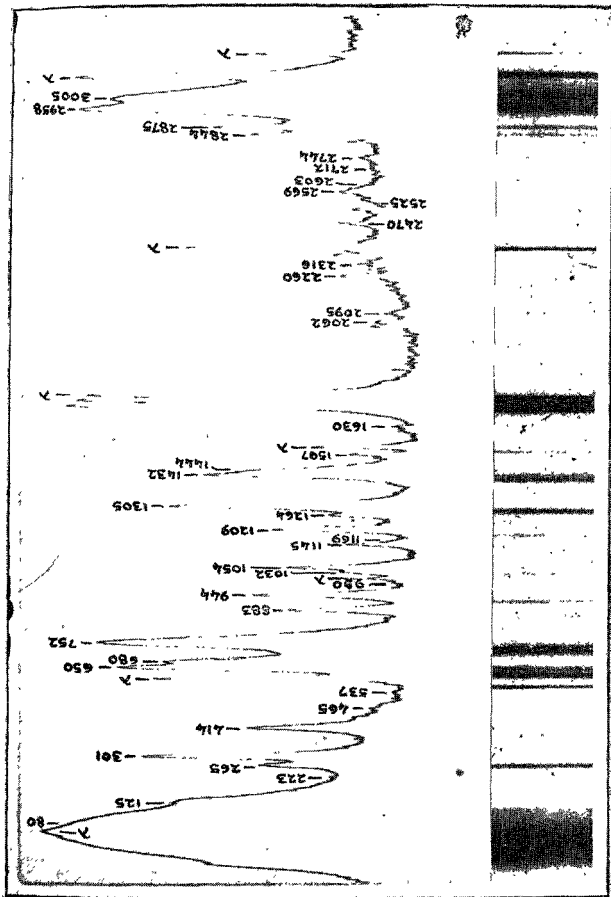
PLATE I*a*

Raman Spectrum and the microphotometer record of 1,2–dichloroethane (2537 Å excitation)
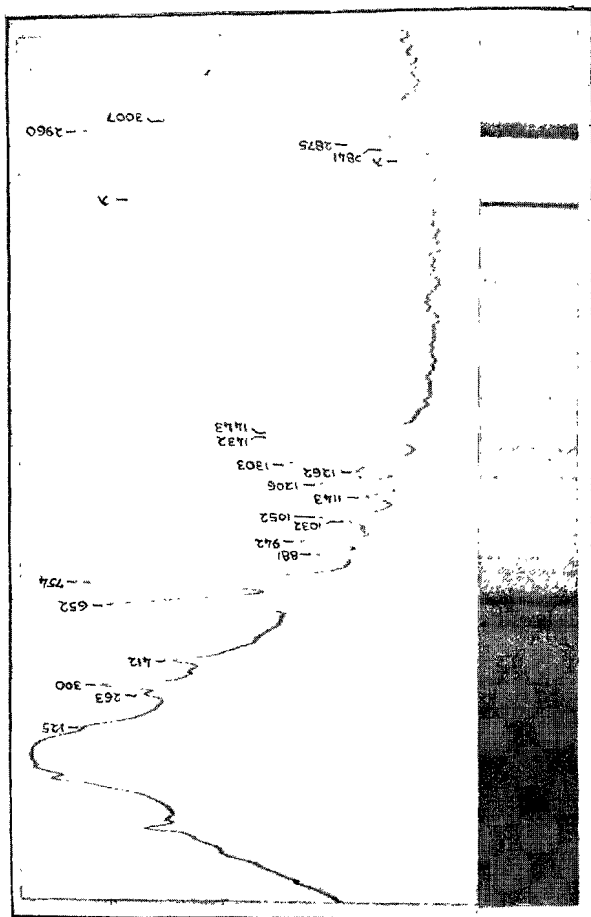
PLATE I *b*

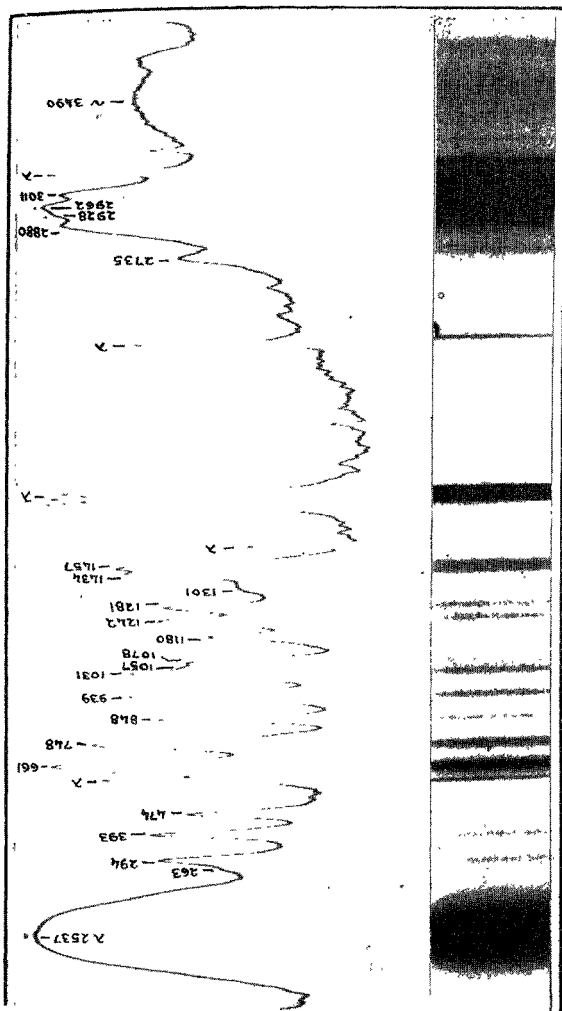Raman Spectrum and the microphotometer record of 1 2—dichloroethane (4358 Å excitation)

Plate IIa

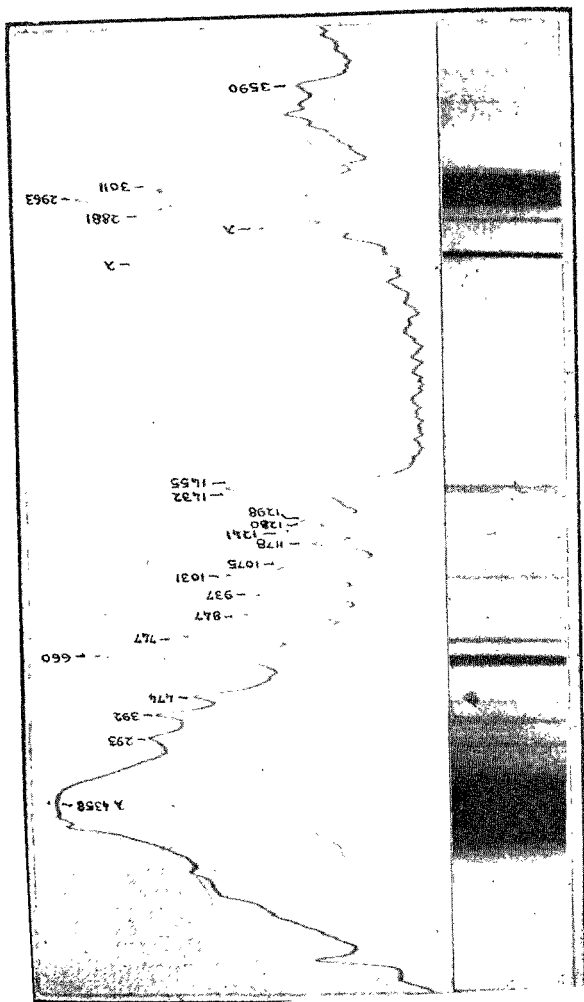Raman Spectrum and the microphotometer record of 2—chloro ethanol (2537 Å A excitation)

PLATE II*b*

Raman Spectrum and the microphotometer record of 2–chloro ethanol (4358 Å A excitation)

TABLE 2

Raman Spectrum of 2-Chloroethanol

Frequencies (cm⁻¹)		Assignments
Present study		
2537 Å excitation	4538 Å excitation	
165(1)		Torsion
263(0)		
294(4)	293(3)	C-C-Cl bending
393(5)	392(4)	
474(3)	473(3)	C-C-O bending
661(10)	660(10)	C-Cl stretching
748(5)	747(4)	
848(4)	847(4)	CH_2 rocking
939(3)	937(5)	
1031(4)	1031(5)	C-C stretching
1057(1)	1056(1)	
1078(2)	1075(2)	C-O stretching
1180(2)	1178(2)	CH_2 twisting
1242(3)	1241(3)	
1281(2)	1280(2)	CH_2 wagging
1301(2)	1293(2)	
1434(5)	1432(4)	CH_2 bending
1457(5)	1455(5)	
1598(0)		Overtones and combinations
1884(1)		
1966(1)		
2492(1)		
2610(1)		
2735(2)		
2880(4)	2881(4)	
2928(3)	2930(3)	C-H stretching
2962(10)	2960(10)	
3011(4)	3011(4)	
3460	3460	O-H stretching

The last column of Tables 2 gives the vibrational assignments for the 2-chloroethane molecule. These assignments have been made by a comparison of the Raman spectrum of 2-chloroethanol with the Raman spectra of 1,2-dichloroethane and 1,2-ethanediol 22.

A comparison of the Raman spectrum of 1,2 dichloroethane excited by the 2537 Å radiation with that obtained by the 4358 Å excitation shows that the relative intensities of the two Raman lines at Ca. 1305 cm^{-1} and a Ca. 1432 cm^{-1} are reversed. A comparison of the depolarization ratios of these two lines shows that in the 2537 Å excited spectrum, these two Raman lines have lower depolarization values. Similary, the Raman lines at 848 and 939 cm^{-1} have their intensities reversed in the 2537 Å excited Raman spectrum of 2−chloroethanol. The changes observed in the relative intensities, though small, are believed to be genuine. In the short wavelength ranges where these Raman lines occur, the variation of the sensitivity of the photographic plate cannot introduce any appreciable error. And, in our depolarization measurements, any error in the determination will only tend to increase the depolarization ratio to the limiting value. Thus the decrease in the depolarization ratios of the two 2537 Å excited Raman lines of 1,2-dichloroethane must also be genuine.

It is well known that in the phenomenon of the resonance Raman effect there is a many fold increase in the intensities of some of the Raman lines of the molecule, when the exciting frequency approaches the electronic absorption frequency of the molecule[23]. If the molecule has a non-degenerate ground and excited electronic states, the depolarization ratio tends to 0.50 as the exciting frequency approaches the electronic absorption frequency. This has been verified experimentally in the case of substituted nitrobenzenes by Rea[24]. However, in the case of saturated molecules, such as cyclohexane, 1, 4-dioxne, etc., there does not seem to be a consistent pattern in the intensity changes as the exciting frequency is in the resonance region[25,26]. In the latter case, however, Bernard and Dupeyrat[27] have shown that the depolarization values do tend to 0.5.

Thus we can conclude that the changes observed in the spectra of 1,2 dichloroethane and 9-chloroethanol, when the exciting frequency is increased, arise due to the resonance effect. It is quite possible, in both cases, that all the lines that do change in intensity in the 2537 Å excitation, actually increase in intensity; only, say, in the case of 1,2-dichloroethane, the Ca. 1305 cm^{-1} Raman line increases intensity much more than the line at Ca. 1432 cm^{-1}.

The Raman lines at Ca. 1305 and Ca. 1432 cm^{-1} in 1,2-dichlorethane arise from the twisting and bending vibrations of the methylene group. The 848 cm^{-1} and 939 cm^{-1} lines of 2-chlorethanol arise from the methylene rocking vibrations. It is interesting to note that in cyclohexane and also in 1,4-dioxane, it is the CH_2 group frequencies which show the resonance effects[25,26].

The electronic absorption spectrum of 1,2-dichloroethane was recorded using a Unicam absorption spectrophotometer, and it was found to be continuous below 2520 Å. This is very similar to the absorption spectrum of ethane[28], and can be connected with the fact that all the valance electrons are used up in forming the single bonds and the only non-occupied orbitals arising from the valence electrons will be antibonding ones and so will lie fairly high. In this case, therefore, it will be a good approximation to think of the continum level to be replaced by a single non-degenrate level and this might account for the changes observed in the intensities and depolarization ratios of the Raman lines on going to the resonance region. Similar explanations have been given by Albrecht[29], Tsenter and Bobovich[30] and Leite and Porto[31] to explain the resonance Raman scattering from various substances.

5. ACKNOWLEDGEMENT :

REFERENCES

1. Kholrauch, K. W. F. and Wittek, H...   *Z phys. Chem* 1940, **B47**, 55.

2. Mizushima, S.   Structure of Molecules and Internal Rotation. Academic Press, 1954.

3. Bishui, B. M.   *Indian. J. Phys.* 1948, **22**, 319.

4. Neu, J. T., Ottenberg, A and Gvinn. W. D.   *J. chem. Phys.* 1948, **16**, 1004.

5. Venkateswaralu, K. and Thyagrajan, G.   *Z. Phys.* 1959, **156**, 569.

6. Nakagawda, I. and Mizushima, S.   *J. chem. Phys.* 1953, **21**, 2195.

7. Lipscomb, W. N. Wang, F. E., May, W. R. and Lippert, E L.   *Acta crystallogr* 1961, **14**, 1100.

8. Ainsworth, J. and Karle, J.   *J chem. Phys.* 1952, **20**, 425.

9. Bernstein, H. J.   *Ibid.* 1949, **17**, 258.

10. Kohlrausch, K. W. F. and Ypsilanti, P.   *Z. phys. chem.* 1935, **B29**, 274.

11. Mizushima, S., Morino, Y. and Nakamura, S.   *Sci. Papers Inst Phys. Chem. Research* (*Tokyo*) 1940, **37**, 207.

12. Mizushima, S., Shimanouchi, T., Miyazaga, T., Abe, K. and Yasumi M.   *J. chem Phys.* 1951, **19**, 1477.

13. Bishui, B. M.   *Indian J. Phys.* 1948, **22**, 333.

14. Mazumder, M.   *Ibid.* 1955, **29**, 361.

15. Hariharan, T. A.   *J. Indian Inst. Sci.* 1954, **36 A**, 224.

16. Mazumder, M.   *Indian J. Phys.* 1959, **33**, 346.

17. Zumwalt, L. R. and Badger, R. M.   . .   *J. Am. Chem. soc.* 1940, **62**, 305.

18. Krueger, P. J. and Mettee, H. D.   .   *Can. J. Chem.* 1964, **42**, 326.

19. Yamaha, M.   . .   . .   *Bull. chem. soc. Japan*, 1956, **29**, 865.

20. Bastiansen, O.   . .   . .   *Acta. chem. scand.* 1949, **3**, 415.

21. Battacharayya, T. J.   . .   . .   *Indian J. Phys.* 1959, **33**, 498.

22 Krishnan, K. and Krishnan, R.S.   . .   *Proc. Indian Acad Sci.* 1966, **64A**, 111.

23. Behringer, J. nnd Brandmuller, J.   . .   *Z. Elektrochem.* 1956, **56**, 643.

24. Rea, D. G.   . .   . .   *J. molec. Spetrosc* 1960, **4**, 499.

25. Bernard, L. and Dupeyrat, R.   . .   *J. chim. Phys.* 1964, **61**, 1334.

26. Bernard, L.   . .   . .   *Ibid.* 1966, **63**, 641 & 772.

27. Bernard, L. and Dupeyrat, R.   . .   Compt. Rend. 1967, **265B**, 986.

28. Herzberg, C.   . .   . .   Electronic Spectra of Polyatomic Molecules. Van Nostrand Co. Inc., 1966, p. 545.

29. Albrecht, A. G.   . .   . .   *J. chem. Phys.* 1961, **34**, 1476.

30. Tsenter, M. Ya. and Bobovisch, Ya. S.   . .   Optics spectrosc. (Eng. trans.) 1964, **16**, 134 & 228.

31. Leite, R.C.C. and Porto, S.S.P.   . .   *Phys. Rev. Lett.*, 1966, **17**, 10.

A NOTE ON THE HOT WIRE METHOD FOR MEASURING HEAT CAPACITY OF GASES AT LOW PRESSURES

By K. GOVINDARAJAN AND E. S. R. GOPAL

(Department of Physics, Indian Institute of Science, Bangalore-12, India

[Received : June 3, 1970]

ABSTRACT

A hot wire cell has been devised for measuring the specific heat of gases at low preasures, in particular of vapours below their normal boiling point. The method is based on the heat loss from an electrically heated fine wire immersed in the fluid. When the pressures are greater than about 10 torr, the heat loss is proportional to the thermal conductivity of the gas, while at pressures below 1 torr, the heat loss depends on the specific heat. Thus, in a single experiment the thermal conductivity, the accommodation coefficient and the specific heat of the gas are determined. Measurements on dry air at 0°C and 40°C are reported.

1. INTRODUCTION

The hot wire cell method of evaluating the heat capacity of gases at constant volume has some advantages over the other methods. Firstly, only a small amount of gas sample is required and secondly it is possible to measure the heat capacity of gases at low pressures. The low pressure specific heat is the ideal value which can be directly compared with the spectroscopic calculations. Moreover it is possible to study the specific heat of vapours at a temparature below their normal boiling point. This feature is valuable because the region of interest in a few gases is at a temperature below their normal boiling point.

The hot wire assembly is widely used in other areas also. For example, it can be used to evaluate the thermal conductivity of gases[1] and has indeed been used for the measurement of thermal conductivity of vapours below their normal boiling point[2]. It is also used in aerodynamic studies to evaluate the velocity of flow of gases[3]. The present note is confined to a brief discussion of the specific heat measurements.

21

2. PRINCIPLE OF THE METHOD

The hot wire cell consists of an electrically heated wire of radius r_1, length L, mounted along the axis of a tube of radius r_2. The gas under investigation of molecular weight M is at a pressure p. A study of the heat transfer through gases[4,5] shows that when the mean free path λ of the gas is much smaller than r_1 the heat loss is proportional to the thermal conductivity of the gas. Molecular flow conditions occur near the wire when $\lambda >> r_1$ and over the whole tube if $\lambda >> r_2$. In the molecular flow region the heat loss from the wire at an absolute temparature T_2 to the tube at a temparature T_1 is given by

$$Q_g = 2\pi r_1 \, Lp \, \alpha \, (\beta + \tfrac{1}{2}) \, [R/(2\pi MT_1)]^{1/2} \, (T_2 - T_1) \, \ldots \quad [1]$$

In this expression, originally due to Knudsen[6], $\beta = C_v/R$ and α is the accommodation cofficient.

It is evident from Eqn. [1] that by studying the heat conductivity of the gas at low pressures it is possible to evaluate C_v, prov ded α can be obtained. Now the mechanics of gas interaction on the solid surface are quite complicated[4], and it is best to consider the a.c. as an effective parameter to be determined under the operating conditions. Therefore attempts have been made to evaluate α as well as C_v from the same arrangement.

Following the earlier suggestion of Eucken[7], Kistiakowsky and coworkers[8], assumed that the ratio of the α's for different gases approach unity at low temparatures and studied the specific heats of ethane etc, in relation to a standard gas, *viz.*, Argon. A d fferent procedure was used by Vanderkooi and de Vries[9] following the earlier arrangement of Eucken and Krome[10]. A wire and a flat ribbon are both used inside the same outer tube. The heat losses determined in the usual way will be of the form

$$Q_{\text{wire}} = A_w \, (T_2 - T_1) \, p \, (MT_2)^{-1/2} + A_{wr} \, (T_2 - T_1) \, p \, (MT_2)^{-1/2} \quad [2]$$

where A_w depends in addition to the geometrical parameters, on the a c. α_{wire} and $(\beta + \tfrac{1}{2})$. A_{wr} is a coupling term depending on α_w and α_R. A similar equation holds for the ribbon also. α_w and C_v are obtained by studying the heat loss from the wire at different settings. A third procedure has been suggested by Gregory and coworkers[11]. They have used Eqn. [1] at low pressures. At high pressures the heat loss, including the temperature jump, is written as

$$\frac{1}{Q} = \frac{ln(r_2/r_1)}{2\pi KL \, (T_2 - T_1)} + \frac{A}{p \, (T_2 - T_1)} \left[\frac{\sqrt{T_2}}{r_1} + \frac{\sqrt{T_1}}{r_2} \right]$$

where $\qquad A = \left(\frac{2\pi M}{R}\right)^{1/2} \frac{1}{2\pi L} \frac{2-\alpha}{2\alpha \, (\beta + \tfrac{1}{2})}$ [3]

It is suggested that at 'high' preasures the plot of $1/Q$ against $1/p$ is a straight line from which K and $[(2-\alpha)/\alpha(\beta+\frac{1}{2})]$ can be known. This combined with the value of $\alpha(\beta+\frac{1}{2})$ obtained in the 'low' pressure Eqn. [1] enable all the quantities to be evaluated.

3 EXPERIMENTAL ARRANGEMENT AND RESULTS

Because of the interest in the study of the specific heat of some vapours below their normal boiling point, it seemed worthwhile to investigate the possibility of using a hot wire cell for the evaluation of the specific heats. Of the procedures for estimating α the method suggested by Gregory was adopted. It allows a simpler hot wire cell than the wire and ribbon procedure. Further, the thermal conductivity may also be compared with the standard values to check the procedure, whereas, such a check on K is not possible in the more complicated wire-ribbon method of Eucken. The method used by Kistiakowsky and coworkers does not appear to be free from objections.

Two compensated hot wire cells of the type used by Gregory and coworkers[11], have been used in the present arrangement; one cell was of glass and the other of copper. Platinum wire of radius 0.00375 cm has been used for the central wire. The glass cell had a diameter of 0.830 cm and the copper tube 0 625 cm. The compensating cell had a length of ~ 5 cms which is adequate for the elimination of end conduction. The glass cell had an effective length of 15.72 cms and the copper cell 13.90 cms. The hot wires of the cell were included in the two arms of a Callendar Griffith Bridge. The temperature of the wire was measured by previously calibrating the platinum wire resistance as a functian of temperature. The current through the wire was measured by connecting a series standard resistance and using a Vernier potentiometer. The cells were placed in an ice bath or in an electronically regulated paraffin oil bath.

An all glass high vaccum apparatus was used for the purpose, A Toepler pump was used for adjusting the pressures while a manometer and a McLeod gauge were used to measure the absolute pressures. The vacuum techiques were of conventional design.

The observed heat loss I^2R should be corrected for several factors. The radiation loss is obtained by measuring the heat loss in the highest vaccum $\sim 10^{-6}$ torr. Convection effects under the conditions of the experiment are negligible if the hot wire cell is mounted vertically. Finally, the end losses are eliminated by employing, as mentioned above, a compensated pair of cells.

The two hot wire cells were tested with pure dry air at the two temperatures of 0° and 40°C. Figure (1) shows performance of the glass cell at $t_2=0$°C and Figure (2) that of the copper cell at ~ 40°C. The plots are quite linear and the values of the various quantities obtained from the figures are :
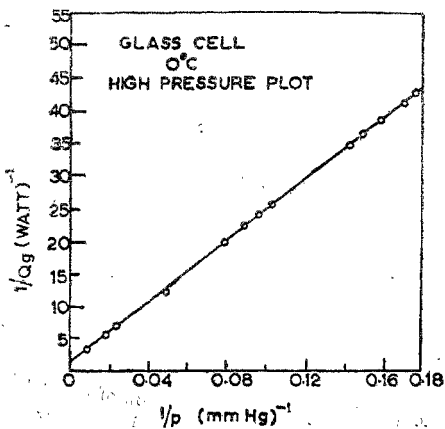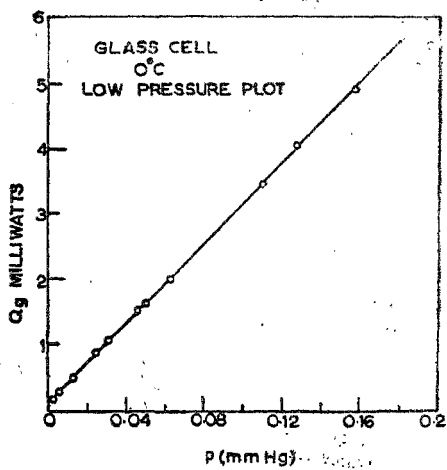
Fig. 1a

Fig. 1b

Behaviour of the glass cell at an ambient temperature of 40°C
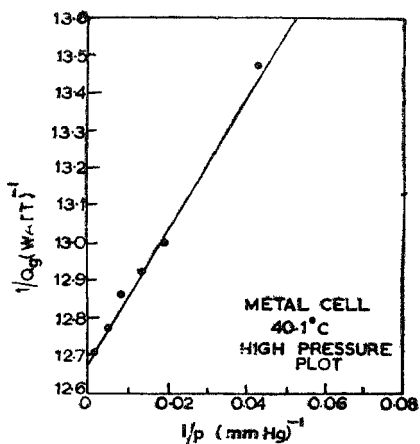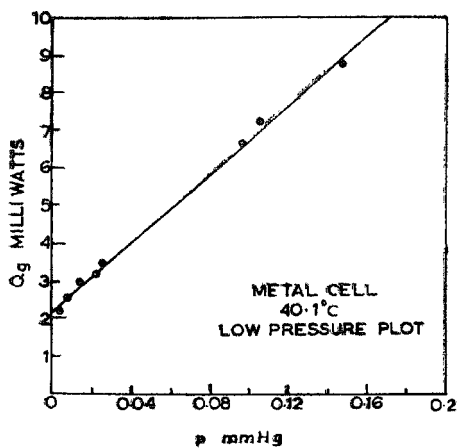(a) high pressure region.   (b) low pressure region.

FIG. II a

FIG. II b

Behaviour of the metal cell at an ambient temperature of 40°C.
(*a*) high pressure region (*b*) low pressure region.

At $0°C$: $K = 5.8_1 \; x \; 10^{-5}$ cal/cm deg. sec ; $C_v/R = 2\,5_0$; $\alpha = 0.48_4$

At $40°C$: $K = 6.2_9 \; x \; 10^{-5}$ cal/cm deg. sec ; $C_v/R = 2.4_9$; $\alpha = 0.55_8$

The value of the specific heat is as expected very close to that of an ideal diatomic gas $C_s = (5/2)R$. The values of K compare well with the values summarized for example, by Dickins[12]; K at $0°C = 5.84 \; x \; 10^{-5}$ can/cm sec. deg. and K at $40°C = 6.5_1 \; x \; 10^{-5}$. The value of the a.c. are not comparable for they refer to the specific experimental conditions. They are of the same order as those for fully absorbed surfaces. It is only for very clean surfaces in much higher temperatures that smaller values of α are obtained.

In conclusion, Gregory's method of evaluating the a.c. appears to be suited for using the hot wire cell to evaluate the specific heat vapours and that the present arrangement is suitable for studying gases under various conditions.

4.   ACKNOWLEDGEMENT

REFERENCES

1. Westenberg, A. A.   .. 'Critical Survey of Methods for measurement of dilute gas transport properties 'in Advances in Heat Transfer, Vol. III, p. 253, Eds. Irvine Jr. T. F. and Hartnett, J. P., Academic Prsss, N. Y, 1966.

2. Vines, R. G.   ..   .. *Aust. J. Chem.* 1953, 6. 1.

3. Bradshaw, P.   ..   .. Experimental Fluid Mechanics, Pergamon Press, 1964, pp. 90-99.

4. Devienne, F. M.   ..   .. 'Low density Heat Transfer', Ch. III in Advances in Heat Transfer, Vol. II, Eds. Hartnett, J. P. and Irvine Jr. T. F., Academic Press, N. Y., 1965.

5. Kennard, E. H.   ..   .. Kinetic Theory of Gases,- McGraw Hill, N. Y., 1938. pp. 312-315.

6. Knudsen, M   ..   .. *Annln. Phys.*, 1911. 34, 593.

7. Eucken, A. and Weigert, K.   .. *Zeits Phys. Chem.* 1933, B25, 265.

8. Eucken, A. and Franck, E. U.   .. *Z. Electro chem*, 1948, 52, 195.

8. Kistiakowsky, G. B. and Nazmi, F.   .. *J. chem. Phys.* 1938, 6, 18.

Kistiakowsky, G. B., Lacher, J. R .. *J. chem. Phys.* 1939, 7, 289.
and Stitt F. J.

Kistiakowsky, G. B. Lacher, J. R .., *Ibid.* 1940, 8, 970.
and Ransom, W. W.

9. Vanderkooi, N. and de Vries, T. .. *J. phys. Chem.* 1956, 60, 636.

0. Eucken, A. and Krome, H. .. *Z. phys. Chem.* 1933, B.45, 144.

1, Gregory, H. S. .. .. *Phil. Mag.* 1936, 22(7), 257,

Gregory. H. S. and Stephen, .. *Nature* 1937, 139, 28.
R. W. B.

Gregory H, S. and Sherif, I. I. .. *Ibid.* 1951, 168, 1123.

Sherif, I. I. .. .. Nuovo Cim 1956, 3 (Ser. X), 6.

2. Dickins, B. G. .. .. *Proc. R. Soc.* 1934, A143, 517.

BUCKLING COEFFICIENTS OF VARIOUSLY SUPPORTED SKEW PLATES[*]

By M. S. S. PRABHU AND S. DURVASULA

(Department of Aeronautical Engineering, Indian Institute of Science, Bangalore-12, India)

[Received : October 5, 1970]

ABSTRACT

The buckling problems of skew plates with different edge support conditions involving simple support and clamping are considered. The in-plane stresses are represented in terms of oblique components. Rayleigh-Ritz method is used employing a double series of functions appropriate to the combination of the edge conditions. Numerical results are presented for several combinations of side ratio, skew angle and different loadings.

1. INTRODUCTION

Skew plates have their application in construction of modern swept wing aircraft. The buckling problems of plates of such shape are of interest to the designer. The boundary conditions obtaining on individual panels are more nearly in the nature of elastic restraint against rotation. Analytical treatment of this boundary condition, however, is somewhat tedious and it is even more so for skew geometry. Consequently, the ideal boundary conditions of simple support or clamping are usually analysed.

While considerable literature is available on buckling of rectangular plates under different loadings (Refs. 1,2,3) yet buckling coefficients for the many different combinations of edge conditions involving simple support and clamping are not fully available.

The problem of buckling of clamped skew plate under uniform compression was studied by Guest[4]. He applied the Lagrangian Multiplier method to get upper bounds and rather doubtful lower bounds (see Ref. 5). In another paper[6] he considered the buckling of clamped rhombic plate under bending and compression. Using Rayleigh-Ritz method, Wittrick studied the buckling problem of clamped skew plates under uniform compression[7]

---

and pure shear[8]. He used Iguchi functions and found that the convergence was slow particularly in the case of positive shear. Hasegawa[9] calculated the buckling coefficients of clamped rhombic plate under the action of pure shear by the Rayleigh-Ritz method using polynomials. Hamada[10] used Lagrangian multiplier method to study the problem of buckling of clamped skew plates under the action of uniform compression and oblique shear. Matrix methods have also been applied[11] to find the buckling coefficients of the parallelogramic plates under the action of shear and compression. Durvasula[5] investigated the above problem using Galerkin Method and expressing the deflection as a series of beam characteristic functions. The buckling coefficients have been calculated when direct and shear forces are acting either individually or in combination. Ashton[12] also investigated the problem using beam characteristic functions and Rayleigh-Ritz method. Mansfield[13] obtained a rough estimate for the buckling coefficient under uniform compression.

Yoshimura and Iwata[14] obtained the buckling coefficients for the simply supported skew plates under oblique shear and compression. Durvasula[15] solved the problem using double Fourier sine series and Rayleigh-Ritz method with in-plane stresses expressed in terms of orthogonal components. Durvasula and Nair[16] have also considered the buckling problem of simply supported skew plates with in-plane stresses expressed in terms of oblique components. Extensive numerical results were presented for various combinations of skew angles and side ratios. Interaction curves have also been given.

In this paper, the buckling problems of skew plates supported differently on different edges are considered. The support conditions considered are confined to different combinations of simple support and clamping on the four edges. The in-plane stresses are represented in terms of oblique components. Rayleigh-Ritz method has been used with the buckling mode expressed as a double series of beam characteristic functions appropriate to the combinations of the edge conditions in each case. Numerical calculations have been made to obtain the buckling coefficients mainly when each of the stress components is present individually for different combinations of side ratio, skew angle and boundary condition and for a few combined loadings. Convergence has been examined in a few typical cases and is found to be satisfactory.

Notation:

a, b	dimensions of the plate
C_{rs}	Coefficient in the series expansion of deflection
D	flexural rigidity of the plate. $[Eh^3/12(1-\nu^2)]$
E	Young's Modulus of the material of the plate
$G, H^{(1)}, H^{(2)}, H^{(3)}$	Matrices defined in Equation [15]
G_1	matrix defined in Equation [18]
h	plate thickness
$I_{mr}^{pq} \; J_{ns}^{pq}$	integrals defined in Equation [14]
M	maximum value of indices m, r
N	maximum value of indices n, s
N_x, N_y, N_{xy}	midplane forces (oblique components), $h\,\sigma_x, \; h\,\sigma_y, \; h\,\sigma_{xy}$ respectively
m, n, r, s	integers
M_n	normal bending moment
$\bar{R}_x, \; \bar{R}_y, \; \bar{R}_{xy}$	non-dimensional midplane force parameters $\sigma_x\, b^2 h/\pi^2 D, \; \sigma_y\, b^2 h/\pi^2 D, \; \sigma_{xy}\, b^2 h/\pi^2 D$ respectively.
$\bar{R}_y^*, \; \bar{R}_y^*, \; \bar{R}_{xy}^*$	non-dimensional midplane force parameters $(\sigma_x a^2 h \cos^3\psi)/D, \; (\sigma_y\, a^2\, h \cos^3\psi)/D, \; (\sigma_{xy}\, a^2 h \cos^3\psi)/D,$ respectively.
U	strain energy of the plate
V	potential energy of the middle surface forces.
$W(\xi, \eta)$	deflection of the plate
$X_m(\xi), Y_n(\eta)$	beam characteristic functions
x, y, z	oblique coordinate system defind in Fig. 1
ξ, η	non-dimensional coordinates, x/a and y/b respectively
ν	Poisson's ratio
$\sigma_x, \sigma_y, \sigma_{xy}$	oblique stress components defined in Fig. 1
∇^2	Skew differential operator $= \mathrm{Sec}^2\,\psi\,[\partial^2/\partial x^2 - 2\,\mathrm{Sin}\,\psi(\partial^2/\partial x\,\partial y) + (\partial^2/\partial y^2)]$
∇_1^2	Non-dimensional skew differential operator $= \mathrm{Sec}^2\,\psi\,[\partial^2/\partial\xi^2 - 2\lambda\,\mathrm{Sin}\,\psi\,(\partial^2/\partial\xi\partial\eta) + \lambda^2\,(\partial^2/\partial\eta^2)]$
ψ	Skew angle as defined in Fig. 1
λ	a/b. side ratio

2.   FORMULATION OF THE PROBLEM

A sketch of the skew plate is shown in Fig. 1 along with the in-plane stresses represented in terms of oblique components. Since the geometry of the plate is oblique in nature, the use of oblique stress components instead of usual orthogonal components is preferable. In terms of oblique components, expressions for the strain energy of the plate and the potential energy of the middle surface forces are simpler and the structure of these expressions is similar to those in the case of rectangular plates with orthogonal stress components. The plate is assumed to be thin, uniform and isotropic.

Using the classical, small deflection thin plate theory, the differential equation for the deflection of a plate of constant thickness under the action of middle surface forces is given by [17],

$$D \cos \psi \, \nabla^4 W = - h \, [\sigma_x \, (\partial^2 W / \partial x^2) + 2\sigma_{xy} \, (\partial^2 W / \partial x \, \partial y) + \sigma_y \, (\partial^2 W / \partial y^2)] \quad [1]$$

In terms of oblique coordinates, the boundaries of the skew plate are given by,

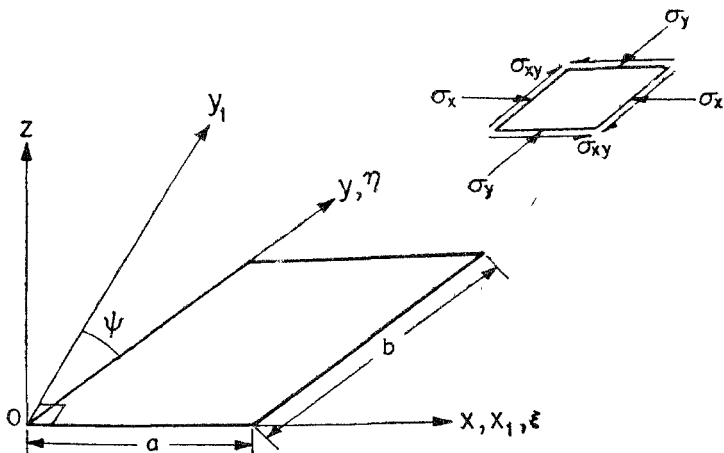$$x = 0, \; x = a \; ; \quad y = 0, \; y = b. \tag{2}$$

FIG. 1

Sketch of the Skew Plate and the in-plane Stress System (Oblique Components)

The boundary conditions considered are confined to combinations of simple support and clamping. These conditions are stated as follows :

Simple support : $W = M_n = 0$ [3a]

or alternatively for a polygonal plate[18]

$$W = \nabla^2 \ W = 0$$ [3b]

Clamping : $W = [(\partial W/\partial n)] = 0$ [3c]

If the edge $x = a$, for example, is simply supported, then boundary condition, Eq (3b) takes the form,

$$W = [(\partial^2/\partial x^2) - 2 \sin \psi (\partial^2/\partial x \ \partial y)] \ W = 0$$ [4]

If the edge $y = b$ is clamped, then the boundary condition Eq. (3c) takes the form[4].

$$W = [(\partial W/\partial y)] = 0$$ [5]

In this paper, the buckling problems with different edges supported differently are considered.   An approximate solution of the buckling problem stated by Equation [1], together with boundary conditions such as given by Equations [3b, 3c] appropriate to each edge is solved using the Rayleigh-Ritz method.

Non-dimensional coordinates ξ and η are defined as follows :

$$\xi = x/a ; \ \eta = y/b$$ [6

For the stress system shown in Fig. 1. the expressions for the strain energy of the plate and the potential energy of the middle surface forces are given respectively by [17],

$$U = \frac{D \cos \psi \ b}{2a^3} \int_0^1 \int_0^1 \ [\ (\nabla_1{}^2 W)^2 - 2\lambda^2(1-\nu) \ \sec^2\psi \left\{ W_{,\xi\xi} \ W_{,\eta\eta} - W_{,\xi\eta}^2 \right\} \ ]d\xi \ d\eta \ [7]$$

$$V = \frac{hb}{2a} \int_0^1 \int_0^1 \ (\sigma_x W^2{}_{,\xi} + 2\lambda \ \sigma_{xy} W_{,\xi} W_{,\eta} + \lambda^2 \sigma_y W_{,\eta}^2) \ d\xi \ d\eta$$ [8]

For polygonal boundaries with $W = 0$ along the edges the expression for U reduces to [17,4]

$$U = \frac{D \cos \psi \ b}{2a^3} \int_0^1 \int_0^1 \ (\nabla_1{}^2 W)^2 d \xi \ d\eta$$ [9]

The deflection W is expressed as a double series in terms of " admissible functions ", *i.e.*, functions which satisfy the geometric boundary conditions. Beam characteristic functions which have been widely used in the literature have been made use of in the present analysis. The series is written as,

$$W(\xi, \eta) = \sum_{m=1}^{M} \sum_{n=1}^{N} C_{mn} X_m(\xi) Y_n(\eta) \qquad [10]$$

where $X_m(\xi)$, $Y_n(\eta)$ are the beam characteristic functions which are appropriate to the particular boundary conditions specified. For example, if the edges $\xi = 0$ and $\xi = 1$ are both clamped, the clamped-clamped beam functions are taken for $X_m(\xi)$. Similarly, if the edge $\eta = 0$ is clamped and edge $\eta = 1$ is simply supported, the clamped-simply supported beam functions are taken for $Y_n(\eta)$.

Substituting the expressions for W in Eqs. [8] and [9], we get,

$$U = \frac{D \sec^3 \psi\, b}{2a3} \int_0^1 \int_0^1 \sum_{m=1}^{M} \sum_{n=1}^{N} \sum_{r=1}^{M} \sum_{s=1}^{N} C_{mn} C_{rs} \left[X_m'' Y_n - 2 \lambda \sin \psi\, X_m' Y_n' \right.$$

$$\left. + \lambda^2 X_m Y_n'' \right] \left[X_r'' Y_s - 2 \lambda \sin \psi\, X_r' Y_s' + \lambda^2 X_r Y_s'' \right] d\xi\, d\eta \qquad [11]$$

$$V = - \frac{hb}{2a} \int_0^1 \int_0^1 \sum_{m=1}^{M} \sum_{n=1}^{N} \sum_{r=1}^{M} \sum_{s=1}^{N} C_{mn} C_{rs} \left[\sigma_x X_m' X_r' Y_n Y_s \right.$$

$$\left. + 2\lambda\, \sigma_{xy} X_m' X_r Y_n Y_s' + \lambda^2 \sigma_y X_m Y_n' X_r Y_s' \right] d\xi\, d\eta \qquad [12]$$

The coefficient C_{mn} are determined from the condition[19]

$$[(\partial/\partial C_{mn})](U+V) = 0 \text{ for } m=1, 2. \ldots M, \text{ for } n=1, 2, \ldots N \qquad [13]$$

The integrals involving the functions $X_m(\xi)$, $Y_n(\eta)$ and their derivatives are defined as follows :

$$I_{mr}^{pq} = \int_0^1 X_m^p(\xi) X_r^q(\xi)\, d\xi \; ; \; J_{ns}^{pq} = \int_0^1 Y_n^p(\eta) Y_s^q(\eta)\, d\eta \qquad [14]$$

where p and q represent the order of the derivative. The formulae for such integrals were given by Felgar[20] and the numerical values of some of these integrals are given in Ref. 21. Using the expressions for U and V from Eqs. [11] and [12] in Eq. [13], and using the relationships between the integrals, we get, finally, a set of linear simultaneous algebraic equations in C_{rs} which can be expressed in the form of a matrix equation as follows :

$$[G] \{C_{rs}\} = \bar{R}_x^* [H^{(1)}] \{C_{rs}\} + \bar{R}_y^* [H^{(2)}] \{C_{rs}\} + \bar{R}_{xy}^* [H^{(3)}] \{C_{rs}\} \qquad [15]$$

where

$$G_{mnrs} = \{I_{mr}^{22} J_{ns}^{00} + \lambda^4 (I_{mr}^{00} J_{ns}^{22}) - 2\lambda \sin \psi [I_{mr}^{21} J_{ns}^{01} + I_{mr}^{12} J_{ns}^{10} + \lambda^2 (I_{mr}^{10} J_{ns}^{12}$$

$$I_{mr}^{01} J_{ns}^{21})] + 2\lambda^2 (1 + 2 \sin^2 \psi) \ I_{mr}^{11} J_{ns}^{11}\} \tag{16}$$

$$H_{mnrs}^{(1)} = I_{mr}^{11} J_{ns}^{00}; \ \ H_{mnrs}^{(2)} = \lambda^2 I_{mr}^{00} J_{ns}^{11}; \ \ H_{mnrs}^{(3)} = 2\lambda I_{mr}^{01} J_{ns}^{01} \tag{17}$$

This is an algebraic eigenvalue problem. To get the buckling loads when N_x, N_y, N_{xy} are present individually or in combination, numerical values are given to two of the three parameters $\bar{R}_x^*$, $\bar{R}_y^*$, $\bar{R}_{xy}^*$ and the third is treated as the eigenvalue. For example, if we wish to determine the buckling parameter $\bar{R}_x^*$, when both N_{xy} and N_y are acting, we assign appropriate numerical values to $\bar{R}_y^*$ and $\bar{R}_{xy}^*$ and obtain the G_1 matrix as,

$$[G_1] = [G] - \bar{R}_x^* \ [H^{(2)}] - \bar{R}_{xy}^* [H^{(3)}] \tag{18}$$

Equation [15] then reduces to

$$[G_1] \ \{C_{rs}\} = \bar{R}_x^* \ [H^{(1)}] \ \{C_{rs}\} \tag{19}$$

which can be written as,

$$[G_1^{-1}] \ [H^{(1)}] \ \{C_{rs}\} = (1/\bar{R}_x^*) \ \{C_{rs}\} \tag{20}$$

For combinations of boundary conditions symmetric about the diagonals, the Equation [15] splits into two cases : $(m+n)$ Even and $(r+s)$ Even ; $(m+n)$ Odd and $(r+s)$ Odd. The Even case corresponds to skew symmetric case consisting of modes which are doubly symmetric and doubly antisymmetric. The Odd case corresponds to skew antisymmetric case consisting of modes which are symmetric-antisymmetric and antisymmetric-symmetric. This splitting reduces the order of the matrix to be considered for finding out the eigenvalues and eigenvectors. If $K(=M \times N)$ is the order of the original matrix, then the size of matrix for the even case will be $(K+1)/2$ if K is Odd and $K/2$ if K is Even ; and the matrix size for the Odd case will be $(K-1)/2$ if K is Odd and $K/2$ if K is Even.

The eigenvalue $\bar{R}_x^*$ can now be determined by using any of the standard methods. The two groups give two eigenvalues ; the lower of the two is the desired critical buckling load. Similar procedure can be adopted to determine the eigenvalues for other combinations of loads.

For cases where such symmetry of boundary conditions about the diagonals is not present, this splitting is not possible and the full matrix of order K will have to be handled.
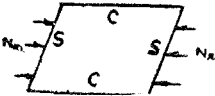
3. NUMERICAL CALCULATIONS

Numerical calculations have been made for different combinations of side ratio a/b and skew angle ψ for different edge conditions. Since the accuracy of the eigenvalues decreases with increasing value of ψ, more terms have been considered for higher skew angles. For skew $\psi \leqslant 30°$, the number of terms considered is upto $M = N = 6$ except in the case of N_x acting alone in which case the number of terms considered is upto $M = N = 5$ only. For $\psi = 45°$, terms upto $M = N = 8$ have been taken. The calculations made are mainly for N_x, N_y or N_{xy} acting alone, though the combined action of N_x, N_y and N_{xy} has also been studied in a typical case. Convergence study has been made for one representative boundary condition when N_x and N_{xy} are each acting alone. The numerical values are presented in Tables 1 to 5.

4. RESULTS AND DISCUSSION

Results of the convergence study for one typical boundary condition in the case of a rhombic plate with $\psi = 30°$ are given in Tables 1 and 2. **Table 1**

TABLE 1

Convergence Study : N_x Acting Alone

$$\lambda = a/b = 1, \quad \psi = 30°$$

Boundary conditions	M	N	Matrix size	Eigen value* $\bar{R}_x$
	2	2	2	12.89
	3	3	4	10.41
	4	4	8	9.663
	5	5	12	9.510
	6	6	18	9.391
	7	7	24	9.352
	8	8	32	9.302
	9	9	41	9.282

*These values are all from $(M+N)$ ODD case; $(M+N)$ EVEN case gives higher values.

TABLE 2

Convergence Study : N_{xy} Acting Alone

$$\lambda = a/b = 1 \; ; \; \psi = 30°$$

Positive Shear   Negative Shear

Boundary conditions	M	N	Matrix size	Eigenvalue* $\bar{R}_{xy}$	
				Positive	Negative
	2	2	2	18.69	-37.78
	4	4	8	8.550	-34.84
	6	6	18	8.314	-34.79
	8	8	32	8.233	-34.75

* These values are all from $(M+N)$ EVEN case. $(M+N)$ ODD case gives higher values.

gives the eigenvalues when N_x alone is acting. Table 2 gives the eigenvalues when N_{xy} alone is acting. It can be seen from Table 1 that the convergence of the eigenvalues is satisfactory. When N_{xy} is acting the convergence is equally good for positive as well as negative shears (Table 2).

The buckling coefficient $\bar{R}_x$ has been obtained for seven different combinations of boundary conditions for a/b equal to 0.5 and 1 and ψ equal to $0°$, $15°$, $30°$ and $45°$. These are given in Table 3 along with results, where available, for comparison. Similarly for the same combinations of a/b and ψ and different boundary conditions, the buckling coefficients $\bar{R}_{xy}$ and $\bar{R}_y$ are given in Tables 4 and 5 respectively. In Table 6, the buckling coefficient $\bar{R}_x$ in the presence of inplane forces N_{xy} and N_y is given for a rhombic plate with skew angle $\psi = 30°$ for a typical boundary condition. From Table 3 it may be seen that even for rectangular plates complete results are not available. For skew plates with different combinations of boundary conditions no results could be found in the literature for comparison. The results of the present paper are in good agreement with the available results.

The buckling coefficient $\bar{R}_x = N_x b^2/\pi^2 D$ increases with the skew angle, as may be expected, and decreases with a/b. Also the values in Table 3 are indicative of the relative stiffnesses of the plates with different combinations of boundary conditions for a given combination of a/b and ψ. One can expect that for a given a/b and ψ the buckling coefficient for a plate with combination of clamped edge conditions (C) and simply supported edge conditions (S) should be in between the values for a plate of the same geometry with all edges clamped and all edges simply supported; this is borne out by the present results except for $a/b = 0.5$, for the obvious reason that in this case the order of approximation is lower ($M = N = 4$).

In Table 4, the buckling coefficients under positive and negative shears are given along with some available results for rectangular plates. The agreement between the present results and available results is quite good. As in the case of $\bar{R}_x$, the buckling coefficient $\bar{R}_{xy}$ decreases with a/b and increases with ψ. The buckling coefficient $\bar{R}_{xy}$ for positive shear is less than that for negative shear irrespective of a/b, ψ and boundary condition. This is in conformity with the observation made previously[16].

In Table 5, the critical buckling coefficient $\bar{R}_y$ is given for differnt combination of a/b, and boundary condition. The buckling coefficient $\bar{R}_y$, for a certain a/b and ψ and boundary condition, can be related to $\bar{R}_x$ for corresponding b/a and ψ, for appropriate boundary conditions. For example for $\psi = 0°$, $a/b = 0.5$ for boundary conditions (Case 6) $\bar{R}_y$ can be interpreted as the value of $\bar{R}_x$ for $\psi = 0$ and $a/b = 2$ for boundary conditions (Case 5). For this to be valid, the corresponding orders of approximations have to be necessarily equal; the slight difference that is seen in the case of $\bar{R}_x$ for $a/b = 1$ (Table 3) and $\bar{R}_y$ for $a/b = 1$ (Table 5) is because the corresponding orders are not the same.

In Table 6, the critical buckling coefficient $\bar{R}_x$ in the presence of different combinations of inplane forces N_{xy} und N_y is given for a typical combination of a/b, ψ and boundary condition. The computer programme, however, can generate data for other combinations of a/b, ψ and any combined loading and is thus capable of generating interaction surfaces which should prove useful in design.

TABLE 3

Buckling Coefficient $\overline{R}_x$ For Different Edge Conditions

Case	Boundary Condition	$\psi = 0°$ $a/b=0.5$	1	$\psi = 15°$ 0.5	1	$\psi = 30°$ 0.5	1	$\psi = 45°$ 0.5	1
1*	(S S S)	6.25	4.00	6.84	4.32	9.17	5.55	15.7	8.40
2	(C S S)	10.4	4.85	11.3	5.21	14.9	6.51	24.1	9.22
3	(S C S)	6.86 $(6.85)^a$	5.74 $(5.74)^a$	7.45	6.16	9.68	7.62	15.2	10.2
4	(C S S)	10.9	6.22	11.8	6.55	15.3	7.87	24.3	10.4
5	(C S C)	18.2	6.75 $(6.74)^a$	19.8	7.14	25.6	8.51	38.0	11.3
6	(S C S)	7.70 $(7.69)^a$	7.70 $(7.69)^a$	8.30	8.10	10.5	9.51	15.9	12.0
7	(C S C)	18.7	8.07	20.2	8.47	25.9	9.83	38.3	12.5
8	(C C S)	11.6	8.09	12.6	8.58	16.0	10.2	24.8	13.1
9	(C C C)	19.4	10.1	20.8	10.5	26.3	11.8	38.8	14.3

(a) Ref. 18 (Levy's Method)   (c) Ref. 2 (Taken from the graph)
   * The eigenvalues corresponding to this case are taken from Ref. 16
(note that for $a/b=0.5$, M=N=4 and for $a/b=1$, M=N=6.)
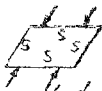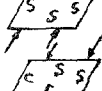
TABLE 4

 Positive Shear   Negative Shear
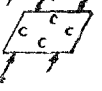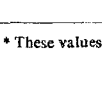
Buckling Coefficient $\overline{R}_{xy}$ For Different Edge conditions

Case	Boundary Conditions	$\psi=0°$ $a/b=0.5$	$\psi=0°$ 1	$\psi=15°$ 0.5	$\psi=15°$ 1	$\psi=30°$ 0.5	$\psi=30°$ 1	$\psi=45°$ 0.5	$\psi=45°$ 1
1*	S S S		±9.40	7.15 / −14.71		6.52 / −27.4			
2	S C / S	±26.5 (26.88)[a]	±10.7 (10.98)[a]	20.3 / −40.3	8.05 / −16.7	17.8 / −72.5	7.09 / −30.6	18.0 / −163	7.26 / −70.0
3	C S / S	±32.4 (33.72)[a]	±10.7 (10.98)[a]	24.6 / −49.6	8.05 / −16.7	21.7 / −89.5	7.09 / −30.6	22.2 / −199	7.06 / −70.9
4	C / C S	33.1 / −33.2	11.7 / −11.9	24.9 / −50.9	8.79 / −18.4	21.9 / −90.7	7.63 / −33.6	22.4 / −201	7.66 / −76.2
5	S / S C	±40.1 (40.16)[a]	±12.6 (12.6)[a,b]	30.8 / −60.3	9.52 / −19.3	26.7 / −107	8.31 / −34.8	26.8 / −238	8.37 / −78.5
6	S C / C	±26.9 (2.688)[a]	±12.6 (12.6)[a,b]	20.5 / −41.0	9.52 / −19.3	18.2 / −73.9	8.31 / −34.8	18.3 / −166	8.37 / −78.5
7	C S C	±40.5	±13.4	30.9 / −61.1	10.1 / −20.5	27.0 / −109	8.75 / −37.0	26.9 / −242	8.71 / −83.1
8	C / C S	±34.2	±13.4	25.7 / −51.8	10.1 / −20.5	22.3 / −91.7	8.75 / −37.0	22.5 / −203	8.71 / −83.1
9	C C / C	±41.0	±14.7	31.2 / −62.2	11.1 / −22.3	27.2 / −111	9.50 / −40.0	27.1 / −246	9.35 / −89.3

* Eigenvalues for this case are taken from Ref. 16 ; a) Ref. 23, b) Ref. 3.

M. S. S. Prabhu and S. Durvasula

Table 5

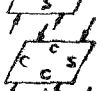Buckling Coefficient $\bar{R}_y$ For Different Edge Condition
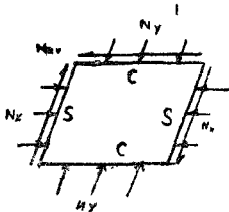
Case	Boundary Conditions	$\psi=0°$		$\psi=15°$		$\psi=30°$		$\psi=45°$	
		$a/b=0.5$	1	0.5	1	0.5	1	0.5	1
1*			4.00		4.32		5.55		8.40
2		22.4	5.74	23.5	6.15	27.3	7.56	34.5	10.2
3		17.0	4.85	18.0	5.19	21.5	6.46	28.0	9.22
4		22.7	6.22	26.1	6.53	27.8	7.80	34.8	10.4
5		27.9	7.70	29.4	8.08	34.2	9.39	42.3	12.0
6		19.4	6.75	20.2	7.13	23.0	8.47	28.5	11.3
7		28.9	8.09	30.3	8.56	34.6	10.1	42.8	13.1
8		24.9	8.07	25.9	8.46	29.3	9.78	36.0	12.5
9		31.6	10.1	32.5	10.5	35.8	11.8	43.1	14.3

* These values are taken from Ref. 16.

TABLE 6

Buckling Coefficient $\bar{R}_x$ under combined Loading for SCSC case

$a/b = 1$; $\psi = 30°$; $N_y = \alpha N_x$; $N_{xy} = \beta N_x$

Boundary conditions	$\dot{\alpha}$	β	$\bar{R}$ critical
	0	0	9.51
	0	0.5	6.66
	0	1 0	4.93
	0.5	0	6.77
	0.5	0.5	5.08
	0.5	1.0	3.96
	1.0	0	4.87
	1.0	0.5	3.96
	1·0	1.0	3.27

5. CONCLUSIONS

The buckling problems of skew plates with different edge conditions involving simple support and clamping are considered with the in-plane stresses represented in terms of oblique components. Rayleigh-Ritz method is used expressing the deflection in terms of beam characreristic functions in oblique coordinates. Buckling coefficients have been obtained mainly when the in-plane forces N_x, N_{xy}, N_y are acting individually for different combinations of a/b, ψ and boundary condition and for a few combined loadings. For buckling under shear loading (oblique components) two critical values exist ; the positive shear (acting in a way so as to reduce the skew angle) is found to be less than the negative shear in magnitude for all the plate configurations and boundary conditions considered. The computer programme developed can be used for generating extensive design data in the form of buckling charts and interaction surfaces for buckling under combined loading.

6. ACKNOWLEDGEMENTS

7. REFERENCES

1.	Anonymus	Data Sheets, Stressed Skin Structures, R Aero. Soc., 2.
2.	Gerard, G. and Becker, H.	Handbook of Structural Stability, 1957, NACA TN 3781.
3.	Leggett, D. M. A.	*A. R. C. Tech. Rep.* 1941. R & M No. 1991.
4	Guest J.	Rep. SM. 172, Aero. Res. Lab., Melbourne, 1951.
5.	Durvasula, S.	Rep, No AE 2458, Dept. Aero. Engg., I.I Sc., 1959.
6.	Guest, J.	Rep. SM. 227, Aero. Res. Lab, Melbourne, 1955.
7.	Wittrick, W. H.	*Aero, Quart.*, 1953, 4, 151.
8.	———	*Ibid*, 1954, 5. 39.
9.	Hasegawa, M.	*J. Aero. Soc.*, 1954, 21, 720.
10.	Hamada, M.	*Bull. Jap. Soc. Mech Engrs.*, 1959, 2, 520.
11.	Argyris, J. H.	Matrix Methods in Structural Mechanics, (Proceedings of the Conference held at Wright-Patterson Air Force Base), 1966, 11.
12.	Ashton, J. E.	*J. Appl. Mech., Trans. ASME*, 1969, E 91, 139.
13.	Mansfield, E. H.	*Aircraft Eng.*, 1952, 24, 48.
14.	Yoshimura, Y. and Iwata	*J. Appl. Mech.*, 1963, 30, 363.
15.	Durvasula, S.	Paper presented at the 17th Annual General Meeting of the Aero. Soc. India. held at Bangalore, 1965.
16.	Durvasula, S and Nair, E. S.	*Israel J. Tech.*, 1969, 7. 303.
17.	Morley, L. S. D.	Skew Plates and Structures, Pergamon Press, 1963.
18.	Timoshenko, S. and Gere. J. M.	Theory of Elastic Stability, McGraw Hill Book Co., 1952.
19.	Bleich, F.	Buckling Strength of Metal Structures, McGraw Hill Book Co , 1952.
20.	Felgar, R. P.	Univ. Texas, Bur Eng. Res. Circular No. 14, 1950
21.	Durvasula, S. Bhatia, P. and Nair, P. S.	Rep No. AE 220, S, Dept. Aero. Engg., I.I.Sc., 1969.
22.	Flugge, W. (Ed.)	Handbook of Engineering Mechanics, McGraw Hill Book Co., 1962, 44-35.
23.	Chilver, A H. (Ed.)	Thin Walled Structuress, Chatto and Windus, 1967, 251.

COMPUTATION OF MATRIX INVERSE BY A POWER SERIES METHOD

By SYAMAL KUMAR SEN

(Central Instruments and Services Laboratory, Indian Institute of Science, Bangalore-12, India)

ABSTRACT

Discussed here is a computational procedure for the inverse of a square matrix by using a power series method[1] that first transforms a matrix into one whose inverse can be equated to a convergent power series and then finds the inverse by a procedure reverse to the aforesaid one that rests on only matrix addition, subtraction and multiplication but no inversion.

1. DISCUSSION

Cofactor method or triangular decomposition methods[2] obtain the inverse of a matrix directly. Almost all these methods are variants of the Gauss's method and they are very susceptible for the ill-conditioned (with respect to inverse) matrices. A suggested method of Maulik[3], since it is independent of the the spacing of the characteristic roots of the matrix and since it does not demand division except at the last step and avoids redundant multiplications, is much more rapid as also more accurate than the co-factor method. This novel method, though not a variant of Gaussian type, can be applied only to matrices of order 2^n, n being a positive integer. The present method cannot be classified in either of the aforesaid two categories. The method, in the first phase, converts any arbitrary square matrix into one whose inverse is replaced by a convergent power series. This inversion then allows the method, in the second phase, to obtain the inverse of the original matrix, that requires matrix addition, subtraction and multiplication but no inversion.

The general form for the conversion of the original matrix $A (= a_{ij})$ of order n into one whose inverse is approximated by a convergent power series is

$$A_{p-1} = A_p + B_p, \quad p = 1, 2, \ldots, n \qquad [1.1]$$

where A_p is identically equal to A_{p-1} excepting the $p-th$ diagonal element of A_{p-1} and $A_0 \equiv A$ and

$$B_p = u_p v_p \qquad [1.2]$$

where the column vector u_p and row vector v_p are

$$u_p = \begin{Bmatrix} 0 \\ 0 \\ \vdots \\ a_{pp} - a'_{pp} \\ 0 \\ \vdots \\ 0 \end{Bmatrix}, \quad v_p = [0 \quad 0 \quad .. \quad 1 \quad 0 \quad . \quad 0] \qquad [1.3]$$

a'_{pp} is the p-th diagonal element of A_p and

$$a'_{pp} > n \left(\sum_{q=1}^{n}{}' a_{pq} \right), \quad q \neq p \qquad [1.4]$$

$a_{pp} - a'_{pp}$ in u_p and 1 in v_p are the $p-th$ elements of u_p and v_p, respectively. We take a'_{pp} such that A_n possesses only non-zero diagonal elements. This is very easy since we are at liberty to choose a'_{pp} satisfying condition [1.4]. The matrix A_n, thus obtained, is the final transformed matrix. For the above procedure of conversion the following theorem will be true.

Theorem : In an arbitrary row, if the diagonal element of a matrix is greater than n times the sum of the moduli of the off-diagonal elements, the inverse of the matrix can be equated to a convergent power series.

We write
$$A_n = P + Q$$

i.e. $$A_n^{-1} = (I - P^{-1} Q + (P^{-1} Q)^2 - (P^{-1}Q)^3 + (P^{-1} Q)^4 - ..) P^{-1} \qquad [2.1]$$

where P is a diagonal matrix having the diagonal elements identical to those of A_n whose diagonal elements are already non-zero as a'_{pp} has been chosen in the manner where no zero can appear on the diagonal of A_n. Q is a matrix identical to A_n excepting its diagonal elements which are exactly zeros.

In Newton-Horner's scheme[4]

$$A_n^{-1} = \{ I - P^{-1} Q \langle I + P^{-1} Q [I + P^{-1} Q (I + P^{-1} Q + ..)] \rangle \} P^{-1} \qquad [2.1a]$$

We determine first $P^{-1} Q (I + P^{-1} Q)$ and call it X. We then obtain $P^{-1} Q (I + X)$ and call it X_1. Next we find $P^{-1} Q (I + X_1)$ and call it X_2 and so on. We stop this procedure when the Erhard-Schmidt's norm[5] of $X_i - X_{i-1}$ *i.e.*,

$$\left\| X_i - X_{i-1} \right\|_{E.S} < \text{a pre-assigned accuracy, say, } 10^{-10}$$
$$i = 2, 3, \ldots.$$

Hence
$$A_n^{-1} = (I - P^{-1} Q X_i) P^{-1} \text{ for sufficiently large } i \qquad [2.1b]$$

The evaluation of A_n^{-1} from [2.1a] is preferred to that of A_n^{-1} from [2.1] as the Newton-Horner's scheme requires less arithmetic operations (n matrix multiplications and n additions) and consequently results in less rounding errors.

It is easy to see that $|P^{-1}Q|_{E.S.} < 1$. It can, furthermore, be noted that we can increase the speed of convergence indefinitely by taking the diogonal elements of A_n sufficiently large. We should, however, refrain from taking too large diagonal elements for too rapid convergence, since these introduce rounding errors due to matrix addition operations the effect of which, however, is very much dependent on the precision of the computer employed. This fact is illustrated through numerical examples that find description in subsequent pages.

The method, in the second phase, obtains A^{-1} using the knowledge of A_n^{-1}. The general form of the recurrence relations for obtaining A^{-1} is

$$\gamma_p = 1 + v_p A_p^{-1} u_p \qquad [3.1]$$

$$B_p = u_p v_p \qquad [3.2]$$

$$A_{p-1}^{-1} = A_p^{-1} - (1/\gamma_p) A_p^{-1} B_p A_p^{-1} \qquad [3.3]$$

$$p = n, n-1, \ldots, 1$$

The above recurrence relations demand only simple matrix multiplications and additions and no inversion. We can, moreover, see that number of multiplications and additions are only a few because, all elements are zeros except one in u_p and one v_p. An efficient computer program is easy to prepare for the aforesaid procedure.

2. Programming Aspect

(I) Store $A = A_o = (a_{ij})$ $i = 1.2, \ldots, n$; $j = 1, 2, \ldots, n$

(II) $c_p = a_{pp}$ $p = 1, 2, \ldots, n$

c_p ($p = 1, 2, \ldots, n$) are the diagonal elements a_{ii} ($i = 1, 2, \ldots, n$) of A.

(III)
$$\begin{cases} d_p = m.n \sum_{q=1}^{n} {}'|a_{pq}| \quad p = 1, 2, \ldots, n, \quad q \neq p \\ m > 1, \ m = 5, \text{ say} \\ \text{If } d_p = 0 \text{ for any } p, \text{ put } d_p = \text{any non-zero number, say, 1.} \end{cases}$$

d_p ($p = 1, 2, \ldots, n$) are the diagonal elements a_{ii}' ($i = 1, 2, \ldots, n$) of P which is a diagonal matrix.

(IV) $a_{pp} = 0$ $p = 1, 2, \ldots, n$

The matrix A is now our Q.   The problem is to find A_n^{-1}.

(V) $\begin{cases} a_{ii} = 0 & i = 1, 2, \ldots, n \\ a_{ij} = b_{ij} = -\dfrac{a_{ij}}{d_{ii}} & i = 1, 2, \ldots, n; \; j = 1, 2, \ldots, n \end{cases}$

(a_{ij}) and (b_{ij}) are the elements of matrix $-P^{-1}Q$.

(VI) $k = 1$

(VII) $b_{ii} = 1 + b_{ii}$ $i = 1, 2, \ldots, n$

Now (b_{ij}) are the elements of the matrix $I + (-P^{-1}Q)$.   The following two steps, namely, steps VIII and IX obtain the value of $(I + P^{-1}Q)^{-1}$ using Newton-Horner's scheme.

(VIII) $e_{ij} = \sum_{p=1}^{n} a_{ip} b_{pj}$ $i = 1, 2, \ldots, n; \; j = 1, 2, \ldots \;\; n$

(IX) $b_{ij} = e_{ij}$ $i = 1, 2, \ldots, n; \; j = 1, 2, \ldots, n$

(X) $\begin{cases} f_k = (\sum_{i=1}^{n} \sum_{j=1}^{n} b_{ij}^2)^{1/2} \\ \text{if } k > 1 \text{ go to step (XI), if } k \not> 1, \text{ replace } k \text{ by } k+1 \text{ and go to} \\ \text{step (VII).} \end{cases}$

(XI) $\begin{cases} f_3 = \text{mod } (f_1 - f_2) \\ \text{if } f_3 < 10^{-8} \text{ say, go to step (XII) otherwise go to step (VI).} \end{cases}$

(XII) $b_{ii} = 1 + b_{ii}$, $i = 1, 2, \ldots, n$

Now (b_{ij}) produce the $A_n^{-1}P$ matrix.

(XIII) $b_{ij} = \dfrac{b_{ij}}{d_j}$ $i = 1, 2, \ldots, n; \; j = 1, 2, \ldots, n$

(b_{ij}) are now the elements of A_n^{-1} matrix.

$$(XIV) \begin{cases} k = n, \; n-1, \; \ldots, \; 1 \\[6pt] \gamma_k = 1 + b_{kk} \, (c_k - d_k) \\[6pt] e_{ij} = \dfrac{b_{ik} \, (c_k - d_k)}{\gamma_k} \, b_{kj} \, , \; i = 1, \, 2, \, \ldots, \, n \; ; \; j = 1, \, 2, \, \ldots, \, n. \\[6pt] b_{ij} = b_{ij} - e_{ij} \qquad i = 1, \, 2, \, \ldots, \, n \; ; \; j = 1, \, 2, \, \ldots, \, n \end{cases}$$

Relations [3.1], [3.2] and [3.3] are computationally represented in step (XIV). (b_{ij}) thus obtained are the elements of A_0^{-1} or A^{-1}. For $k = n$, we determine γ_n, all e_{ij}'s and all b_{ij}'s. We then take $k = n-1$, and obtain γ_{n-1}, all e_{ij}'s and then all b_{ij}'s and so on. Thus for $k = 1$, we calculate γ_1, all e_{ij}'s and subsequently b_{ij}'s. The latest b_{ij}'s are the elements of A^{-1} matrix. The ' $=$ ' sign in all the aforesaid computational steps has the identical meaning as that in Fortran.

Numerical Results: 8 dit floating point arithmetic has been employed for all the calculations.

Example 1. A matrix that does not satisfy row (or column)-sum criterion.

$$\begin{bmatrix} 1 & 4 & 3 \\ 4 & 2 & 1 \\ 3 & 2 & 2 \end{bmatrix}$$

Three times the sum of the off-diagonal elements in the first, second and third rows are 21, 15 and 15 respectively. If we choose their multiplying factor 10, the number of effective terms in the power series becomes 6 and the final inverse (A^{-1}) is correct up to 6 significant figures.

Any additional terms in the power series will not contribute anything towards improving or diminishing the accuracy of A_n^{-1}. An extra term in the series does, however, improve the accuracy when the precision of calculations is considerably increased.

If the multiplying factor (m. f.) is 10^2, the A^{-1} is correct up to 5 significant figures. The number of effective terms in this power series for A_n^{-1} is 4. For the m.f. 10^3, A^{-1} becomes less accurate and the accuracy is up to 4 significant figures. When the m. f. is 10^4, A^{-1} is correct up to 3 significant figures, the number of terms in the power series for A_n^{-1} being 3. The inverse is, for m. f. $= 1.1$,

$$\begin{bmatrix} -.1666667 \times 10^0 & .1666667 \times 10^0 & .1666667 \times 10^0 \\ .4166667 \times 10^0 & .5833333 \times 10^0 & -.9166667 \times 10^0 \\ -.1666667 \times 10^0 & -.8333333 \times 10^0 & .1166667 \times 10^1 \end{bmatrix}$$

and AA^{-1} is

$$\left(\begin{array}{ccc} .1000000 \times 10^{1} & .1862645 \times 10^{-8} & .3725290 \times 10^{-8} \\ -.2980232 \times 10^{-7} & .1000000 \times 10^{1} & -.1490116 \times 10^{-7} \\ .1490116 \times 10^{-7} & .0000000 \times 10^{0} & .1000000 \times 10^{1} \end{array}\right)$$

The number of terms in the series for the aforesaid m. f. is 16 and the result is correct up to all significant figures noted. When m. f. is 10^{5}, the accuracy of A^{-1} comes down still further and it is correct up to 2 significant figures. When it is 10^{6}, the A^{-1} is correct up to 1 significant figure.

The m f., when increased, reduces the number of terms (in the power series) and consequently the computing time at the cost of introducing more error due to matrix addition. The other examples which we have attempted produce good results for m. f. lying between 1.1 and 10.

Example 2. A matrix satisfying row (or column)-sum criterion

$$\left|\begin{array}{cccc} 10 & 5 & 3 & 1 \\ 2 & 8 & 2 & -3 \\ 3 & 2 & 19 & 7 \\ 5 & 2 & 1 & 15 \end{array}\right|$$

When m. f. $= 10$, number of terms in the power series is 5 and the inverse is correct up to 7 significant figures. When it is 10^{2}, the result is correct up to 6 significant figures with effective number of terms in the series $= 4$. The inverse, for m. f. 1.1, is

$$\left(\begin{array}{cccc} .1265405 \times 10^{0} & -.7185299 \times 10^{-1} & -.1149868 \times 10^{-1} & -.1744058 \times 10^{-1} \\ -.4467430 \times 10^{-1} & .1462368 \times 10^{0} & -.1028829 \times 10^{-1} & .3702685 \times 10^{-1} \\ -.1980634 \times 10^{-2} & -.5831866 \times 10^{-2} & .5496259 \times 10^{-1} & -.2668354 \times 10^{-1} \\ -.3609155 \times 10^{-1} & .4841549 \times 10^{-2} & .1540493 \times 10^{-2} & .6932218 \times 10^{-1} \end{array}\right)$$

and AA^{-1} is

$$\left(\begin{array}{cccc} .1000000 \times 10^{1} & .3259629 \times 10^{-8} & .1804437 \times 10^{-8} & .1862645 \times 10^{-8} \\ .9313226 \times 10^{-9} & .1000000 \times 10^{1} & -.1746230 \times 10^{-8} & .0000000 \times 10^{0} \\ .0000000 \times 10^{0} & -.4656613 \times 10^{-9} & .1000000 \times 10^{1} & -.1862645 \times 10^{-8} \\ .1862645 \times 10^{-8} & -.1862645 \times 10^{-8} & -.4656613 \times 10^{-9} & .1000000 \times 10^{1} \end{array}\right)$$

The number of effective terms here is 12 and the result is correct in all the significant figures shown. For m. f. $= 1.5$, the number of terms in the series is 10 and the result is identical to the above result up to all the significant figures retained. When m. f. $= 10^5$, number of terms in the power series is 2 and A^{-1} is correct up to 3 significant figures.

Example 3. A near-singular matrix

$$\begin{bmatrix} 1 & 5 & 3 & 7 \\ 2 & 4 & 1 & 6 \\ 3 & 1 & -2 & 3 \\ 2 & 9.90 & 6 & 14 \end{bmatrix}$$

The (4,2)-th element is made 9.9 instead of 10 to make it slightly near-singular.

When the multiplying factor $= 10$, number of terms in the power series is 6 and the inverse is correct up to 4 significant figures. The inverse is, for m. f. 1 5 with number of terms in the series 12,

$$\begin{bmatrix} .6750068 \times 10^2 & -.1150010 \times 10^2 & .5500045 \times 10^1 & -.3000031 \times 10^2 \\ .2000022 \times 10^2 & -.3179908 \times 10^{-4} & .1478940 \times 10^{-4} & -.1000010 \times 10^2 \\ .4600046 \times 10^2 & -.9000064 \times 10^1 & .4000030 \times 10^1 & -.2000021 \times 10^2 \\ -.4350045 \times 10^2 & .5500064 \times 10^1 & -.2500030 \times 10^1 & .2000021 \times 10^2 \end{bmatrix}$$

and AA^{-1} is

$$\begin{bmatrix} 1000003 \times 10^1 & -.3814697 \times 10^{-5} & -.1907349 \times 10^{-5} & -.1335144 \times 10^{-4} \\ .1072884 \times 10^{-5} & .9999990 \times 10^0 & -.4768372 \times 10^{-6} & -.3814697 \times 10^{-5} \\ .2145767 \times 10^{-5} & -.1907349 \times 10^{-5} & .9999981 + 10^0 & -.1144409 \times 10^{-4} \\ -.2145767 \times 10^{-5} & .9536743 \times 10^{-6} & .1907349 \times 10^{-5} & .1000010 \times 10^1 \end{bmatrix}$$

When the (4,2)-th element is made 9 99, the inverse becomes, for m, f. 10 with number of terms in the series 6,

$$\begin{bmatrix} .6076449 \times 10^3 & -.1150218 \times 10^2 & .5501015 \times 10^1 & -.3000717 \times 10^3 \\ .2000490 \times 10^3 & -.7378161 \times 10^{-3} & .3428161 \times 10^{-3} & -.1000242 \times 10^3 \\ .4060965 \times 10^3 & -.9001453 \times 10^1 & .4000676 \times 10^1 & -.2000478 \times 10^3 \\ -.4035970 \times 10^3 & .5501461 \times 10^1 & -.2500679 \times 10^1 & .2000480 \times 10^3 \end{bmatrix}$$

and AA^{-1} is

$$\begin{pmatrix}
.1000088 \times 10^1 & .4577637 \times 10^{-4} & .7629394 \times 10^{-5} & -.1831055 \times 10^{-3} \\
.2670288 \times 10^{-4} & .1000004 \times 10^1 & .0000000 \times 10^0 & -.7629395 \times 10^{-4} \\
.5531311 \times 10^{-4} & .1525879 \times 10^{-4} & .1000008 \times 10^1 & -.1525879 \times 10^{-3} \\
-.5722046 \times 10^{-4} & -.2288818 \times 10^{-4} & .7629394 \times 10^{-5} & .1000137 \times 10^1
\end{pmatrix}$$

When the m. f. $= 1.5$, the accuracy of A^{-1} is nearly the same as above; the number of effective terms, however, is doubled.

When $(4,2)$-th element is made 9.999, the inverse becomes, for m. f. 1.1 with number of effective terms 14,

$$\begin{pmatrix}
.6006932 \times 10^4 & -.1150117 \times 10^2 & .5500659 \times 10^1 & -.2999716 \times 10^4 \\
.1999808 \times 10^4 & -.3841519 \times 10^{-3} & .2170578 \times 10^{-3} & -.9999039 \times 10^3 \\
.4005622 \times 10^4 & -.9000781 \times 10^1 & .400044 \times 10^1 & -.1999811 \times 10^4 \\
-.4003120 \times 10^4 & .5500776 \times 10^1 & -.2500438 \times 10^1 & .1999810 \times 10^4
\end{pmatrix}$$

and AA^{-1} is

$$\begin{pmatrix}
.1000488 \times 10^1 & .0000000 \times 10^0 & .0000000 \times 10^0 & .9765625 \times 10^{-3} \\
.1678467 \times 10^{-3} & .1000061 \times 10^1 & .3051758 \times 10^{-4} & .3662109 \times 10^{-3} \\
.3204346 \times 10^{-3} & .0000000 \times 10^0 & .1000061 \times 10^1 & .6103516 \times 10^{-3} \\
-.3356934 \times 10^{-3} & -.1220703 \times 10^{-3} & -.6103516 \times 10^{-4} & .9992676 \times 10^0
\end{pmatrix}$$

Any result better than above can only be achieved by using higher precision arithmetic.

We have, in all the aforesaid examples, used Newton-Horner's[5] scheme for the evaluation of the power series $(I + P^{-1}Q)^{-1}$.

ACKNOWLEDGMENT

REFERENCES

1. Sen, S. K.   ..   ..   A Power Series Method for the Inverse of Matrices, communicated to Computer J.

2. Sen, S. K.   ..   ..   Proc. 1st Mastech Conference on Matrix Analysis held at NAL, Bangalore, (Sept. 25—Oct. 3, 1969) pp 113-123.

3. Maulik, T. N.   ..   ..   *Ibid*, 1969, pp 149—160.

4. Eve, J.   ..   ..   *Num. Math.*, 1964, 6, 17.

5. Collatz, L.   ..   ..   Functional Analysis and Numerical Maths., Academic Press (1966), 174.

NUMERICAL DIFFERENTIATION BY EXTRAPOLATION

By MANAS CHANDA

(Department of Chemical Engineering, Indian Institute of Science, Bangalore-12, India)

AND

SYAMAL KUMAR SEN

(Central Instruments and Services Laboratory, Indian Institute of Science, Bangalore-12, India)

ABSTRACT

Presented in this paper is a simple extrapolation technique to obtain numerical derivative of an analytic function, complex or real. The function may be in tabular form or in functional form. A few numerical examples are added for the purpose of illustration.

1. DISCUSSION

The method of finding the temperature at which the volume of a gas becomes zero (a situation which cannot be reached in practice) by extrapolating the curve of relative volume versus temperature (°C) to zero volume, prompted the idea of obtaining the numerical derivative of a function (that cannot be obtained numerically using the theoretical definition.

$$\underset{\triangle x \to 0_{\pm}}{Lt} \frac{\triangle y}{\triangle x} = \frac{dy}{dx}$$

for any analytic function because of the precision limitation of any arbitrary computer used) by extrapolation.

Let us first consider a real function of a single real variable. The generalization to many variable functions and to complex functions then follows readily from it. Let $\triangle x_1$, $\triangle x_2$, $\triangle x_3$ be three small positive real numbers satisfying the inequality

$$\triangle x_1 > \triangle x_2 > \triangle x_3$$

and let x_0 be the point at which we want to obtain the derivative of $f(x)$. The problem is then posed as follows :

$$\triangle x_1 \longrightarrow \frac{f(x_0 + [\triangle x_1/2]) - f(x_0 - [\triangle x_1/2])}{\triangle x_1}$$

51

$$\triangle x_2 \longrightarrow \frac{f(x_0 + [\triangle x_2/2]) - f(x_0 - [\triangle x_2/2])}{\triangle x_2}$$

$$\triangle x_3 \longrightarrow \frac{f(x_0 + [\triangle x_3/2]) - f(x_0 - [\triangle x_3/2])}{\triangle x_3}$$

$$0 \longrightarrow ?$$ [1]

Evidently, the answer to the question mark (?) is the numerical derivative of the function at x_0, and it can be obtained only by extrapolation since the quantities

$$\frac{f(x_0 + [0_+/2]) - f(x_0 - [0_+/2])}{0_+}$$

or

$$\frac{f(x_0 + [0_-/2]) - f(x_0 - [0_-/2])}{0_-}$$

cannot be obtained numerically due to obvious physical limitation. (0_+ indicates that $\triangle x \longrightarrow 0$ from the positive direction and 0_- indicates that $\triangle x \longrightarrow 0$ from the negative direction.)

2.   EXTRAPOLATION METHOD

The aforesaid problem is one of quadratic extrapolation since r. h. s. informations are provided corresponding to three quantities $\triangle x_1$, $\triangle x_2$, $\triangle x_3$ only.   One can as well pose the problem as cubic, biquadratic or any other extrapolation considering 4, 5 or more r.h.s. informations corresponding to 4, 5 or more quantities $\triangle x_1$, $\triangle x_2$, $\triangle x_3$, $\triangle x_4$, $\triangle x_5$ etc.   It is, however, the fact that the use of biquadratic or higher-order extrapolation does not offer any significant advantage over quadratic or cubic extrapolation which is simpler and more economic[1].   It is worth mentioning that the aforesaid situation is analogous to the fact that the Wilkes-Harvard and Newton-Raphson iterative division scheme with an order of convergence more than two or three are uneconomical for realization in computers[1].   We therefore restrict ourselves to the discussion of quadratic and cubic extrapolation. The next problem is how to choose $\triangle x_1$, $\triangle x_2$, $\triangle x_3$ etc.   Since we do not possess definite knowledge about what $\triangle x$'s should be so that the numerical derivative turns out to be the most accurate within the allowed precision of the computer, we devise the fllowing iteration process.

We extrapolate the r.h.s. quantities to $x = 0$, using Lagrange's interpolation formula of order 2 or 3.   We choose for this purpose $\triangle x_2$ as $[\triangle x_1/2]$, $\triangle x_3$ as $[\triangle x_2/2]$, $\triangle x_4$ as $[\triangle x_3/2]$ and so on.   We can, however, choose any other spacing of $\triangle x$'s, equidistant or non-equidistant.   After

obtaining the numerical derivative of $f(x)$ by extrapolation, we reduce $\triangle x_1$ to half and pass through the identical procedure to obtain the second iteration value of numerical derivative. The process is repeated, halving the interval $\triangle x_1$ at each iteration till the continuously increasing or continuously decreasing numerical derivative attains a maximum or minimum value. The maximum or minimum value is the required numerical derivative. For greater accuracy, $\triangle x_1$ should be small (starting with, say, 1 or 2) but not too small.

It can be seen that we have used in [1] the central difference scheme and not forward or backward difference schemes for initial approximate derivatives. This is because central difference scheme produces a truncation error of the order of h^2 while forward or backward difference scheme produces an error of the order of h.

The suggested technique is also true for complex functions. The arithmetic employed here has to be complex. Functions of many variables do not pose any extra problem ; in this case we obtain numerical partial derivatives.

If we use both the quadratic and cubic extrapolations, then the difference between the values of $f'(x_0)$, so obtained, provides us in the first place an idea of the accuracy and also an idea about the interval size to be chosen for the argument of the function. If the interval is big, so far as the nature of the variation of $\triangle f(x)/\triangle x$ is concerned, both quadratic and cubic fittings may produce results almost completely different, thereby indicating that the interval should be reduced.

A function $f(x)$ is said to be ill-conditioned with respect to its derivatives if $f(x)$ is violently fluctuating, *i.e* , a little change in x causes a very large change in $f(x)$. The degree of ill-conditioning[2] is dependent on the degree of fluctuation of $f(x)$. Such a function of $f(x)$, however, is a problem under any treatment. The basic fact is that the function $f(x)$ is a near approach to a discontinuous function.

If we denote $\triangle x_1$, $\triangle x_2$, $\triangle x_3$, by p_1, p_2, p_3 respectively and the corresponding right hand quantities in [I] by q_1, q_2, q_3 respectively, we then write, by Lagrange's interpolation formula, the extrapolated numerical derivative as

$$q(0) = \frac{p_2 p_3}{(p_1-p_2) (p_1-p_3)} q_1 + \frac{p_1 p_3}{(p_2-p_1) (p_2-p_3)} q_2 + \frac{p_1 p_2}{(p_3-p_1) (p_3-p_2)} q_3 \quad [\text{II}]$$

The formula in [II] is the result of quadratic fitting. Similarly we can obtain $f'(x)$ using cubic fitting.

3. NUMERICAL RESULTS

We have taken the Bessel functions $J_0(x)$, $J_1(x)$, $Y_0(x)$, $Y_1(x)$, $I_0(x)$, $I_1(x)$, $K_0(x)$ and $K_1(x)$ with real argument x as examples.   The calculations are carried out in about 8 digit floating point arithmetic.   The computer used is National Elliott 803 computer with fixed word-length of 40 bits.   Numerical derivatives of the aforesaid functions at $x=2$, obtained by the present method are presented in Table 1.   The starting value of $\triangle x_1$ is 2 in each case.   The calculation of the functions J_0, J_1, Y_0, Y_1, I_0, I_1, K_0, K_1 are carried out using Chebyshev polynomial expansion[3].

TABLE I

| Function | Quadratic Fittings | | Cubic fitting | |
$f(x_0)$	$f'(x_0)$	No. of iteration	$f'(x_0)$	No. of iteration
$J_0(2)$	$-.57672439$ (min)	5	$-.57672486$ (max)	3
$J_1(2)$	$-.64470331 x 10^{-1}$ (min)	7	$-.64471851 x 10^{-1}$ (max)	3
$Y_0(2)$	$.10703253$ (min)	5	$.10703247$ (max)	3
$Y_1(2)$	$.56389175$ (min)	5	$.56389244$ (max)	5
$I_0(2)$	$.15906365 \times 10$ (min)	4	$.15906397 \times 10$ (max)	4
$I_1(2)$	$.14842662 \times 10$ (min)	5	$.14842662 \times 10$ (max)	3
$K_0(2)$	$-.13986553$ (min)	5	$-.13986603$ (max)	3
$K_1(2)$	$-.18382511$ (min)	6	$-.18382710$ (max)	4

It is noted that in the quadratic fitting the derivative value decreases with iterations and after attaining a minimum value with 4 or 5 iterations starts increasing.   The situation is just reverse in case of cubic fitting.   In

Table I the word 'min' within closed parenthesis under the heading ' quadratic fitting ' indicates the minimum value attained by the derivative at the corressonding number of iterations mentioned alongside; this minimum value is our required numerical derivative. Similarly, in the case of cubic fitting, the maximum value of the derivative is the required derivative. The results are seen to be correct up to about 6 significant figures.

4. ACKNOWLEDGEMENT

The authors wish to express their sincere thanks to Prof. S. Dhawan for his constant encouragement.

5. REFERENCES

1. E. V. Krishnamurthy   ..   " Economical Iterative and Range-Transformation Schemes for Division ", to appear in IEEE Trans. on Computers.

2. S. K. Sen   ..   .:   *J. Indian Inst. Sci*, 49, 1967, pp 37.

3. M. Abramowitz and I. A. Stegun ..   Handbook of Math. Functions, Dovet Publication, New York, 1965, pp. 355-435.

ETHANOL DEHYDRATION OVER SHEVAROY BAUXITE

By G. S. Pant, N. Subrahmanyam, M Chanda and S. S. Ghosh

(Department of Chemical Engineering, Indian Institute of Science, Bangalore-12, India)

ABSTRACT

Vapour phase dehydration of ethanol to ethylene over Shevaroy bauxite has been studied in a fluidised-bed reactor. Factorial design of experiments has been carried out. A mathematical expression representing the dependence of conversion as a function of temperature and time factor has been proposed.

1. INTRODUCTION

Vapour phase dehydration of ethanol to ethylene using bauxite/alumina as catalysts has been a well studied reaction. However, most of the work reported in literature is for the reaction in fixed-bed reactors. Therefore, in the present study of alcohol dehydration over bauxite from Shevaroy (Tamilnadu State) a fluidised bed reactor was employed. Factorical design of experiments was carried out to determine the nature of dependence of conversion as a function of temperature and time factor.

2. CATALYST

Bauxite obtained from Shevaroy was first washed to remove clay material present and dried to remove free water. It was then activated to remove combined water and to increase its adsorptive power.

A few important characteristics of this bauxite are :

(1)	Particle size	$-65 + 80$ T.S.S.
(2)	Bulk density	1.30 gms/cc.
(3)	Surface area	68.34 sq. cm./gm.

The surface area of bauxite was determined by benzene adsorption method in a desiccator.[1]

3. EXPERIMENTAL

The equipment was of laboratory scale, as illustrated schematically in Figure 1. It consisted of feed system, vaporiser, reactor, condenser and
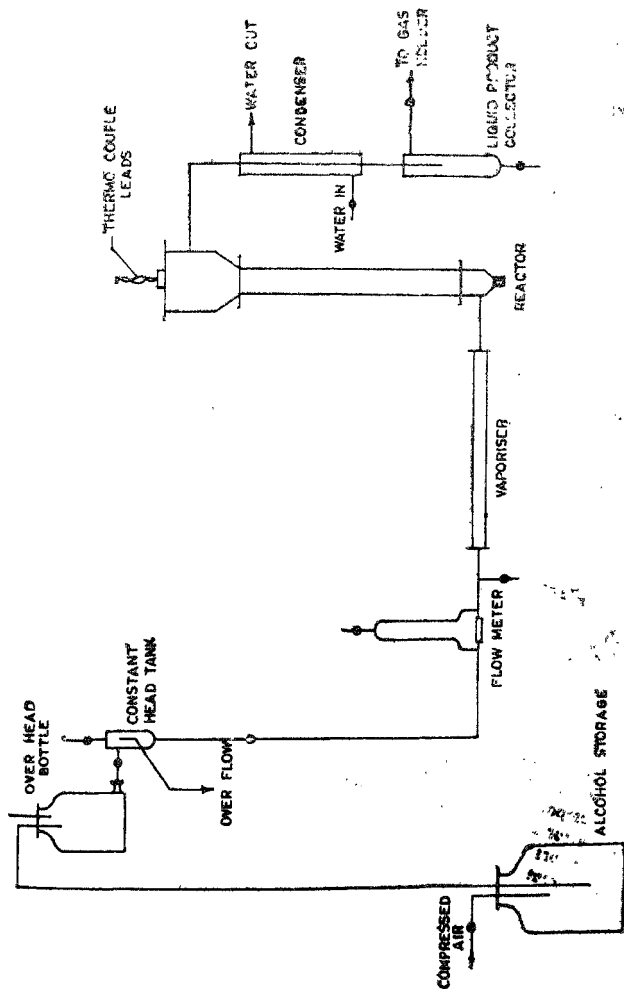
Fig. 1 FLOW DIAGRAM OF SET-UP.

FIG. 1

Flow diagram of Set-up

gas collection system. Ethanol from storage carboy was pumped to the overhead by using compressed air, from where it was fed continuously to a vaporiser at constant rate. The vaporiser was $1/4'' \times 3/8''$ stainless steel tube of 24'' length, packed with porcelain beads and electrically heated. The temperature of the vaporiser was maintained at $125 \pm 1°C$. The reactor was a stainless steel tube 2'' dia. and 12'' long. A stainless steel wire mesh was used as the catalyst support and feed distributor. The reactor was heated by external resistance coils to the required temperature and controlled to within $\pm 5°C$ by a simmerstat. Hot gases leaving the reactor were passed through a double walled surface condenser to condense out the water produced by the dehydration of alcohol, as also any unconverted alcohol. The gas collection system consisted of a low pressure gas holder of 250 litres capacity. Suitable weights were used for the gas collection under positive pressure. A T-stop cock was placed midway between the liquid-product collector and the gas holder for tapping gas samples for analysis.

The vaporiser and the reactor were heated to the desired temperature and then alcohol was allowed to flow at a predetermined rate. The vapours then passed through the reactor containing a known weight of bauxite for a period of one hour. The condensate was collected in a flask and the gaseous product in the gas holder.

The gaseous product was analysed in a modified Orsat gas analysis set-up. The liquid product being mainly water and unreacted alcohol was not analysed even though very small amounts of acetic acid, ethyl acetate and acetaldehyde were present.

A design was used involving two factors namely temperature (A) and time factor (B), each at four levels with equal intervals. The experimental runs were carried out in a random order so as to improve the experimental efficiency. Care was taken to avoid batch to batch variation in the raw materials.

5. RESULTS AND DISCUSSION

The responses obtained at various levels of temperature and time factor are presented in Table 1. The method of analysis employed is as suggested by Davies.[2] The first step is to calculate the linear, quadratic and cubic components of the effect of factor A for each level of factor B and that of factor B for each level of factor A. The interaction of components of the factors A and B are then calculated. The analysis of variance of Table 1 is presented in Table 2.

The conclusion that can be drawn within the range of experiment are therefore :

> (i) There is a significant linear increase in conversion with increase in temperature.

(ii) There is a significant linear decrease in conversion with increase in time factor.

(iii) The quadratic and cubic effects of temperature are small, so that a linear function provides an adequate representation.

(iv) The interactions of linear temperature with linear and quadratic time factor are significant which means that slope of the line is not the same for different levels of time factor.

All the components of the effect of temperature and the linear and cubic components of the effect of time-factor are significant which imply that there occurs a minimum or maximum conversion at some intermediate combination of temperature and time factor, or a point outside the range examined. Taking into consideration only those effects and interactions which are significant at 5% level (see Table 2) the conversion of ethanol to ethylene as a function of temperature and time factor could be represented as:

$$x = K_1 y + K_2 z + K_3 y^2 + K_4 z^2 + K_5 y^3 + K_6 yz + K_7 yz^2 \qquad [1]$$

TABLE 1

Responses obtained at various levels of temperature and time factor

Temperature (A) $A_1 = 380°C$

$A_2 = 420°C$

$A_3 = 460°C$

$A_4 = 500°C$

Time factor (B) $B_1 = 28.97$

$B_2 = 36.30$

$B_3 = 47.63$

$B_4 = 56.96$

Response :   Mole% conversion of ethanol to ethylene.

	B_1	B_2	B_3	B_4
A_1	34.78	38.25	28.63	26.54
A_2	46.22	55.03	43.10	39.64
A_3	80.70	92.37	71.70	47.63
A_4	78.30	89.43	75.20	51.28

TABLE II

Analysis of Variance of Table 1

Source of variation	Sum of squares		Degrees of freedom		Mean square	Variance ratio
Main Effects						
Linear	4597.00		1		4597.00	200.20*
A Quadratic	182.00	5096.10	1	3	182.00	7.93*
Cubic	317.10		1		317.00	13.81*
Linear	988.30		1		988.30	43.04*
B Quadratic	491.00	1590.70	1	3	491.00	21.38*
Cubic	111.40		1		111.40	4.84
Interactions						
Linear A x Linear B	183.80		1		183.80	8.01*
Linear A x Quadratic B	156.30		1		156.30	6.81*
Quadratic A x Linear B	6.02	480.86	1	9	6.02	0.26
Remainder = Error	134.74		6		22.47	-----
Total		7167.66	15			

* Significant at 5% level of the F statistic, because with 1 and 6 degrees of freedom, 5% significance level requires a variance ratio of 5.99.

where x is the mole% conversion of ethanol to ethylene

    y is the temperature

    z is the time factor, and

    $K's$ are constants.

By least square fitting their values are found to be :

$$K_1 = 1.09 \times 10^2$$
$$K_2 = -1.06 \times 10^3$$
$$K_3 = -3.28 \times 10^{-1}$$
$$K_4 = 1.21 \times 10$$
$$K_5 = 2.43 \times 10^{-4}$$
$$K_6 = 1.82$$
$$K_7 = 2.09 \times 10^{-2}$$

Given a temperature and time factor, within the range studied in the present investigation, Eq. [1] can be employed to calculate the conversion.
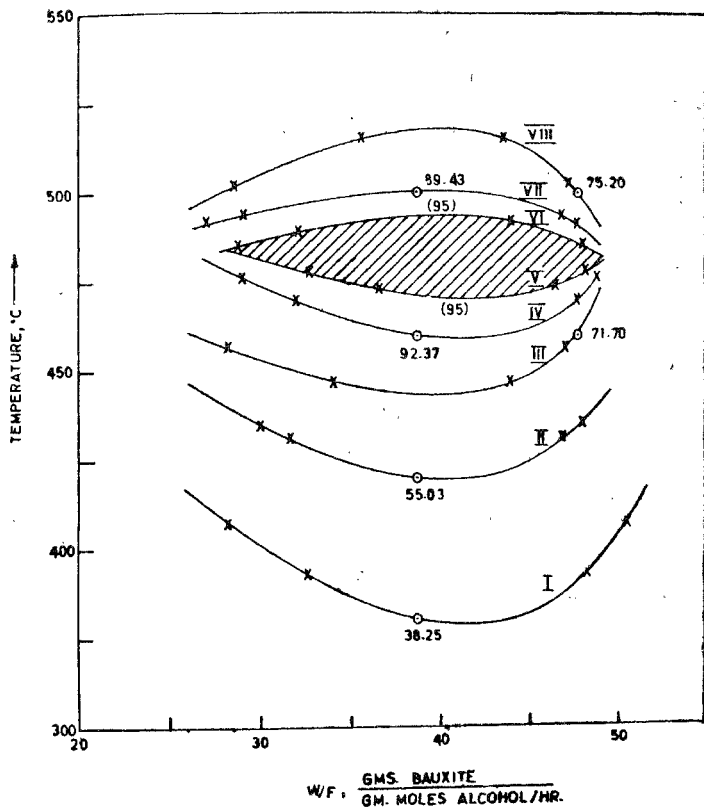
FIG. 2

Pilot of constant conversion contours.

6.   Optimum Conditions

The relationship between mole% conversion and the two independent variables *viz.*, temperature and time factor, is represented as a contour diagram consisting of lines of constant mole% conversion as parameter, the coordinates being temperature and time factor.   Figure 2 shows such contours, on which the circles represent experimental points, while the crosses represent theoretical points calculated from Eq. [1].   In order to obtain theoretical points on any contour the corresponding value of the mole% conversion (x) is put in Eq. [1] and a value is assumed for temperature (y), so that the equation reduces to a quadratic equation by solving which one gets two values of time factor (z).   It is evident from the contour diagram that an optimum point of temperature and time factor lies inside the region bounded by the contours V and VI

7.   Conclusions

In the range of variables employed in the present factorial study *viz.*, temperature, 380°C to 500°C and time factor, 28.97 to 56.96 gms. of bauxite per gm.mole alcohol per hour, the effects and interactions which are significant (at 5% level) are the linear, quadratic and cubic effects of temperature, the linear and quadratic effects of time factor and the interaction of linear temperature with linear-time factor and quadratic-time factor.

At all combinations of temperature and time factor in the shaded region of Fig- 2 the conversion is more than 95%.

References

1. Emmett, P. H.   . .   . .   Catalysis, Vol. 1, Reinhold, New York, 1964, pp. 1-26.

2. Davies, O. L.   . .   . .   The Design and Analysis of Industrial Experiments, Oliver & Boyd, 1956, pp. 247-327.

THEORETICAL STUDIES ON SOMMERFELD
SURFACE WAVE RESONATOR

By S. K. Chatterjee, Miss H. M. Girija, Miss Rukmini,
Miss Glory John and N. Narasimhan
[Received October 21, 1970]

Abstract

*The present report consists of a brief vé .sumé of the properties of microwave
resonators, such as,.mode degeneracy, coupling of companion modes etc , and the
derivation of the equivalent circuit by using Lagrangian method.   After making a
comparative study of the Sommerfeld and Harms--Goubau surface wave lines,
the report deals with the theory of surface wave resenator excited in E_0 and EH
and HE modes. As each of the latter two modes are coupled modes it is expected
that the Q factor will be very low, so emphasis is laid on the E_0 --mode resonator,
which may be called the Sommerfeld surface wave resonator.   Numerical
Computations for $Q (E_0)$ and guide wavelength $\lambda_g (E_0)$ as function of the length l
of the resonator and frequency of excitation for the Sommerfeld resonator show
that $Q (E_0)$ increases linearly with increasing length of the resonator for different
frequencies of excitation, whereas, λ_g decreases almost exponentially with increase
in frequency.*

1. Introduction

The study of electromagnetic oscillations in resonators is inherently
associated with Maxwell's equations and the concept of standing waves.
The study of standing waves in resonant cavities first made by Lord Rayleigh
remained for many years a subject of theoretical speculation.   Almost half a
century elapsed before the piactical importance of standing waves could be
realised and resonators became very useful practical tools for microwave
work.   The obvious answer as to why standing waves were for such a long
period of only academic interest is that the technique of generation of
microwave power was not sufficiently advanced so as to make microwave
work possible ; and yet this is hardly an adequate answer as the original
experiments of Hertz were done with millimeter waves.   The practical

application of resonators to microwave work was made possible due mainly to the work of Southworth and Schelkunoff at the Bell Telephone Laboratories, and Barrow, C hu and Stratton at the Massachusetts Institute of Technology in the middle of 1930's.

The resonance phenomena in microwave resonators of simple and some complicated shapes have been studied by several authors[1-35]. The concept of resonance in enclosed type of microwave cavities has been utilised by several authors[36 41] to study the surface-wave properties of Sommerfeld and Harms-Goubau lines. The investigations on electromagnetic wave propagation[42] initiated by Sommerfeld and Zenneck[43] and followed by Wait[44-46], Bowwkamp[47], Barlow and many others[48-66] have led to the modern concept of surface-waves and the evalution of different types of surface-wave structures which can be used as waveguides or antennas depending on the nature of surface-reactance.

The present investigations have been motivated with the object of making a theoretical study of the resonance properties of a surface-wave resonator consisting of Sommerfeld surface-wave line of radius terminated by identical plane metalic circular plates of each of radius a ($a > > d$) at both ends such that the surface-wave line forms the axis of the resonator (Fig. 1). The resonator has been developed with a view to make a systematic experimental study of the surface-wave properties such as field distribution, attenuation constant, etc. of a corrugated cylindrical metallic structure. The present study is the first step towards undertaking the more involved problem of surface wave modulated structures. It is thought worth while to give a brief re'sume' of some of the fundamental properties of a microwave cavity resouator[21] which will have some bearing on the study of the resonance properties of the Sommerfeld surface wave resonator.
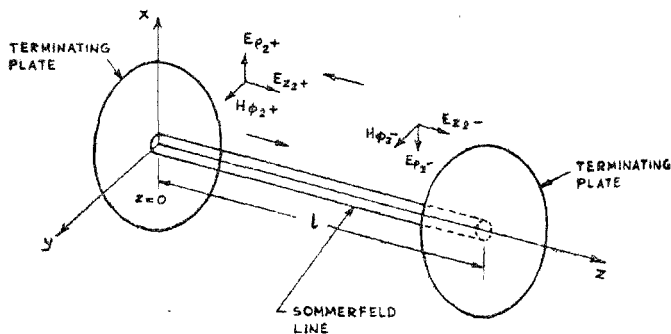

FIG. 1

Field components and coordinate system in surface wave resonator.

2. MICROWAVE RESONATOR—BRIEF RÉSUMÉ

2.1 *Equivalent Circuit*

A microwave cavity resonator, like the conventional resonant circuit, can be described as composed of an inductance—capacitance network with the help of the Lagrangian equation, which for a holonomic system is expressed as follows, in terms of the generalised co-ordinates q_1, q_2, $q_3 \ldots q_n$ and the corresponding velocities $\dot{q}_1$, $\dot{q}_2$, $q_3 \cdots \dot{q}_n$

$$p\,(\partial L/\partial \dot{q}_k) - (\partial L/\partial q_k) = F_k\,; \quad k = 1,\ 2,\ 3 \ldots n \qquad [1]$$

where, $p = d/dt$. F_k represents the dissipative forces and any external applied forces present in the system. The symbol L representing the Lagrangian is a function of q and $\dot{q}$ and is expressed in terms of the kinetic energy T and the potential energy V of the system as $L = T - V$. The charges Q_1, Q_2, $Q_3 \ldots Q_n$ and the currents $\dot{Q}_1$, $\dot{Q}_2$, $\dot{Q}_3 \ldots \dot{Q}_n$ in an electrical network can be considered as equivalent[66] to q_1, q_2, q_3, $\ldots q_n$ and $\dot{q}_1$ $\dot{q}_2$, $\dot{q}_3 \cdots \dot{q}_n$ respectively. So, the Lagrange equation for a single lossless cavity can be written as

$$p\,(\partial T/\partial \dot{Q}) + (\partial V/\partial Q) = 0 \qquad [2]$$

The kinetic and the potential energies of the cavity of volume **V** can be written as

$$T = 1/2\ \mu \sum_a k_a^2 \, v, \ \dot{Q}_a^2 = 1/2 \sum_a \mathcal{L}_a \, \dot{Q}_a^2, \ V = 1/2 \ \epsilon \sum_a k_a^4 \, v, \ Q_a^2 = 1/2 \sum_a (Q_a^2/C_a) \ [3]$$

where k_a represents the wave number for the ath mode of oscillation. The constants of the medium inside the cavity are represented by μ and ϵ. The equivalent lumped inductance and capacitance of the cavity are represented by L_a and C_a respectively.

From equations [2] and [3], the differential equation for a lossless cavity is obtained as follows :

$$\mathcal{L}_a \ddot{Q} + Q/C = 0 \qquad [4]$$

which represents a parallel inductance and capacitance network having resonant frequency.

$$\omega_a = \sqrt{(1/\mathcal{L}_a C_a)} \qquad [5]$$

A microwave cavity is usually coupled to external circuits by means of loops or coupling holes. The equivalent circuit of a single or a double loop coupled cavity can be similarly found with the help of Lagrange's equation.

2.2   *Resonant Frequencies of a Cavity*

Let us consider the case of an ideal right circular cylindrical cavity having infinitely conducting walls and end-plates and enclosing completely a lossless dielectric.   Natural electromagnetic oscillations once started in such a cavity will persist indefinitely and would be subject to Maxwell's equations expressed as follows in m.k.s. rationalised units.

$$\nabla \times \vec{E} = -\mu \, (\partial \vec{H}/\partial t) \, ; \quad \nabla \times \vec{H} = \epsilon \, (\partial \vec{E}/\partial t) \, ; \quad \nabla \cdot \vec{H} = 0 \, ; \quad \nabla \cdot \vec{E} = 0 \qquad [6]$$

inside the volume of the cavity.   The following boundary conditions should be satisfied.

$$\vec{n} \cdot \vec{H} = 0 \, ; \quad n \times E = 0. \qquad [7]$$

at the inside surface of the cavity. The symbols have their usual significance.

Let us assume that an oscilating electromagnetic field whose $\vec{E}$ and $\vec{H}$ components are given by the following equations has been set up inside the cavity

$$\vec{E} = \frac{1}{\sqrt{\epsilon}} \, \vec{e} \, \sin\left(\frac{k}{\sqrt{\epsilon\mu}} \, t + \phi\right) \, ; \quad \vec{H} = \frac{1}{\sqrt{\mu}} \, \vec{h} \, \cos\left(\frac{k}{\sqrt{\epsilon\mu}} \, t + \phi\right) \qquad [8]$$

where, the electric and the magnetic field configurations are given by the mode vectors $\vec{e}$ and $\vec{h}$ which are vector functions of position only. k and ϕ are constants.

The field satisfies Maxwell's equations
if

$$\nabla \times \vec{h} = k\vec{e} \, ; \quad \nabla \times \vec{e} = k\vec{h} \qquad [9]$$

within the volume of the cavity and

$$n.\vec{h} = n \times \vec{e} = 0 \qquad [10]$$

at the boundary wall of the cavity.

These equations when solved show that any given cavity can sustain an infinite number of modes of oscillation having eigen frequencies $k_1 \lfloor 2\pi\sqrt{\epsilon}\mu$, $k_2 \lfloor 2\pi\sqrt{\epsilon}\mu. \, . \, . \, , \, . \, . \, , \, k_n \rfloor \, 2\pi\sqrt{\epsilon}\mu$ with eigenvalues $k_1, \; k_2, \; k_3 \ldots k_n$.

The resonant frequencies of a cavity depend on the manner in which the cavity is excited.   Broadly, two general classifications are made, namely transverse electric (H), having the electric field transverse to the axis, and transverse magnetic (E) having the magnetic field transverse to the axis.   The resonant frequencies of a cavity whether it is excited in the H or E mode is given by

$$f_{l,m,n} = \sqrt{[(cn/2L)^2 + (f_o)^2_{lm}]} \qquad [11]$$

where,

$L =$ Length of the cavity

$l =$ number of full period variation of E_r along the angular θ cordinate.

$m =$ number of half period variations of E_θ along the radial r cordinate.

$n =$ number of half period variations of E_r along the axial or z cordinate.

$c =$ velocity of electromagnetic waves in free space.

The cut-off frequencies $(f_o)_{l,m}$ are given by

$$(f_o)_{l,m} = (c\, k'_{l,m}/2\,\pi a) \text{ for } H_{l,m} \text{ mode}$$

and

$$(f_0)_{l,m} = (ck_{l,m}/2\,\pi a) \text{ for } E_{l,m} \text{ mode} \qquad [12]$$

Where, a represents the radius of the cavity. The quantities $k'_{l,m}$ and $k_{l,m}$ are the roots of the following equations :

$$J'_l(k'_{l,m}) = 0; \quad \text{for } H_{l,m} \text{ modes}; \quad J_l(k_{l,m}) = 0; \quad \text{for } E_{l,m} \text{ modes} \qquad [13]$$

There will be a distinct resonance for each combination of l, m, n, which is referred to as a resonant mode of the system. Theoretically, a triple infinity of modes for each class is possible, but only the several lowest modes are of practical interest.

2.3 Mode Degeneracy

In experimental work on cavity resonators, generally the H_{01} mode is used, whereas, for surface-wave work, the mode of primary interest is E_0, since all the other modes have very high attenuation. From eqn. [13], $k'_{01} = k_{11} = 3.832$ as $J'_0(x) = -J_1(x)$. So, the resonant frequencies eqn. [11] f_{01n} and f_{11n} for the H_{01n} and E_{11n} modes respectively are identically the same. This is an important case of double degeneracy. When a cavity is excited in the desired mode H_{01}, the other mode E_{11} which is the companion mode invariably appears.

2.4. Field Components

The Field components for these two modes are given by the following expression.

H_{011} mode :

$$E_\rho = E_z = H_\theta = 0; \qquad E_\theta = J_0'(k_1\rho)\sin k_3 z; \qquad H_\rho = (k_3/k)\,J_0'(k_1\rho)\cos k_3 z;$$

$$H_z = (k_1/k)\,J_0(k_1\rho)\sin k_3 z \qquad [14]$$

E_{111} mode :

$$E_{\rho} = -(k_3/k) \; J_1{}' \, (k_1\rho) \, \cos\theta \, \sin k_3 z$$
$$E_{\theta} = (k_3/k) \; [J_1 \, (k_1\rho)/k_1\rho] \sin\theta \, \sin k_3 z$$
$$E_z = (k_1/k) \; J_1 \, (k_1\rho) \, \cos\theta \, \cos k_3 z$$
$$H_{\rho} = -[J_1{}' \, (k_1\rho)/k_1\rho] \sin\theta \, \cos k_3 z$$
$$H_{\theta} = -J_1{}' \, (k_1\rho) \, \cos\theta \, \cos k_3 z$$
$$H_z = 0 \qquad\qquad\qquad\qquad\qquad\qquad\qquad\qquad\qquad [15]$$

2 5 H_{01} *mode*

In spite of the double degeneracy, the H_{01} mode is invariably used for cavity excitation for the following reasons :

(i)   The field distribution of the H_{01} mode shows that the wall currents flow in circles perpendicular to the axis of the cylinder and hence no current can cross the contact surface of an adjustable plunger used to resonate the cavity to the excitation frequency. So, a non-contact type of plunger can be used for turning a cavity, This avoids any fluctuating loss taking place at the surface of contact with the walls of the cavity.

(ii) When a cavity is excited in any desired mode, a number of crossing and interfering modes appear depending on the volume of the cavity and the wavelength of excitation. For a cavity of of volume V and wavelength λ of excitation, the number of modes N that can appear is given approximately by the following relation[35]

$$N \approx (8\pi/3) \; (v/\lambda^3) \qquad\qquad\qquad\qquad\qquad\qquad [16]$$

But the Q of the cavity is given by the following relation :

$$Q = 2\pi \, f \, (\bar{W}/P) \qquad\qquad\qquad\qquad\qquad\qquad\qquad [17]$$

As the mean energy $\bar{W}$ stored in the resonator is given by a volume integral, whereas, the rate of dissipation of energy P is given by a surface integral, it is evident from eqn. [17] that, in order to obtain high Q, the volume of the cavity must be large. This is undesirable as it will make a larger number of spurious modes appear in a cavity. It can also be shown that H_{01} is the mode which gives the highest possible Q with minimum volume of the cavity.

2.6   *Interaction of H_{01} and E_{11} modes*

In the absence of perturbation, it can be shown[67], that there is very little interaction between the two modes H_{01} and E_{11} so that the two modes

can co-exist without interacting with each other. It has been shown by Wien[34] that the interaction between the free vibrations of two resonators depend on the coupling coefficient k' and the ratio of the resonance frequencies of the two resonators. We shall calculate the coupling coefficient k' of the two companion modes under normal condition with the help of the field theory.

The coupling coefficient between the two modes is defined broadly as follows :

$$k' = (W_{1,2})/\sqrt{(W_1 W_2)} \tag{18}$$

Where, W_1 and W_2 represent the energies stored in the H_{01} and E_{11} modes respectively and $W_{1,2} = W_{2,1}$ represents the mutual energy, or the energy interchanged between the two modes. The total energy of the two modes in the resonator is given by the following relations[68] in m.k.s. rationalised units.

$$W = \frac{1}{2\mu} \int_v (\vec{B_1} + \vec{B_2}) \cdot (\vec{B_1} + \vec{B_2}) \, dv$$

$$= \frac{\mu}{2} \left[\int_v H_1^2 \, dv + 2 \int_v \vec{H_1} \cdot \vec{H_2} \, dv + \int_a H_2^2 \, dv \right] \tag{19}$$

The first and the last terms of the right hand side in eqn. [19] give the energy stored in the desired and the companion modes respectlvely. The second term gives the energy used in bringing the two modes into interaction, or, in other words, the mutual energy between the two coupled modes.

Hence

$$W_{1,2} = \mu \int_v H_1 \cdot H_2 \, dv \tag{20}$$

For a cylindrical cavity resonator having radius a and length L, the expression equation [20] for the mutual energy becomes

$$W_{1,2} = \mu \int_0^a \int_0^{2\pi} \int_0^L \vec{H_1} \cdot \vec{H_2} \, \rho \, d\rho \, d\theta \, dz$$

The expressions for the components H_1 and H_2 for the two modes H_{01} and E_{11} are

$$\left| \vec{H_1} \right| = \left\{ (k_3^2/k^2) \, [J_0'(k_1\rho)]^2 \cos^2 k_3 z + (k_1^2/k^2) \, J_0^2(k_1\rho) \sin^2 k_3 z \right\}^{1/2} \tag{21}$$

$$\left| \vec{H_2} \right| = \left\{ (J_1^2(k_1\rho)/k_1^2\rho^2) \sin^2\theta \cos^2 k_3 z + [J_1'(k_1\rho)]^2 \cos^2\theta \cos^2 k_3 z \right\}^{1/2} \tag{22}$$

Substituting eqns. [21] and [22] in [20] and integrating and making some approximations, the following expression for the mutual energy $W_{1,2}$ is obtained[21]

$$W_{1,2} \simeq -\frac{2\pi\mu k_1^3}{4\,k\,k_3} \left[\frac{L}{2} - \frac{\sin 2k_3 L}{4\,k_3} \right] \times \frac{128\,k_1}{9\pi} \left[\frac{a^4}{8} - \frac{a^3}{4k_1}\cos 2k_1 a \right.$$
$$\left. + \frac{3}{8k_1^2}a^2 \sin 2k_1 a + \frac{3}{8k_1^3}a \cos 2k_1 a - \frac{3}{16k_1^4}\sin 2k_1 a \right] \qquad [23]$$

The maximum energies stored in the electric field of the resonator operating in the H_{01} and E_{11} modes respectively are given by the following expressions[21]

$$W_1 = \frac{\epsilon}{2} \int_0^a \int_0^{2\pi} \int_0^L \rho\,[J_0'(k_1\rho)]^2\,\sin^2 k_3 z\,\,d\rho\,\,d\theta\,\,dz$$

$$= + \frac{\epsilon\,\pi\,a^2\,L}{4}\,J_0^2\,(k_{01}) \qquad [24]$$

$$W_2 = \frac{\epsilon}{2} \left[\frac{k_3^2}{k^2} \int_0^a \int_0^{2\pi} \int_0^L \rho\,[I_1'(k_1\rho)]^2\,\cos^2\theta\,\sin^2 k_3 z\,\,d\rho\,\,d\theta\,\,dz \right.$$

$$+ \frac{k_3^2}{k^4} \int_0^a \int_0^{2\pi} \int_0^L \rho\,\frac{J_1^2(k_1\rho)}{k_1^2\rho^2}\,\sin^2\theta\,\sin^2 k_3 z\,\,d\rho\,\,d\theta\,\,dz$$

$$\left. + \frac{k_1^2}{k^2} \int_0^a \int_0^{2\pi} \int_0^L \rho\,J_1^2\,(k_1\rho)\,\cos^2\theta\,\cos^2 k_3 z\,\,d\rho\,\,d\theta\,\,dz \right]$$

$$= \frac{\epsilon L}{4} \left[\frac{\pi\,a^2}{2} - \frac{\pi\,k_3^2}{k^2\,k_1^2} + \frac{\pi k_3^2}{k^4 k_1} \right] J_0^2\,(k_{11}) \qquad [25]$$

The coupling coefficient k' between the two modes is found from equations [18], [23-25] as follows :

$$k' = -256\,\mu\,k_1^4 \left[\frac{L}{2} - \frac{\sin 2k_3\,L}{4\,k_3} \right]$$

$$\times \left\{ \frac{[a^4/8 - (1/4k_1)a^3\cos 2k_1 a + (3/8k_1^2)a^2\sin 2k_1 a + (3/8k_1^3)a\cos 2k_1 a - (3/16k_1^4)\sin 2k_1 a]}{9\,a \in L\,k\,k_3\,J_0\,(k_{01})\,J_0\,(k_{11})\,\sqrt{\{\pi(\pi a^2/2 - \pi k_3^2/k^4 k_1^2 + \pi k_3^2/k^4 k_1)\}}} \right\}$$
$$[26]$$

2.7. *Coupled Frequencies* :

When the two modes H_{01n} and E_{11n} coexist, the cavity will oscillate in two different resonant frequencies, one slightly above and the other slightly below the uncoupled resonant frequencies $f_{01n} = f_{11n} = f_0$ of the two individual modes. These coupled frequencies depend on the coupling coefficient k' and are given by

$$f_{c1} = f_0 / \sqrt{(1 + k')} \; ; \quad f_{c2} = f_0 / \sqrt{(1 - k')} \tag{27}$$

If the coupling is loose these two coupled resonance frequencies may be quite close together and the effect is that the the cavity will oscillate over a band of frequencies $\triangle f$ given by the difference of the two frequencies $f_{c2} - f_{c1}$. This can be reduced to $\triangle f = k' \, f_0 / \sqrt{[1 - (k')^2]}$, provided k' is small.

3. SOMMERFELD SURFACE WAVEGUIDE

Sommerfeld surface waveguide (see Fig. 2) consists of an infinitely long straight metallic wire of circular cross-section having finite conductivity imbedded in a dielectric of infinite extent and excited by E_0 wave. Treating this as a boundary value problem and matching the fields at the surface $(\rho = d)$, the following characteristic equation for the E_0 wave is obtained.

$$\frac{k_1^2}{\mu_1 \, u} \frac{J_1(u)}{J_0(u)} = \frac{k_2^2}{\mu_2 \, v} \frac{H_1^{(1)}(v)}{H_0^{(1)}(v)} \tag{28}$$

where

$$u = \gamma_1 \, d \; ; \quad v = \gamma_2 \, d \; ; \quad \gamma_1^2 = k_1^2 - h^2 \; ; \quad \gamma_2^2 = k_2^2 - h^2 \; ;$$
$$k_1^2 = \omega^2 \, \mu_1 \, \epsilon_1 + i \, \omega \, \sigma_1 \, \mu_1 \; ; \quad k_2^2 = \omega^2 \, \mu_2 \, \epsilon_2.$$
$$h = \text{axial propagation constant.}$$

The following cases are of interest :

For $\sigma_1 = \infty$ eqn. [28] reduces to

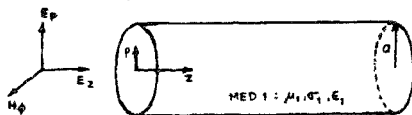$$\frac{H_0^{(1)}(v)}{H_1^{(1)}(v)} = 0 \tag{29}$$

FIG. 2

Sommerfeld surface wave guide : Coordinats system

If ν is small *i.e.* for a very thin conductor

$$H_0^{(1)}\,(\upsilon)\cong\frac{2i}{\pi}\ln\frac{\gamma\,\upsilon}{2i}\;;\qquad H_1^{(1)}\,(\upsilon)\cong\frac{2i}{\pi\upsilon} \tag{30}$$

The principal branch of $H_n^{(1)}(\upsilon)$ vanishes at all infinite points of the positive imaginary half-plane. The roots of only the principal branch of the multi-valued Hankel function are of interest, but the principal branches of $H_0^{(1)}(\upsilon)$ and $H_1^{(1)}(\upsilon)$ have no roots so,

$$\frac{H_0^{(1)}\,(\upsilon)}{H_1^{(1)}\,(\upsilon)}=-\upsilon\,\ln\,\frac{\gamma\upsilon}{2i}=0 \tag{31}$$

where, $\gamma=1.781$

possesses the only solution $\upsilon=0$ *i.e.* $h=k_2$.

This means that when a cylindrical conductor of infinite conductivity imbedded in a dielectric medium is excited by the fundamental E wave, the field is propagated in the axial direction with a velocity which is solely determined by the characteristics of the external medium. If the conductor is imbedded in free space, the field is propagated along the cylinder without attenuation and with phase velocity equal to the free space velocity c.

If σ is large but not equal to infinity, $h\neq k_2$ but the difference $h\sim k_2$ for E_0 wave is very small. So, υ is small but $|k_1| >> k_2$ since $k_2\cong|h|$ and $u\simeq k_1\,d >> 1$. Therefore, representing $J_0(u)$ and $J_1(u)$ by asymptotic expansions and $H_0^{(1)}(\upsilon)$ and $H_1^{(1)}(\upsilon)$ by small argument approximations, the following equation is obtained from equation [28].

$$\upsilon^2\,\ln\frac{\gamma\upsilon}{2i}=i\,\frac{\mu_1}{\mu_2}\,\frac{k_2^2\,d}{k_1} \tag{32}$$

$$\text{which reduces to}\quad \xi\,\ln\xi=\eta \tag{33}$$

where,

$$\xi=\left(\frac{\gamma\,\upsilon}{2i}\right)^2$$

and

$$\eta=-\frac{i\gamma^2}{2}\,\frac{\mu_1}{\mu_2}\,\frac{k_2^2\,d}{k_1}$$

Equation [33] is the basic Sommerfeld equation which when solved gives the characteristics, such as the propagation factor in the axial direction, attenuation constant, phase constant and phase velocity of the Sommerfeld surface wave .

Sommerfeld's analysis leads to the following conclusions.

(i) A solid cylindrical conductor of circular cross-section can support an infinite number of propagating modes. The amplitudes of these modes are coefficients involved, in the field components. These coefficients are determined by the nature of the source,

(ii) of all the modes, only the Eo mode possesess relatively low attenuation. All the other symmetric E and symmetric H and all the asymmetric modes suffer rapid attenuation within a very short distance from the source, even at very low frequencies, and as such are of no practical interest.

(iii) In order that the Eo mode may be bound to the surface of the conductor. the conductivity of the conductor can be high but must be finite.

(iv) The electric lines of forces outside the conductor are almost perpendicular but not exactly to the surface of the conductor. The wave front in the external medium is slightly tilted forward in the direction of propagation. The Poynting vector being directed towards the conductor, the energy flow into the conductor accounts for the Joule heat losses.

(v) The phase velocity of the wave is slightly less than the free space velocity for conductors having high conductivity and radius of curvature greater than the skin depth.

(vi) The radial field decay in the region outside the conductor is governed by the Hankel function $H_1^{(1)}(\gamma_2\rho)$. The field extension in the radial direction is large and can be reduced by decreasing the conductivity and radius of the conductor and by increasing the frequency of excitation.

(vii) Since the wave is guided along the conductor, its attenuation in the x-direction is produced solely due to definite conductivity of the wire. In the conceptual limit of infinite conductivity, the E wave passes to a T-wave and decreases in amplitude in the radial direction as $1/\rho$

(viii) An ohmic loss on the surface of the guide is essential for the Sommerfeld surface wave to be supported by the conductor.

Sommerfeld surface waveguide is not of much use in practice, as the *Eo* wave supported by the structure is not tightly bound to the surface *i.e.* the extent of the field in the radial direction is inconveniently large. As such any discontinuity in the path of the wave such as a bend or kink in the wire produces considerable loss of power by radiation. The inherent short-coming of the Sommerfeld guide is that its ohmic loss is essential to its operation in contrast with the conventional waveguide for which the ohmic loss is only incidental. This difficulty has been obviated by Goubau[56] by coating the

wire with a thin layer of dielectric. The dielectric coating loads the surface in such a way that the E_o wave is guided by the structure and the extent of the field spread in the radial direction is comparatively much smaller even in the case of the conductor having infinite conductivity. In a surface wave structure of this type, the ohmic loss is only incidental and the extent of the radial field spread is controlled solely by the thickness and dielectric constant of the dielectric film. The characteristics of the dielectric coated structure was first studied by Harms[69] and then more exhaustively by Goubau[56].

4. HARMS-GOUBAU SURFACE WAVEGUIDE

Harms[69] made a theoretical study of the problem of wave propagation along a cylindrical wire of radius d coated with a dielectric of thickness $(b-d)$ and dielectric constant E_1 (see Fig. 3). Goubau[56;59] made a detailed theoretical and experimental study of the problem and evaluated its practical usefulness as a transmission line for microwaves. Treating this as a boundary-value problem and using the impedance matching technique at $\rho = b$ for E_o wave, the following characteristic equation isobtained.

$$\frac{1}{\epsilon_1} \frac{\gamma_1 J_0 (\gamma_1 b) Y_0 (\gamma_1 d) - J_0 (\gamma_1 d) J_0 (\gamma_1 b)}{J_1 (\gamma_1 b) Y_0 (\gamma_1 d) - J_0 (\gamma_1 d) Y_1 (\gamma_1 b)} = -\frac{\gamma_2}{\epsilon_2} \frac{H_0^{(1)} (i \gamma_2 b)}{H_1^{(1)} (i \gamma_2 b)} \tag{34}$$

which yields the following equation[56] after some simplication.

$$(\mu_2/\epsilon_2)^{1/2} (\gamma_2^2/k_2) b \ln 0,89 \gamma_2 b = -(\mu_1/\epsilon_1)^{1/2} (\gamma_1/k_1) b \ln (b/a) \tag{35}$$

where $k_1^2 = \omega^2 \mu_1 \epsilon_0$ and $k_2^2 = \omega^2 \mu_0 \epsilon_2$.

In order that the radial impedances at $\rho = b$ be continuous, it is necessary that the axial propagation constant in the two media be the same, *i.e.*

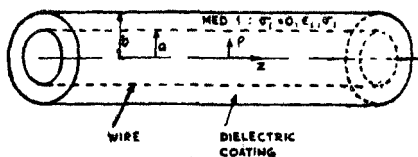$$\sqrt{(k_1^2 - \gamma_1^2)} = \sqrt{(k_2^2 + \gamma_2^2)} \tag{36}$$

FIG. 3

Harms—Goubau surface wave guide

The radial constant γ_2 and hence the phase velocity $v_p = \omega \sqrt{(k_2{}^2 + \gamma_1{}^2)}$ of the wave can be determined from equations [35] and [36]. Since, γ_2 is positive and real $v_p < \omega/k_2$ which is the free space velocity in the case of the medium 2 being air.

The division of power between the two media 1 and 2 is calculated from the Goubau relation

$$\frac{P_1}{P_2} = -\frac{\epsilon_2}{\epsilon_1} \frac{ln\,(b/d)}{ln\,0.89\ \gamma_2\,b + 0.5} \tag{37}$$

where, P_2 represents the power of the surface wave which is contained in the external medium. This equation is used to determine the thickness of the dielectric coating $(b-d)$ required for a dielectric material to constrain a certain percentage of power of the surface wave within a specified distance from the surface of the structure. The above results are derived on the basis of no loss. The effect of dissipation is determined by using the perturbation method *i e.* by assuming that the field distribution in an equiphase plane is the same as that in the case when there is no loss. The conclusions drawn from the foregoing analysis are:

(i) The field structure of Harms-Goubau guide is the same as that of Sommerfeld guide.

(ii) The extent of the field spread in the radial direction decreases with increasing dielectric constant and thickness of coating *i.e.* the radial extension of the field can be controlled by modifying the surface of Sommerfeld guide.

(iii) In the case of Sommerfeld guide, if the conductivity is increased indefinitely, the radial extension of the field would increase in such a way that the power carried by a wave of finite amplitude would become infinite which is physically inadmissible. But in the case of Harms-Goubau guide, the wave will still remain a guided wave with a limited radial extension of the field. even in the case when the conductivity of the wave is increased indefinitely, The field is only slightly affected,

(iv) Compared to the Sommerfeld guide the Harms-Goubau guide possesses higher loss. Losses of this type of guide consists of (*a*) the ohmic loss in the conductor which is also present in the Sommerfeld guide (*b*) the loss in the dielectric film which is not present in the Sommerfeld guide (c) the loss due to the finite size of the launching device. As the radial field spread is more in Sommerfeld guide, it requires a much longer dimension of the launching device than Goubau guide. For the same dimension of the launching device, Sommerfeld line will have more loss.

(v) The phase velocity of the wave guided by the dielectric coated structure is less than the free space velocity.

(vi) As $H_0^{(1)}$ ($i\ \gamma_2 b$) is negative imaginary and $H_1^{(1)}$ ($i\ \gamma_2 b$) is negative real for positive imaginary argument, it follows that the surface impedance is negative imaginary, *i. e.* the surface impedance of this guide is purely inductive. Or, in other words, coating the wire with a dielectric amounts to loading inductively the surface of the conductor.

(vii) The axial component of the Poynting vector integrated over a plane perpendicular to the axial direction yields a finite value which leads to the physical realisability of Goubau wave.

5. ATTENUATION CONSTANTS

5.1 *Sommerfeld Line* :

From the relations

$$h = \alpha + j\beta ; \quad \gamma_2 = a_2 - jb_2 ; \quad k_2^2 = \omega_2\ \mu_0\ \epsilon_0 = -(h_2 + \gamma_2^2) \qquad [38]$$

and assuming that at microwave frequencies

$$k_2^2 >\ > (a_2^2 - b_2^2) ; \quad a_2 >\ > b_2 \qquad [39]$$

the attenuation constant of the Sommerfeld line is[53]

$$a(\text{sommerfeld}) = (c/\omega)\ (a_2 b_2) \qquad [40]$$

5.2 *Harms-Goubau Line*

Assuming that there is no loss due to radiation, the total loss in Harms-Goubau line is due to the ohmic loss in the wire (α_c) and dielectric loss in the coating (α_d). The attenuation constants α_c and α_d are[56]

$$\alpha_c \simeq \frac{1}{2d}\sqrt{\frac{\epsilon_0\ \omega\ \mu_w}{2\mu_0\sigma_w}}\ \frac{1}{ln\ \gamma_2 b + 0.38}\text{Nepers}/m \qquad [41]$$

$$\alpha_d \simeq \frac{\gamma_2^2}{2k}\ \frac{\epsilon_0}{\epsilon_d - \epsilon_0}\ \left(1 - \frac{0.5}{ln\ \gamma_2 b + 0.38}\right)\ \tan\delta\text{Neper}/m \qquad [42]$$

The radial propagation factor is obtained from

$$G\ (\gamma_2 b) = -(\gamma_2 b/2\ \pi)^2\ ln\ (0.89\ \gamma_2 b) \qquad [43]$$

where,

$$G\ (\gamma_2 b) = \frac{ln\ (b/d)}{(\epsilon_d/\epsilon_d - \epsilon_0)\ (\lambda/b)^2}$$

The attenuation constant α (Harms-Goubau line) $= \alpha_d + \alpha_c$

where,

$k =$ free space wave propagation

constant $= \omega \, (\mu_0 \, \epsilon_0)^{1/2}$

$\epsilon_d =$ dielectric constant of the dielectric coating

6. COMPARATIVE STUDY OF THE SOMMERFELD AND HARMS GOUBAU LINES

A comparative study of the characteristics such as radial decay factor (γ) as a function of the radius of the Sommerfeld line and as a function of the dielectric constant for different coating thickness in the case of the Harms-Goubau line for different wavelength of excitation, ratio of the radii of the constant percentage power contour as a function of coating thickness $b-d=a$ for different wavelength of excitation and percentage reduction in phase velocity as a function of wire radius are presented in figures (4-7) respectively. Fig. 8 shows the percentage power flow for the Harms Goubau and Sommerfeld line as a function of the radial distance from the line. Fig. 9 shows a comparative study of the conduction and dielectric loss in the case of the Harms-Goubau line as a function of dielectric coating thickness in the X and K band.

7. THEORY OF THE SURFACE WAVE RESONATOR

The resonator (see Fig. 1) consists of a metallic wire of radius d terminated at both ends by large circular metallic plates each of radius $a >> d$. The length l of the wire is adjusted such that it is an integral multiple of half the guide wavelength λ_g corresponding to the mode of excitation. The resonator is open on all sides except at the two ends.

7.1 *Field Components of Resonant Waves*

The components of resonant waves, when the resonator oscillates in pure E or H modes are respectively[42].

E mode :

$$E_{zr}(\rho) = 2 \, \chi \cos \theta \cos (m_z \pi / l) \, z \, J_1 (\gamma_e \rho)$$

$$E_{\rho r}(\rho) = 2j \, (h \, \gamma_e / \omega^2 \, \mu_0 \epsilon_0) \, \chi \cos \theta \sin (m_z \pi / l) \, z \, J_1' (\gamma_e \rho)$$

$$E_{\theta r}(\rho) = -2j \, \chi \, (h / \omega^2 \, \mu_0 \epsilon_0) \, 1/\rho \sin \theta \sin (m_z \pi / l) \, z \, J_1 (\gamma_e \rho)$$

$$H_{\rho r}(\rho) = -2j \, \chi \, (1 / \omega \mu_0) \, (1/\rho) \sin \theta \cos (m_z \pi / l) \, z \, J_1 (\gamma_e \rho)$$

$$H_{\theta r}(\rho) = -2j \, \chi \, (\gamma_e / \omega \mu_0) \cos \theta \cos [(m_z \pi) / l] \, z \, J_1' (\gamma_e \rho) \tag{44}$$
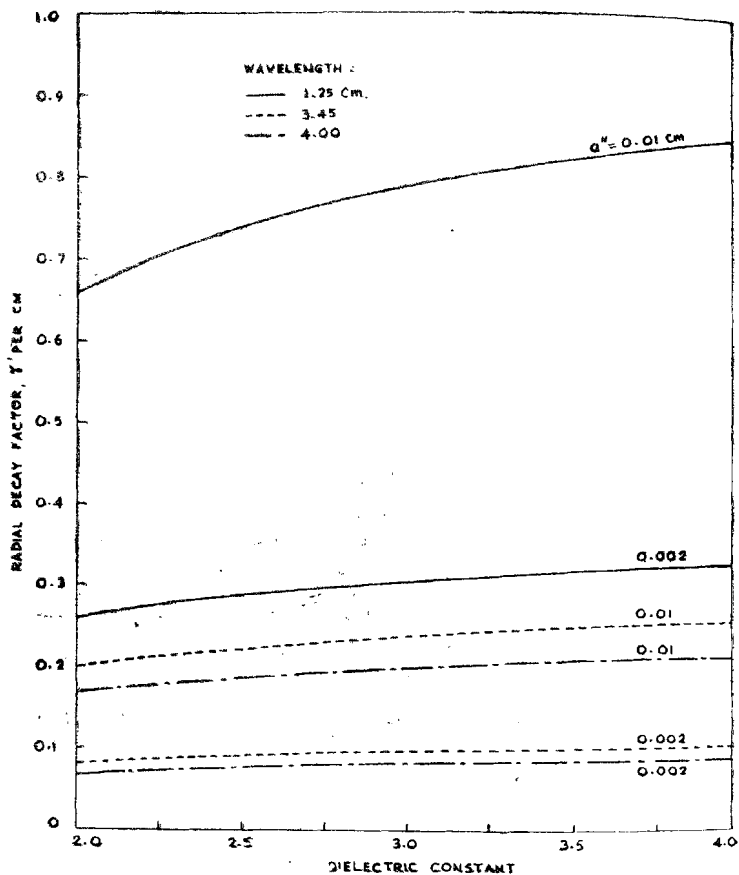
S. K. CHATTERJEE, *et. al.*

FIG. 4

Radial decay factor as a function of dielectric constant of the coating
for different wavelengths   Wire radius, $a = 0.10$ cm.

Fig. 5

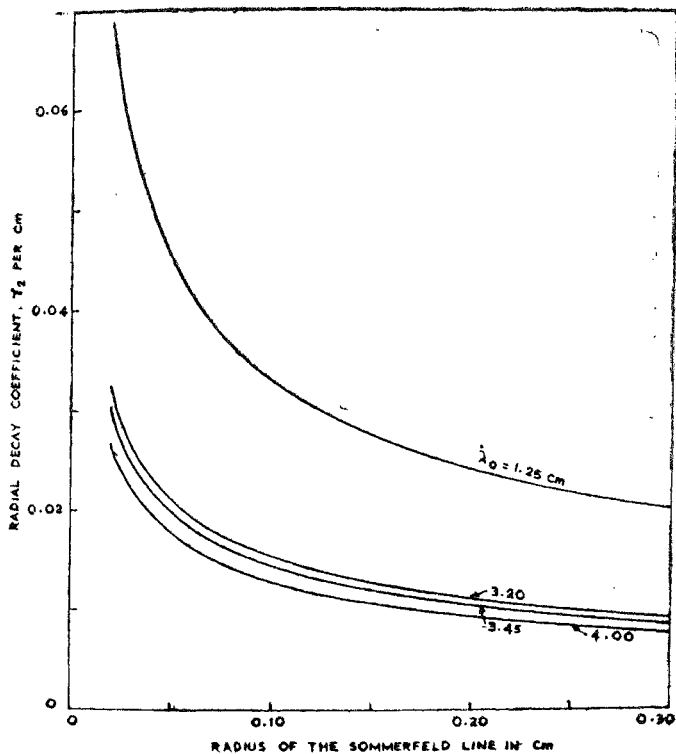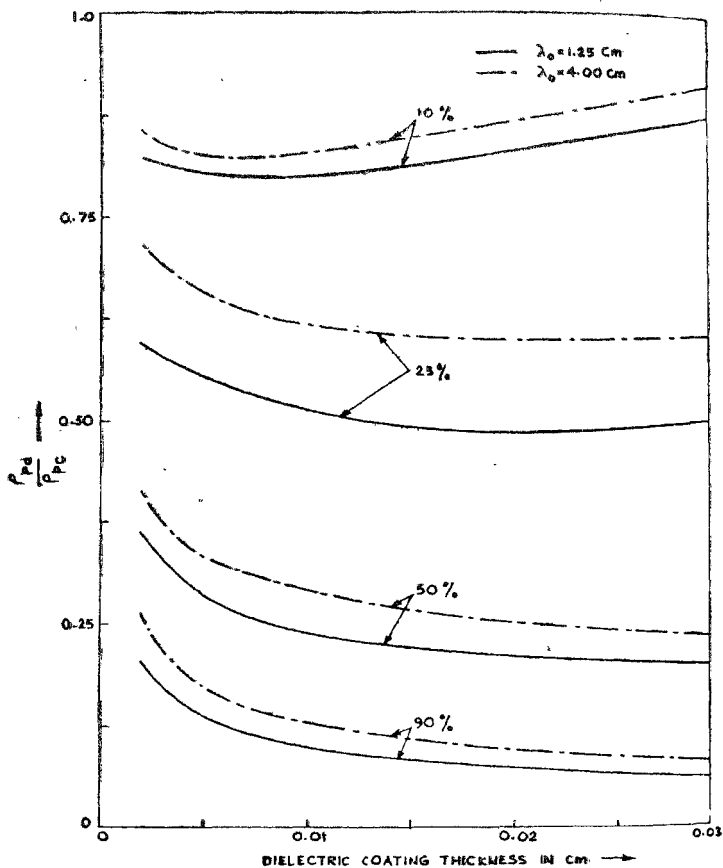Radial decay factor as a function of wire radius for different wavelengths.

S. K. CHATTERJEE, *et. al.*

FIG. 6

Ratio of radii of the constant percentages power contour as a function of the dielectric coating thickness for different wavelengths. $a = 0.10$ cm, $\epsilon = 2.4$.
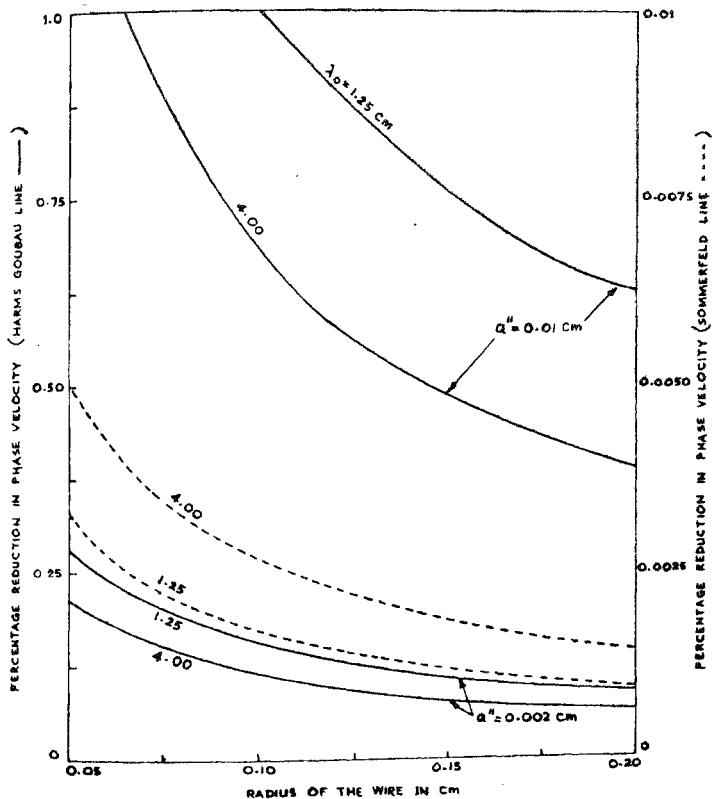
FIG. 7

Percentage reduction in phase velocity as a function of wire radius
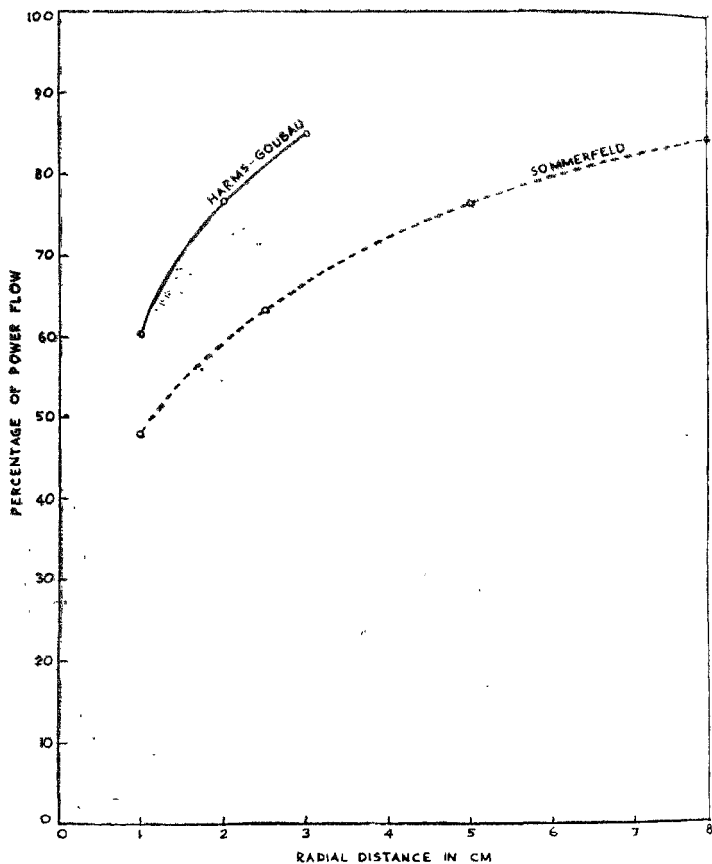for different wavelengths. $\epsilon = 2\cdot4$.

FIG. 8

Power distribution curves for a wire of radius $a=0.08$ cm,
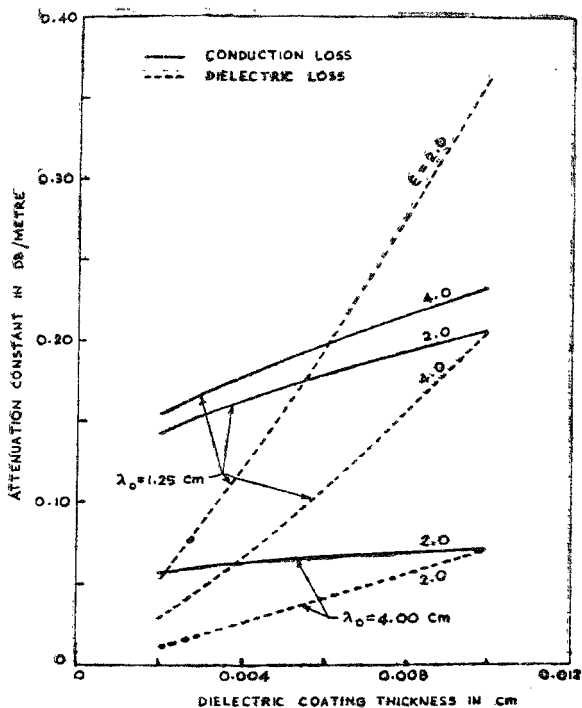coating thickness $a''=0.005$ cm. $\lambda_0=3.57$ cm.

FIG. 9

Attenuation constant as a function of dielectric coating thickness for different dielectric constants and wavelengths. Wire radius $a = 0.10$ cm.

H mode :

$$H_{zr}(\rho) = -2j\psi \sin\theta \sin(m_z\pi/l) z J_1(\gamma_h\rho)$$

$$H_{\rho r}(\rho) = 2\psi (h \gamma_h/\omega^2\mu_0\epsilon_0) \sin\theta \cos(m_z\pi/l) z J_1'(\gamma_h\rho)$$

$$H_{\theta r}(\rho) = 2\psi (h/\omega^2\mu_0\epsilon_0) (1/\rho) \cos\theta \cos(m_z\pi/l) z J_1(\gamma_h\rho)$$

$$E_{\rho r}(\rho) = -2\psi (1/\omega\epsilon_0) (1/\rho) \cos\theta \sin(m_z\pi/l) z J_1(\gamma_h\rho)$$

$$E_{\theta r}(\rho) = 2\psi (\gamma_h/\omega\epsilon_0) \sin\theta \sin(m_z\pi/l) z J_1'(\gamma_h\rho)$$

$$E_{zr}(\rho) = 0$$

The above field components are derived on the assumption that the electromagnetic energy is contained wholly within the volume $\pi a^2 l$ of the resonator and that there is no loss of energy by radiation.

7.2 *Conditions of Resonance*

The conditions of no radiation leads to

$$H_1^{(2)}(\gamma_e d) = -H_1^{(1)}(\gamma_e d)$$

which yields

$$J_1(\gamma_e d) = 0 \tag{46}$$

as the condition of resonance when the resonator is oscillating in a pure *E*-mode. The condition of resonance when the resonator is oscillating in a pure *H*-mode and the energy is completely enclosed within the volume of the resonator is

$$H_1^{(2)\prime}(\gamma_h d) = -H_1^{(1)\prime}(\gamma_h d)$$

which yields

$$J_1'(\gamma_h d) = 0 \tag{47}$$

The eigen values $\gamma_h d$ which satisfy the above equation is obtained when $J_1(\gamma_h d)$ is maximum *i.e.* $\gamma_h d = 1.84, 8.54, 14.86$, etc.

7.3 *Coupled E and H modes*

In the case of a conventional type of cavity resonator enclosed on all sides by highly conducting metallic walls, no loss of energy occurs by radiation and *E* or *H* modes can exist independently, whereas, in the case of an open type resonator, due to the discontinuity which is invariably present at the edge $(\rho = a)$ of the end plates, some energy will be lost by radiation. As the radiated wave in free space is a *T*-wave, E_ρ^e, H_ρ^e and E_ρ^h, H_ρ^h of the *E* and *H* modes respectively, must vanish inside the resonator or approach zero value at $\rho = a$. But the radial components of *E* and *H* modes of the non-radiating standing wave part of the total field within the resonator cannot independently become zero. So, it may be said that

$$E_\rho^e + E_\rho^h = 0 \qquad [48]$$

or
$$H_\rho^e + H_\rho^h = 0 \qquad [49]$$

at $\rho = a$, which signifies that the E and H modes are coupled.

The characteristic equation for the coupled mode obtained by imposing proper boundary conditions on appropriate field components and utilising the no-radiation condition is

$$-\frac{j\,\omega\,\mu_0}{h\,\gamma a}\;\frac{y\,H_1^{(1)}(\gamma a) - H_1^{(2)}(\gamma a)}{x\,H_1^{(1)}(\gamma a) - H_1^{(1)}(\gamma a)} = -j\frac{\gamma d\,\omega,\mu_0}{h}\;\frac{y\,H_1^{(1)\prime}(\gamma d) - H_1^{(2)}(\gamma d)}{x\,H_1^{(1)}(\gamma d) - H_1^{(2)}(\gamma d)} \quad [50]$$

where,
$$x = \frac{H_1^{(2)}(\gamma_e d)}{H_1^{(1)}(\gamma_e d)} \qquad [51]$$

and
$$y = \frac{H_1^{(2)\prime}(\gamma_h d)}{H_1^{(1)\prime}(\gamma_h d)}$$

and
$$\gamma = \gamma_{eh}$$

It can be shown that for the resonance conditions $J_1(\gamma_e d) = 0$, $x = 1$ and similarly $y = -1$ from the definition of x and y. By using appropriate recurrence relations and $x = 1$, $y = -1$ eqn. [50] reduces to

$$\frac{J_1(\gamma a)}{\gamma a\,J_0(\gamma a) - J_1(\gamma a)} = \frac{\gamma d\,J_0(\gamma d) - J_1(\gamma d)}{J_1(\gamma d)} \qquad [52]$$

which yields on differentiation with respect to γa

$$\gamma a\,J_0^2(\gamma a) - 2\,J_1(\gamma a)\,J_0(\gamma a) + \gamma a\,J_1^2(\gamma a) = 0 \qquad [53]$$

since
$$\frac{J_1(\gamma a)}{\gamma a\,J_0(\gamma a) - J_1(\gamma a)} = \text{constants.}$$

Let the roots of eqn. [53] be δ_n $(n = 1, 2, 3, \ldots)$. For mth mode, the eigen values $\gamma_{eh} = \gamma$ is given by $\gamma_{eh} = \delta_m/a$ and the condition of resonance for the coupled mode is

$$\left[\frac{m_z\,\pi}{l} = \frac{4\,\pi^2}{\lambda_0^2} - \frac{\delta_m^2}{a^2}\right]^{1/2} \qquad [54]$$

since, $m_2\pi/l$ is positive and real $(\delta_m/a) < (2\pi/\lambda_0)$ and $(\delta_m^2/a^2) < < (4\pi^2/\lambda_0^2)$. Hence,

$$l = m_2\,\lambda_0/2 \qquad [55]$$

which states that the resonance condition is established, when the distance between the two terminating end plates is an integral multiple of half wavelength.

In practice $d < < a$ and if $\gamma d < < 1$, then by making small argument approximation of $J_0(\gamma d) \cong 1$ and $J_1(\gamma d) \cong \gamma d/2$, eqn. [52] reduces to

$$J_0(\gamma_{eh} a) = 0 \tag{36}$$

which gives the successive eigen values when resonator is oscillating under the condition that the modes are coupled.

7.4. *Q of the Resonator*

The Q of the resonator is defined as

$$Q = \omega \frac{W_E}{P} \text{ or } \omega \frac{W_M}{P} \tag{37}$$

where, ω is the angular frequency at resonance, W_E and W_M represent the maximum energy stored in the electric and magnetic fields respectively inside the resonator and P is the total power loss inside the resonator.

The total power lost is equal to the sum of the power lost in the end plates (P_e) and power lost in the wire (P_w) and the power lost by radiation. Assuming that there is no loss of power by radiation and that the resonator is oscillating in pure E or H modes and calculating

$$W_E = \frac{\epsilon_0}{2} \int_{\theta=0}^{2\pi} \int_{\rho=d}^{a} \int_{z=0}^{l} |E|^2 \, \rho \, d\rho \, d\theta \, dz$$

$$W_M = \frac{\mu_0}{2} \int_{\rho=}^{2\pi} \int_{\rho=}^{a} \int_{z=0}^{l} |H|^2 \, \rho \, d\rho \, d\theta \, dz$$

$$P_e = 2 \times 1/2 \sqrt{\frac{\pi f \mu_0}{\sigma_e}} \int_{\theta=0}^{2\pi} \int_{\rho=d}^{a} |H_{tan}|^2 \, \rho \, d\theta \, d\rho \tag{58}$$

for both the end plates and

$$P_w = \sqrt{\frac{\pi f \mu_0}{\sigma_w}} \int_{\theta=0}^{2\pi} \int_{z=0}^{l} |H_{tan}|^2 \, d \, d\theta \, dz$$

the Q factor for the E (Q^E) and H (Q^H) modes are

$$Q^E = \langle [\{2 - \gamma_e^2 a^2\} \, J_1^2 \, (\gamma_e a) - \{\gamma_e^2 a^2 - 2 \, \gamma_e - 2\} \, J_0^2 \, (\gamma_e a)$$
$$+ \{\gamma_e^2 d^2 + 2 \, \gamma_e - 2\} \, J_0^2 \, (\gamma_e d)] \, f^{-3/2} h^2 \, l \times 81.64 \times 10^{29}$$
$$+ [a^2 \, J_1^2 \, (\gamma_e a) - a^2 \, J_0 \, (\gamma_e a) \, J_2 \, (\gamma_e a) - d^2 \, J_0^2 \, (\gamma_e d)] f^{5/2} \times 1.57 \rangle$$
$$\div \{ -120.31 \times 10^{-39} [-\tfrac{1}{2} \, \gamma_e^2 d^2 \, J_0^2 \, (\gamma_e d) - \tfrac{1}{2} \, \gamma_e^2 \, a^2 \, J_0^2 \, (\gamma_e a)$$
$$- (1 - \tfrac{1}{2} \, \gamma_e^2 \, a^2)] \, J_1^2 \, (\gamma_e a)] - 52.2 \times 10^{-39} \, \gamma_e^2 \, d \, l \, J_0^2 \, (\gamma_e \, d)\} \qquad [59]$$

$$Q_H = 179 \times 10^8 f^{-1} \, l \, [\tfrac{1}{2} \, \gamma_h^2 \, a^2 - 1) \, J_1^2 \, (\gamma_h a) + \tfrac{1}{2} \, \gamma_h^2 a^2 \, J_0^2 \, (\gamma_h a)$$
$$- (\tfrac{1}{2} \, \gamma_h^2 d^2 - 1) \, J_1^2 \, (\gamma_h d) - \tfrac{1}{2} \, \gamma_h^2 \, d^2 \, J_0^2 \, (\gamma_h d)]$$
$$\div \{694.22 \times 10^{22} \, h^2 f^{-7/2} \, [(\tfrac{1}{2} \, \gamma_h^2 a^2 - 1) \, J_1^2 \, (\gamma_h a) + \tfrac{1}{2} \, \gamma_h^2 a^2 \, J_0^2 \, (\gamma_h a)$$
$$- (\tfrac{1}{2} \, \gamma_h^2 d^2 - 1) \, J_1^2 \, (\gamma_h d) - \tfrac{1}{2} \, \gamma_h^2 d^2 \, J_0^2 \, (\gamma_h d)]$$
$$+ 2 \, 61 \times 10^{-7} \, d \, l f^{1/2} \, [52 \times 10^{29} \, (h^2/d) f^{-4} - 1] \, J_1^2 \, (\gamma_h \, d)\} \qquad [60]$$

The Q factor for the coupled EH and HE modes are respectively

$$Q_{EH} = 81.64 \times 10^{29} f^{-3/2} \, h^2 \, l \, [\{2 - \gamma^2 a^2\} \, J_1^2 \, (\gamma a) - \{2 - \gamma^2 d^2\} \, J_1^2 \, (\gamma d)$$
$$+ \{\gamma^2 d^2 + 2 \, \gamma - 2\} \, J_0^2 \, (\gamma d) + 1.57 f^{5/2} \, l \, [a^2 \, J_1^2 \, (\gamma a)$$
$$- d^2 \, J_1^2 \, (\gamma d) + d^2 \, J_0 \, (\gamma d) \, J_2 \, (\gamma d)] \div \{ -120.31 \times 10^{-39} \times$$
$$[-\tfrac{1}{2} \, \gamma^2 d^2 \, J_0^2 \, (\gamma d) + (1 - \langle \gamma^2 d^2/2 \rangle) \, J_1^2 \, (\gamma d) - (1 - \tfrac{1}{2} \, \gamma^2 a^2) \, J_1^2 \, (\gamma a)]$$
$$- 52.2 \, \gamma^2 \, d \, l \times 10^{-39} \, [J_0^2 \, (\gamma d) + \langle J_1^2 \, (\gamma d)/\gamma^2 \, d^2 \rangle$$
$$- \langle 2 \, J_0 \, (\gamma d) \, J_1 \, (\gamma d)/\gamma \, d \rangle \,] \} \qquad [61]$$

where, $\gamma = \gamma_{eh.}$

$$Q^{HE} = 179 \times 10^8 \, l f^{-1} \, [(\tfrac{1}{2} \, \gamma^2 a^2 - 1) \, J_1^2 \, (\gamma a)$$
$$- (\tfrac{1}{2} \, \gamma^2 d^2 - 1) \, J_1^2 \, (\gamma d) - \tfrac{1}{2} \, \gamma^2 d^2 \, J_0^2 \, (\gamma d) \,]$$
$$\div 694.22 \times 10^{22} f^{-7/2} \, h^2 \, [(\tfrac{1}{2} \, \gamma^2 a^2 - 1) \, J_1^2 \, (\gamma a)$$
$$- (\tfrac{1}{2} \, \gamma^2 d^2 - 1) \, J_1^2 \, (\gamma d) - \tfrac{1}{2} \, \gamma^2 d^2 \, J_0^2 \, (\gamma d) \,]$$
$$+ 2.61 \times 10^{-7} \, l \, d f^{1/2} \, [52 \times 10^{29} f^{-4} \, h^2 \, d^{-1} - 1] \, J_1^2 \, (\gamma \, d) \, \} \qquad [62]$$

where, $\gamma = \gamma_{he}$

7.5 *Guide Wavelength*

The values of the axial propagation constant h in the case of the resonator oscillating in pure E or H mode are obtained from the condition $W_E = W_M$ at resonance from the following equations.

E mode :

$$26 \times 10^{29} f^{-4} h^2 \{ -\gamma_e^2 a^2 \{ J_1^2 (\gamma_e a) + J_0^2 (\gamma_e a) \}$$
$$+ \gamma_e^2 d^2 J_0^2 (\gamma_e d) + 2 J_1^2 (\gamma_e a) + 2 \gamma_e \{ J_0^2 (\gamma_e a)$$
$$+ J_0^2 (\gamma_e d) \} + 2 \{ J_0^2 (\gamma_e a) - J_0^2 (\gamma_e d) \}]$$
$$= 22 \times 10^{14} f^{-2} [J_1^2 (\gamma_e a) + \frac{1}{2} \gamma_e^2 d^2 J_0^2 (\gamma_e d) - [(\gamma_e^2 a^2)/2]$$
$$\times \{ J_0^2 (\gamma_e a) + J_1^2 (\gamma_e a) \}]$$
$$- \frac{1}{2} a^2 \{ J_1^2 (\gamma_e a) - J_0 (\gamma_e a) J_2 (\gamma_e a) \} - \frac{1}{2} d^2 J_0^2 (\gamma_e d) \qquad [63]$$

H *mode* :

$$26 \times 10^{29} f^{-4} h^2 [-\gamma_h^2 d^2 J_1^2 (\gamma_h d) + 2 \{ J_1^2 (\gamma_h d)$$
$$+ J_0^2 (\gamma_h d) \} + \gamma_h^2 a^2 \{ J_1^2 (\gamma_h a) + J_0^2 (\gamma_h a) \} - 2 \{ J_1^2 (\gamma_h a) + J_0^2 (\gamma_h a) \}]$$
$$= 22 \times 10^{14} f^{-2} [\gamma_h^2 a^2 / 2) \{ J_1^2 (\gamma_h a) + J_0^2 (\gamma_h a) \}$$
$$- (\gamma_h^2 d^2 / 2) \{ J_1^2 (\gamma_h d) + J_0^2 \gamma_h d) \} - \{ J_1^2 (\gamma_h a)$$
$$- J_1^2 (\gamma_h d) \}] - \frac{1}{2} d^2 \{ J_1^2 (\gamma_h d) - J_0^2 (\gamma_h d)$$
$$- J_0 (\gamma_h d) J_2 (\gamma_h d) \} + \frac{1}{2} a^2 \{ J_1^2 (\gamma_h a) - J_0 (\gamma_h a)$$
$$J_2 (\gamma_h a) \} - (\gamma_h^2 / 2) \{ J_1^2 (\gamma_h d) - J_1^2 (\gamma_h a) - J_0^2 (\gamma_h a)$$
$$+ J_0^2 (\gamma_h d) \} - (1/\gamma_h^2 \{ J_0^2 (\gamma_h a) - J_0^2 (\gamma_h d) \} \qquad [64]$$

The total propagation constants *h* for the coupled EH and HE modes is obtained from eqn. [55] and [56] respectively by replacing γ_e by γ_{eh} and γ_h by γ_{he} in equations [53] and [54] respectively and using the resonance condition $J_0 (\gamma_{eh} a) = 0$.

EH Mode :

$$26 \times 10^{19} f^{-4} h^2 [-\gamma^2 a^2 J_1^2 (\gamma a) + \gamma^2 d^2 \{ J_1^2 (\gamma d) + J_0^2 (\gamma d) \}$$
$$+ 2 \{ J_1^2 (\gamma a) - J_1^2 (\gamma d) \} + 2\gamma J_0^2 (\gamma d) - 2 J_0^2 (\gamma d)]$$
$$= -22 \times 10^{11} f^{-2} [\{ J_1^2 (\gamma d) - J_1^2 (\gamma a) \} - \gamma^2 d^2 \{ J_1^2 (\gamma d) + \frac{1}{2} J_0^2 (\gamma d) \}$$
$$+ (\gamma^2 a^2 / 2) J_1^2 (\gamma a)] - \frac{1}{2} a^2 J_1^2 (\gamma a) + \frac{1}{2} d^2 \{ J_1^2 (\gamma d)$$
$$- J_0 (\gamma d) J_2 (\gamma d) \} \qquad [65]$$

where, $\gamma = \gamma_{eh}$

HE Mode :

$$26 \times 10^{29} f^{-4} h^2 \left[- \gamma^2 d^2 J_1^2(\gamma d) + 2 \left\{ J_2^2(\gamma d) + J_0^2(\gamma d) \right\} + \gamma^2 a^2 J_1^2(\gamma a) \right.$$
$$\left. - 2 J_1^2(\gamma a) \right]$$
$$= 22 \times 10^{14} f^{-2} \left[(\gamma^2 a^2/2) J_1^2(\gamma a) - (\gamma^2 d^2/2) \left\{ J_1^2(\gamma d) + J_0^2(\gamma d) \right\} \right.$$
$$- \left\{ J_1^2(\gamma a) - J_1^2(\gamma d) \right\} \right] - \tfrac{1}{2} d^2 \left\{ J_1^2(\gamma d) - J_0^2(\gamma d) - J_0(\gamma d) J_2(\gamma d) \right\}$$
$$+ \tfrac{1}{2} a^2 J_1^2(\gamma a) - (\gamma^2/2) \left\{ J_1^2(\gamma d) - J_1^2(\gamma a) + J_0^2(\gamma d) \right\}$$
$$+ (1/\gamma^2) J_0^2(\gamma d) \tag{66}$$

where, $\gamma = \gamma_{he}$

It is evident that the guide wave length λ_g determined from h in each case is a function of d, a, and f_0.

When γ and the argument of the Bessel functions are large equations [59] to [66] reduce respectively to

$$Q^E = \left\{ \left[-(2\gamma a/\pi) \left\langle \cos^2(\gamma a - 3\pi/4) + \cos^2(\gamma a - \pi/4) \right\rangle \right. \right.$$
$$+ 2\gamma J_0^2(\gamma d) \left] f^{-3/2} h^2 l \times 81.64 \times 10^{29} \right.$$
$$+ \left[(2a/\pi \gamma) \left\langle \cos^2(\gamma a - 3\pi/4) + \cos^2(\gamma a - \gamma/4) \right\rangle \right.$$
$$- (4/\pi \gamma^2) \cos(\gamma a - 3\pi/4) \cos(\gamma a - \pi/4)$$
$$- d^2 J_0^2(\gamma d) \left] f^{5/2} l \times 1.57 \right\}$$
$$\div \left\{ 120.31 \times 10^{-39} \left[\tfrac{1}{2} \gamma^2 d^8 J_0^2(\gamma d) + (\gamma a/\pi) \cos 2\gamma a \right] \right.$$
$$- 52.2 \times 10^{-39} \gamma^2 d l J_0^2(\gamma d) \right\} \tag{67}$$

where, $\gamma = \gamma_e$

$$Q^H = 179 \times 10^8 f^{-1} l \left[(\gamma a/\pi) \left\{ \cos^2 \left\langle \gamma a - (3\pi/4) \right\rangle \right. \right.$$
$$+ \cos^2 \left\langle \gamma a - (\pi/4) \right\rangle \left\} - (\tfrac{1}{2} \gamma^2 d^2 - 1) J_1^2(\gamma d) - \tfrac{1}{2} \gamma^2 d^2 J_0^2(\gamma d) \right]$$
$$\div \left\{ 694.22 \times 10^{22} h^2 f^{-7/2} \left[(\gamma a/\pi) \left\langle \cos^2(\gamma a - 3\pi/4) + \cos^2(\gamma a - \pi/4) \right\rangle \right. \right.$$
$$- (\tfrac{1}{2} \gamma^2 d^2 - 1) J_1^2(\gamma d) - \tfrac{1}{2} \gamma^2 d^2 J_0^2(\gamma d) \right]$$
$$+ 2.61 \times 10^{-7} l d \sqrt{(f)} \left[52 \times 10^{19} (h^2/d) f^{-4} - 1 \right] \times J_1^2(\gamma d) \right\} \tag{68}$$

where $\gamma = \gamma_h$

$$Q^{EH} = 81.64 \times 10^{29} f^{-3/2} h^2 l \left[\left\{ 2 - \gamma^2 a^2 \right\} (2/\pi \gamma a) \cos^2(\gamma a - 3\pi/4) - 2 J_1^2(\gamma d) \right.$$
$$+ (2\gamma - 2) J_0^2(\gamma d) \right] + 1.57 f^{5/2} l \left\langle (2a/\pi \gamma) \cos^2(\gamma a - 3\pi/4) \right.$$
$$- d^2 \left\{ J_1^2(\gamma d) - [2 J_1(\gamma d) J_0(\gamma d)/(\gamma d)] + J_0^2(\gamma d) \right\} \right\rangle$$
$$\div \left\{ 120.31 \times 10^{-39} \left[J_1^2(\gamma d) - (2/\pi \gamma a)(1 - \tfrac{1}{2} \gamma^2 a^2) \times \cos^2(\gamma a - 3\pi/4) \right] \right.$$
$$- 52.2 \gamma^8 d l \times 10^{-39} \left\langle J_0^2(\gamma d) + J_1^2(\gamma d)/(\gamma^2 d^2) \right.$$
$$- 2 J_0(\gamma d) J_1(\gamma d)/(\gamma d) \right\rangle \right\} \tag{69}$$

where, $\gamma = \gamma_{eh}$

$$Q^{HE} = 179 \times 10^8 \, l \, f^{-1} \, [\, (\tfrac{1}{2} \, \gamma^2 \, a^2 - 1) \, (2/\pi \, \gamma a) \, \cos^2 \{ \gamma a - (3\pi/4) + J_1^2 \, (\gamma d]$$

$$\div \, \{ 694.22 \times 10^{22} \, h^2 \, f^{-7/2} \, [\, (\tfrac{1}{2} \, \gamma^2 \, a^2 - 1) \, (2/\pi \, \gamma a) \, \times \, \cos^2 \, (\gamma a - 3\pi/4)$$

$$+ \, J_1^2 \, (\gamma d)] + 2.61 \times 10^{-7} \, l \, d \, f^{1/2}$$

$$\times [52 \times 10^{29} \, h^2 \, f^{-4} \, d^{-1} - 1] \, J_1^2 \, (\gamma d) \} \qquad [70]$$

where, $\gamma = \gamma_{he}$

The variation of λ_g and Q^E with respect to the frequency of excitation and the variation of Q^E with respect to the length of the resonator are shown in figures 10 and 11 respectively. The following values for the constants have been used in computing the results
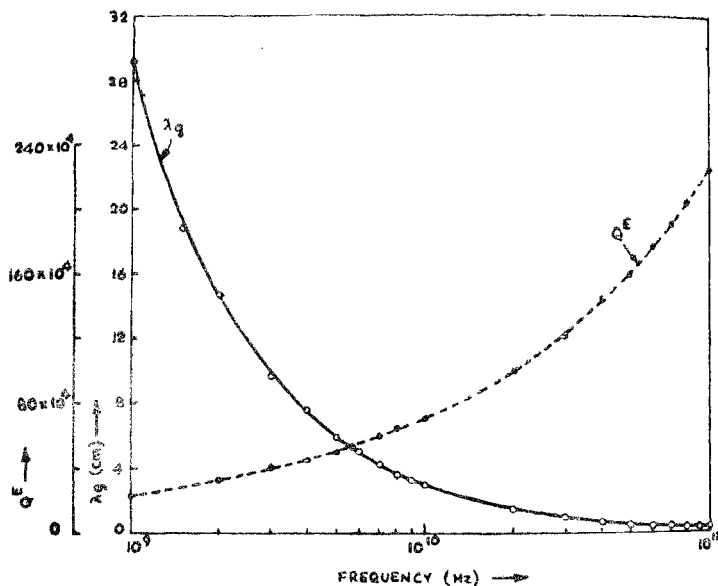
FIG. 10

Variation of guide wavelength and Q factor of E mode with frequency of excitation of the resonator
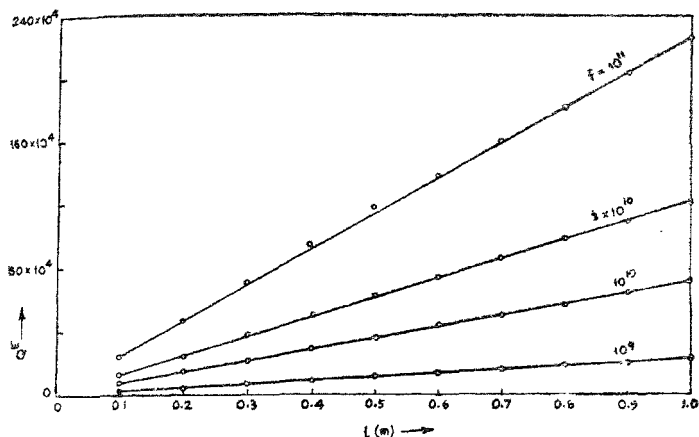
FIG. 11

Variation of Q (E-mode) with respect to the length of the resonator
at different frequencies of excitation.

$$u = 1 \text{ metre}; \quad d = 10^{-3} \text{ metre}; \quad \sigma_e (Al) = 3.54 \times 10^7 \text{ } v/m;$$

$$\sigma_w (Cu) = 5.8 \times 10^7 \text{ } v/m; \quad \mu_0 = 4\pi \times 10^{-7} \text{ } H/m; \quad \epsilon_0 = 8.85 \times 10^{-12} \text{ } F/m.$$

Q OF SOMMERFELD SURFACE WAVE RESONATOR

8.1. *Field Components* :

The mode of practical intest in cylindrical surface wave transmission is rhe E_0 mode, since all other modes have very high attenuation. For Sommerfeld surface wave line having radius d and immersed in air the field components for the resonant waves E_0 are[40]

$$E_{zr} = 2 B \, H_0^{(1)} (j \, \gamma_2 \, \rho) \cos (n \, \pi \, z/l)$$

$$E_{\rho r} = -j \, 2 B \, (n\pi/\gamma_2 \, l) \, H_1^{(1)} (j \, \gamma_2 \, \rho) \sin (n \, \pi \, z/l)$$

$$H_{\theta r} = 2 B \, (\omega \, \epsilon_0/\gamma_2) \, H_1^{(1)} (j \, \gamma_2 \, \rho) \cos (n \, \pi \, z/l) \qquad [71]$$

where

$$\gamma_2 = a_2 - j \, b_2$$

8 2. *Maximum Energy Stored* ;

～ The maximum energy W_M stored inside the resonator is

$$W_M = -\frac{2\pi\mu_0\,B^2\,\omega^2\,\epsilon_0^2\,l}{\gamma_2\,\gamma_2^*\,(\gamma_2^{*2}-\gamma_2^2)}\,[-j\,\gamma_2^*\,d\,\mathrm{H}_1^{(1)}\,(j\,\gamma_2\,d)\,\mathrm{H}_0^{(2)}\,(-j\,\gamma_2^*\,d)$$
$$-j\,\gamma_2\,d\,\mathrm{H}_0^{(1)}\,(j\,\gamma_2\,d)\,\mathrm{H}_1^{(2)}\,(-j\,\gamma_2^*\,d)] \qquad [72]$$

8.3. *Power Lost* :

$$P_e = -\sqrt{\left(\frac{\omega\,\mu_0}{2\,\sigma_e}\right)}\,\frac{8\,\pi\,B^2\,\omega^2\,\epsilon_0^2}{\gamma_2\,\gamma_2^*\,(\gamma_2^{*2}-\gamma_2^2)}\,[-j\,\gamma_2^*\,d\,\mathrm{H}_1^{(1)}\,(j\,\gamma_2\,d)\,\mathrm{H}_0^{(2)}\,(-j\gamma_2^*\,d)$$
$$-j\,\gamma_2\,d\,\mathrm{H}_0^{(1)}\,(j\,\gamma_2\,d)\,\mathrm{H}_1^{(2)}\,(-j\,\gamma_2^*\,d)\,] \qquad [73]$$

$$P_w = \sqrt{\left(\frac{\omega\,\mu_0}{2\,\sigma_w}\right)}\,\frac{2\,\pi\,B^2\,\omega^2\,\epsilon_0^2\,l\,d}{\gamma_2\,\gamma_2^*}\,\mathrm{H}_1^{(1)}\,(j\,\gamma_2\,d)\,\mathrm{H}_1^{(2)}\,(-j\,\gamma_2^*\,d) \qquad [74]$$

8.4.   Q *Factor* :

The Q factor for the Sommerfeld surface wave resonator is

$$Q\,(E_0) = \omega\,(W_M{}'[P_E+P_W])$$
$$= \sqrt{\omega}\,\mu_0\,[-j\,\gamma_2^*\,d\,\mathrm{H}_1^{(1)}\,(j\,\gamma_2\,d)\,\mathrm{H}_0^2\,(-j\,\gamma_2^*\,d)$$
$$-j\,\gamma_2\,d\,\mathrm{H}_0^{(1)}\,(j\,\gamma_2\,d)\,\mathrm{H}_1^{(2)}\,(-j\,\gamma_2^*\,d)]$$
$$- [4/l\,\sqrt{(2\sigma_e)}]\,[-j\,\gamma_2^*\,d\,\mathrm{H}_1^{(1)}\,(j\,\gamma_2\,d)\,\mathrm{H}_0^{(2)}\,(-j\,\gamma_2^*\,d)$$
$$-j\,\gamma_2\,d\,\mathrm{H}_0^{(1)}\,(j\,\gamma_2\,d)\mathrm{H}_1^{(2)}\,(-j\,\gamma_2^*\,d)\,]$$
$$-[d\,(\gamma_2^{*2}-\gamma_2^2)/\sqrt{(2\,\sigma_w)}\,[\mathrm{H}_1^{(1)}\,(j\,\gamma_2\,d)\,\mathrm{H}_1^{(2)}\,(-j\,\gamma_2^*\,d)] \qquad [75]$$

The magnitude of the arguments of the Hankel functions in most of the practical cases is less than 0.05.   Therefore, using the following small argument approximations

$$\mathrm{H}_1^{(1)}\,(j\,\gamma_2\,d) = -(2/\pi\,\gamma_2\,d)$$
$$\mathrm{H}_1^{(2)}\,(-j\,\gamma_2^*\,d) = -(2/\pi\,\gamma_2^*\,d)$$
$$\mathrm{H}_0^{(1)}\,(j\,\gamma_2\,d) = j\,(2/\pi)\,(m+j\,n)$$
$$\mathrm{H}_0^{(2)}\,(-j\,\gamma_2^*\,d) = -j\,(2/\pi)\,(m+j\,n) \qquad [76]$$

where,

$$m = \tfrac{1}{2}\,\ln\,[(0\,89\,d\,)^2\,(a_2^2+b_2^2)]$$
$$n = \text{arc tan}\,(b_1/a_2)$$

the expression for $Q(E_0)$ reduces to

$$Q(E_0) \cong \frac{\sqrt{(\omega \mu_0 \sigma_w \sigma_e)}}{\{2\sqrt{2} \sigma_w / l\} \ \{a_2 b_2 \sqrt{(2} \sigma_e / d [n (a_2^2 - b_2^2) + 2 a_2 b_2 m]\}} \qquad [77]$$

where, the values of $a_2 b_2$ are determined from the solution of the following characteristic equation given by Barlow and Brown[53]

$$\frac{\gamma_2 H_0^{(1)} (j \gamma_2 d)}{\omega \epsilon_0 H_1^{(1)} (j \gamma_2 d)} = \frac{j \gamma_1}{\sigma_w + j \omega \epsilon_1} \frac{J_0 (j \gamma_1 d)}{J_1 (j \gamma_1 d)} \qquad [78]$$

where, γ_1 is the radial propagation constant for the region inside the conductor and ϵ_1 represents the dielectric constant of the conducting medium. By using large argument approximation $|j \gamma_1 d| >> 1$ for the Bessel functions and small argument approximation $|j \gamma_2 d| << 1$ for the Hankel functions, eqn. [78] is solved to yield

$$a_2 = [(1.123 |\xi|^{1/2})/d] \cos \delta/2, \quad b_2 = [(1.123 |\xi|^{1/2})/d] \sin \delta/2 \qquad [79]$$

where,

$$\delta = -\frac{\pi}{4} \left(1 - \frac{1}{ln |\xi| + 1} \right)$$

$$- |\eta| = |\xi| \ ln |\xi|$$

$$\text{and} \ |\eta| = \frac{24 \ 6 \times 10^{-14}}{\sqrt{\sigma_w}} f^{3/2} d \qquad [80]$$

The $Q(E_0)$ of the Sommerfeld resonator at $f = 9500$ *MHz* and with

$$\sigma_e = 3.54 \times 10^7 \ v/m, \quad \sigma_w = 5.8 \times 10^7 \ v/m$$

is

$$Q(E_0) = 10^{-6} \left[\frac{1.74}{l} - \frac{0 \ 678 \ a_2 b_2}{d [n a_2^2 - b_2^2) + 2 a_2 b_2 m]} \right] \qquad [81]$$

which for $l = 0.75 \ m$ and $d = 1.1 \times 10^{-3} \ m$ yields

$Q(E_0) = 18.830$ and for $l = 0 \ 1 \ m \ Q(E_0) = 14660.$

9. Power Flow

In deriving the expression for $Q(E_0)$, it has been assumed that the only losses in the resonator occurs due to ohmic dissipation in the end plates and the wire surface and the loss due to the radiation has been ignored. An idea of the radiation loss can be gained from the power flowing outside a radius ρ_e corresponding to the radius of the terminating end plates.

The total power flow P_t outside the Sommerfelc line is

$$P_t = \frac{1}{2} Re \int_{\theta=0}^{2\pi} \int_{\rho=d}^{\infty} E_{\rho 2} \, H_{\theta 2}^* \, \rho \, d\rho \, d\theta$$

$$= Re \left[\frac{\pi \, \epsilon_0 \, \omega \, h \, B^2}{j \, \gamma_2 \, \gamma_2^\times (\gamma_2^{\times 2} - \gamma_2^2)} \left\{ j \, \gamma_2^\times \, d \, H_1^{(1)} (j \, \gamma_2 \, d) \right. \right.$$

$$\left. \left. H_0^{(2)} (-j \, \gamma_2^* \, d) + j \, \gamma_2 \, d \, H_0^{(1)} (j \, \gamma_2 \, d) \, H_1^{(2)} (-j \, \gamma_2^* \, d) \right\} \right]$$

$$\cong \frac{2 \, \epsilon_0 \, \omega \, B^2 \, \beta}{\pi \, a_2 \, b_2 \, (a_2^2 + b_2^2)^2} \left[\, (b_2^2 - a_2^2) \, n - 2 \, a_2 \, b_2 \, m) \, \right] \tag{82}$$

where, $h = \alpha + j \beta \cong j \beta$ and small argument approximations for the Hankel functions have been used.

The energy flow outside a radius ρ_e is

$$P_{\rho e} = \frac{1}{2} Re \int_{\rho = \rho_e}^{\infty} \int_{\theta=0}^{2\pi} E_{\rho 2} \, H_{\theta 2}^* \, \rho \, d\rho \, d\theta$$

$$= Re \left[\frac{\pi \, \omega \, \epsilon_0 \, h \, B^2}{j \, \gamma_2 \, \gamma_2^* (\gamma_2^{*\,2} - \gamma_2^2)} \left\{ j \, \gamma_2^* \, \rho_e \, H_1^{(1)} (j \, \gamma_2 \rho_e) \right. \right.$$

$$H_0^{(2)} (-j \, \gamma_2^* \, \rho_e) + j \, \gamma_2 \, \rho_e \, H_0^{(1)} (j \, \gamma_2 \rho_e)$$

$$\left. H_1^{(2)} (-j \, \gamma_2^* \, \rho_e) \right. \tag{83}$$

Therefore, the percentage of power flow outside a radius

ρ_e is

$$(P_{\rho e}/P_t) \times 100$$

$$= 100 \, (\pi^2 \, (a_2^2 + b_2^2) \, \rho_e / 8 \, \beta)$$

$$Re \, [h \, \{ j \gamma_2^* \, H_1^{(1)} (j \, \gamma_2 \rho_e) \, H_0^{(2)} (-j \, \gamma_2^* \, \rho_e)$$

$$\frac{+ j \, \gamma_2 \, H_0^{(1)} (j \, \gamma_2 \rho_e) \, H_1^{(2)} (-j \, \gamma_2^* \, \rho_e) \} \,]}{[n \, (a_2^2 - b_2^2) + 2 \, a_2 \, b_2 \, m]} \tag{84}$$

The variation of the percentage of power flow outside a radius $\rho_e = 1$ m and $\rho_e = 0.45$ m as function of the radius of the Sommerfield line having σ_w and σ_e values same as stated previously is shown in fig. 12. It is found that for 25 s.w.g. wire and end plate radius of 1 metre only about .03% power flows outside the resonator, whereas, for end plate of radius 0.45 metre, the percentage of power flow outside the resonator, is about 1%.
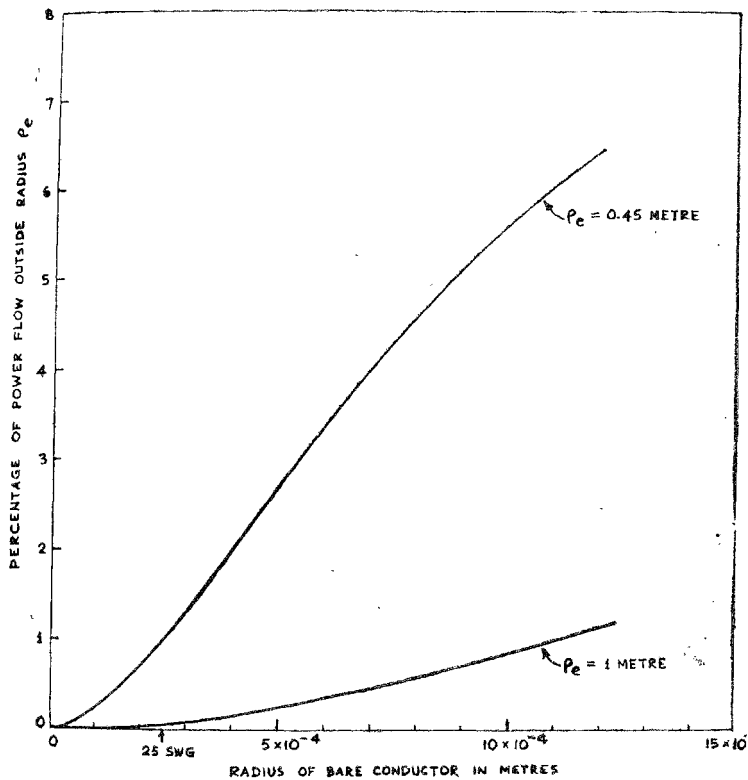
FIG. 12

Power flow outside a radius $P_e = 1$m and $P_e = 0.45$ m as a function of
the radius of Sommerfeld line.

10. FURTHER SCOPE OF WORK

The following work in connection with the surface wave resonator which has been developed (see fig. 13) is under progress.

(i) The effect of the tilt of one of the terminating end plates on the Q of the resonator.

(ii) The problem of excitation of a metallic corrugated surface wave structure.

(iii) Experimental study of the field decay guide wavelength, attenuation of surface wave lines with metal disc loading.

(iv) Extension of the surface wave resonator technique to the study of corrugated dielectric rod characteristic.

11. ACKNOWLEDGEMENT

REFERENCES

|			
1.	Hansen, W. W.	..	..	*J. Appl. Phys.* 1938, **9**, 654.
2.	Borgins, F.	..	..	*Ann. Phys. Lpz.* 1939, **35**, 359.
3.	Jouquet, M.	..	..	*Compt. Rend.* 1939, **209**, 25, 203.
4.	Hansen, W. W.	..	..	*J Appl. Phys.* 1939, **10**, 38.
5.	Richtmyer, R. D.	..	..	*J. Appl Phys.* 1939, **10**, 391.
6.	Barrow, W. L.; Mieher, W. W.	..	Proc. I. R. E. 1940, **28**, 181.
7.	Borgnis, F.	..	..	*Hoch. freq. Tech Elektroakust.* 1940, **56**, 47.
8.	Hahn, W. C.	..	..	*J. Appl. Phys.* 1941, **12**, 62.
9.	Condon, E. U.	..	..	*J. Appl. Phys.* 1941, **12**, 129.
10.	Jouget, M. M.	..	..	*Revue. Gen. Elect.* 1942. **51**, 318.
11.	Jeuget, M. M.	..	..	*Revue. Gen. Elect.* 1942, **51**, 484.
12.	Kinzer, J. P.; Wilson, I. C.	..	*Bell. Sys. Tech. J*, 1947, **26**, 410.
13.	Kinzer, J. P.; Wilson, I. C.	..	*Bell. Sys. Tech. J.* 1947, **26**, 31.
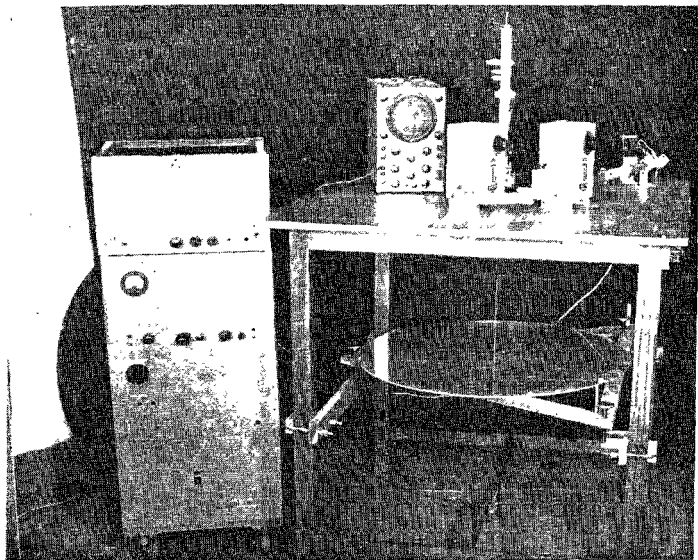
FIG. 13

Photograph of the experimental setup of Sommerfeld surface wave resonator

14. Chatterjee, S. K. . . . . *J. Indian Inst. Sci.*, 1952, **34**, 99.

15. ———, ... *J. Brit. I. R. E*, 1953, **13**, 475.

16. ———, ... *J. Indian Inst. Sci.*, 1953, **35**, 59.

17. ———, ... *Ibid*, 1952, 34, 43.

18. ———, . . , . *Ibid*, 1952, **34**, 77.

19. ———, ... *J I. T. E.* 1965, **11**, 407.

20 ———, ... *J. 1. T E.* 1965, **11**, 528.

21. ———, ... *Proc. I. E. R. E.* 1966, **4**, 53.

22. Szulkin, P. . . . . *Bull Acad. Pol. Sci. Ser. Sci. Tech.*, 1960, **8**, 639.

23. Borgnis, F. and Papas, C. H. . . Randwert, Probleme der. Microwellen Physik, 1955 S. springer verlag.

24. Mayer, E. . . . . *J. Appl.* 1946, **17**, 1046.

25. Klein, W. . . . . *Z. Angew, Phys.*, 1951, **3**, 253.

26. Casimir, H. B. C. . . . . Phillips. Res. Rep., 1951, 6, 162.

27. Waldron, R. A. . . . . Proc. I. E. E., 1960, **107**, 272.

28. Cunltffe, A. and Gould R. N. and Hall, K. D. . . *I. E. E. Monograph*, 1954, 91.

29. Cunliffe, A. and Mathias, L. E. S. . . *Proc. I. E. E.* Pt. III, 1950, **97**, 367.

30. Bethe, H. A and Schwinger, J. . . N.D.R.C. Report D 1-117, March, 1942.

31. Kahan, T. . . . . *C. R. Acad. Sci., Paris*, 1945, **221**, 536, 694.

32. Bernier, J. . . . . Onde Elect., 1946, **26**, 305.

33. Muller, J. . . . . *Hochfrequenz, tech. u. Elektroakust*, 1939, **54**, 157.

34. Wien, M. . . . . *Ann. der. Physik u. Chemie*, 1897, **61**, 151.

35. Kinzer, J.P. and Wilson, I. C. . . *Bell Sys. Tech. J.*, 1947, **26**, 410.

36. Chandler, C. J. . . . . *J. Appl. Phys*, 1949, **20**, 1188.

37. Scheible, E. H. and King, B. G. and Van Zeeland, D. L. . . *Ibid*, 1954, **25**, 790.

38. King, B. G. and Scheibe, E. H., Tatasuguchi, I. . . Ptoc. Nat. Electronics conf., 1955, **11**, 949.

39. King, B. G. and Tatsuguchi, I. Scheibe, E. H. and Goubau, G. . . Spring meeting USRI, Washington, D.C. 1955.

40. Zacharia, K. P. and Chatterjee, S. K. *Radio and Electronic Engineer*, 1968, **36**, 111.

41. Chatterjee, S. K. and Chatterjee, R. *J. Indian Inst. Sci.*, 1968, **50**, 345.

42. Sommerfeld, A. . . . . *Ann. Physik. Chemic, Lpzg.*, 1899, **67**, 233.

43. Zenneck, J. . . . . *Ann. Phy. Lpzg*, 1907, **81**, 1135.

44. Wait, J. R. . . . . *J. Res. Nat. Bur. Stds.* 1957, **59**, 365.

45. ———, ... *Trans. I. R. E.*, 1960, **AP-8**, 445.

46. ———, ... Advances in Radio Research, Academic Press, London, 1964, **4**, 157.

47. Bowwkamp, C. J.   ..   ..   *Phy. Rev.* 1950, **80**, 294.

48. Barlow, H. M.   ..   ..   *Proc. I.R.E.*, 1958, **46**, 1413.

49. ——.   ..   ..   *Proc. I.E.E.*, 1959, **106B**, 179.

50. ——, ...   *Trans. I.R.E.*, 1959, **AP7**, S147.

51. ——, and Cullen, A. L.   ..   *Proc. I.E.E.* Pt. III, 1953, **100**, 329.

52. ——, and Karbowiak, A. E.   ..   *Ibid*, 1953, **100**, 321.

53. ——, and Brown, J.   ..   Radio Surface Waves 13, 1962, Clarendon Press, Oxford.

54. Cullen, A. L.   ..   ..   *Proc. I.E.E.*, Pt. IV, 1954, **101**, 225,

55. Attwood, S. S.   ..   ..   *J. Appl. Phys.* 1951, **22**, 504.

56. Goubau, G.   ..   ..   *Ihid*, 1950, **21**, 111.

57. ——, ...   *Proc. I. R. E.*, 1951, 39, 619.

58. ——, ...   *Trans. I. R. E*, 1956, MTT-4, 197.

59. ——, ...   *Ibid*, 1959, AP-7, S-140.

60. Chatterjee, S. K. and Madhavan P.   *J. Ind. Inst. Sci.*, 1955, 37, 200.

61. ——, and S. N. Contractor   ..   *Ibid*, 1957, **39**, 107.

62. ——, and Chatterjee, R.   ..   *Ibtd*, 1956, **38**, 156.

63. ————————   ..   ..   *Ibid*, 1957, 39, 71.

64. ——   ..   ..   *J. Inst. Engrs. (India)*, 1958, **38**, 875.

65. ——   ..   ..   *J. I. T. E.*, 1958, 4, 90.

66. Wells, D. A.   ..   ..   *J. Appl. Phys.*, 1938, **9**, 312.

67. Albersheim, W. J.   ..   ..   *Bell Sys. Tech. J.*, 1949, **28**, 1.

68. Smythe, W. R.   ..   ..   Static and Dynamic Electricity, 1950, 311, McGraw Hill Book Co.

69. Harms, F.   ..   ..   *Ann. d. Physik*, 1907, **23**, 44.